Research Programme of the Research Fund for Coal and Steel
Steel RTD

Project carried out with a financial grant of the
Research Programme of the Research Fund for Coal and Steel

Robustness of car parks against localised fire

Grant Agreement Number RFSR-CT-2008-00036

Deliverable VI: Development of design recommendations, critical appraisal and application to a study case

March 2012

Authors:

Cheng Fang (ICST)
Bassam Izzuddin (ICST)
Ahmed Elghazouli (ICST)
David Nethercot (ICST)
Ludivine Comeliau (ULGG)
Jean-Pierre Jaspart (ULGG)
Jean-François Demonceau (ULGG)
Clara Huvelle (ULGG)
Long Van Hoang (ULGG)
Cécile Haremza (FCTUCOIMBRA)
Aldina Santiago (FCTUCOIMBRA)
Luís Simões da Silva (FCTUCOIMBRA)
Renata Obiala (ARCELORPROFIL)
Bin Zhao (CTICM)
Dhionis Dhima (CSTB)
Nicolas Taillefer (CSTB)
Frédéric Gens (GREISCH)
Vincent de Ville (GREISCH)

Table of contents

I. Introduction

This deliverable present all the developments performed within WP4 and WP5.

The first objective of WP5 was to design an "actual" reference building, in full agreement with Eurocode recommendations. This building is first presented in § II.

Then, the derivation of practical design recommendations useful for practitioners representing the main outcome of WP4 is presented. The activities of this WP were divided in two tasks:

- derivation of practical recommendations and;
- critical appraisal of the practical recommendations.

For such a complex problem than the one considered in the present project, different design approaches may be contemplated, ranging from the very sophisticated thermal and mechanical simulations through FEM techniques to basic hand design procedures. The sense to give to "practical recommendations" is strongly dependent on the selected level of design sophistication. This being, and recognising the difficulty to approach the problem whatever is this level, it has been decided, in WP4, to gather all recommendations which seemed to be of practical interest for the designer.

In the present deliverable, different questions, corresponding to different sophistication levels, are therefore addressed:

- How to perform experimental tests on substructures so as to simulate the actual response of joints subjected to fire action, (and in which combined bending moment and axial loads are in constant evolution during the column heating) - § IV.
- How to simulate numerically, through FEM techniques, the behaviour of such joints - § III.2.
- How to predict analytically the M-N resistance interaction curves of such joints - § V.1.
- How to predict in a simplified way the actual distribution of temperatures along the beam axis - § III.1.2.
- How to predict analytically the response of a slab located just above the lost column - § V.2.2.
- How to numerically simulate the global frame response according to one of the three following potential approaches: temperature-Dependent Approach, simplified Temperature-Dependent Approach and Temperature-Independent Approach - § III.1.
- How to analytically check the robustness of the car park through simplified "hand" analytical procedures - § V.2.

The higher is the level of sophistication, the greater is the accuracy of the design. But also the greater are the design efforts and the complexity of the approach for the designer. The powerful or more basic character of the calculation tools to be used is also a factor to be accounted for in design offices.

The most practical one is for sure the simplified analytical approach as the latter may be applied using tools available in any design office. It is the reason why the "practice-oriented" partners have mainly focused their work on the applicability of this approach. A critical appraisal of the latter is given in § VI.

After having presented and criticised these recommendations, the applicability of the latter to the reference building has been investigated in § VII and § VIII by the "practice-oriented" partners, in interaction with the "scientific" partners.

II. Case study description

II.1. Design of a reference structure

II.1.1. Introduction

In order to realise tests and studies of this research on the basis of a common structure used in our countries, a standard structure of an open car-park has been designed. This structure will be called in all documents "the reference structure".

The geometry of the designed car-park must be the most general possible in order to cover the greatest number of existing structures. After discussions between the partners of the research, the structure selected is described on Figure 1. Except for the columns, whole the elements have a composite resistance. Thus, the slab is composite and the beams are connected to this one, but are not coated with concrete. The whole structure is supposed to be braced and this is made with the help of the concrete ramps which are not drawn in the field of this project.

It is thus about a car-park having internal columns laid out every 10 m, the beams have a range of 16 m and are spaced of 3,333 m which is the range of the slab.

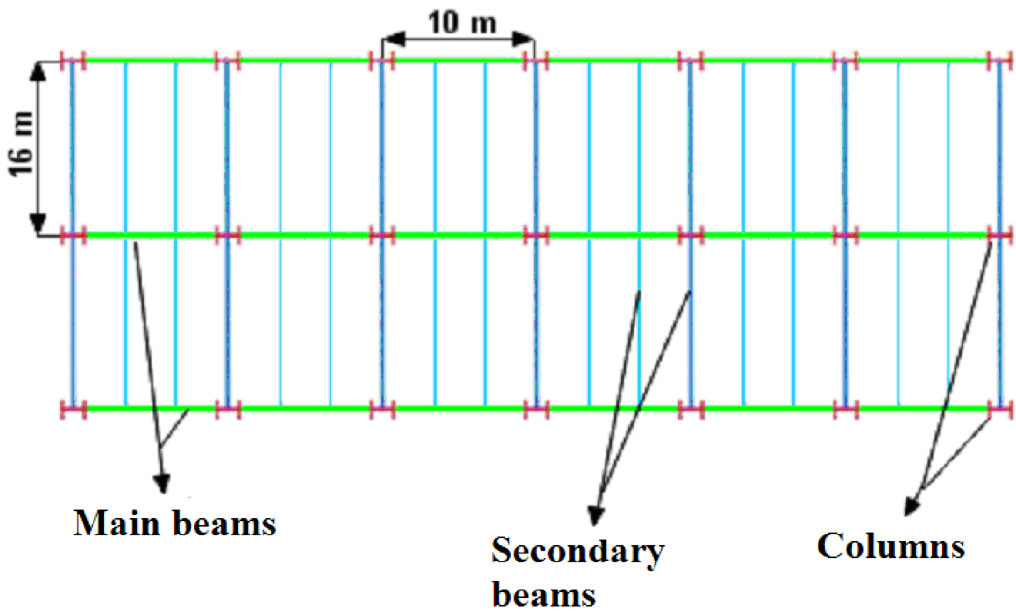

Figure 1 : structure description (plan view)

The height of the 8 stages is fixed at 3 m, which makes a total height of the building equal to 24 m. Moreover, no roof is envisaged on the last stage, this one also being used as level of parking and the selected metal sections will be the same ones on the whole of the structure.

All plans of this reference structure and the details of the design can be found in the Annex A of the present Deliverable (X.1). Only the main results are presented here below.

II.1.2. Cross-sections designed

II.1.2.1. Composite slab

The composite slab is of type COFRAPLUS 60, made up of a ribbed metal sheet of 1 mm of thickness which represents the lower reinforcement in the longitudinal direction of the slab, but also the formwork of this one during the casting of the concrete; this sheet thus has a double function. The thickness of this slab is of 120 mm which is relatively weak.

A basic mesh of Φ8 mm spaced by 200 mm is placed all over in the slab and some reinforcement have to be placed in the joint zone of the main beams.

II.1.2.2. Main beams

The static schemes for those beams consider a semi-rigid joint for the connection with the column. The rigidity is different for the self weight loads and for the variable loads because of the behaviour of concrete

Finally, the dimensioning lead to consider for those main beams a IPE 550 profile (S355). The joint is described on Figure 2

II.1.2.3. Secondary beams

The static schemes for those beams consider a pinned connection with the column and with the main beam. This is valid for the self-weight when the steel structure acts alone and also for the variable load because the composite sections is not able to carry loads in case of dissymetrical loading.

Finally, the dimensioning lead to consider for those secondary beams a IPE 450 profile (S355). The joint is described on Figure 2

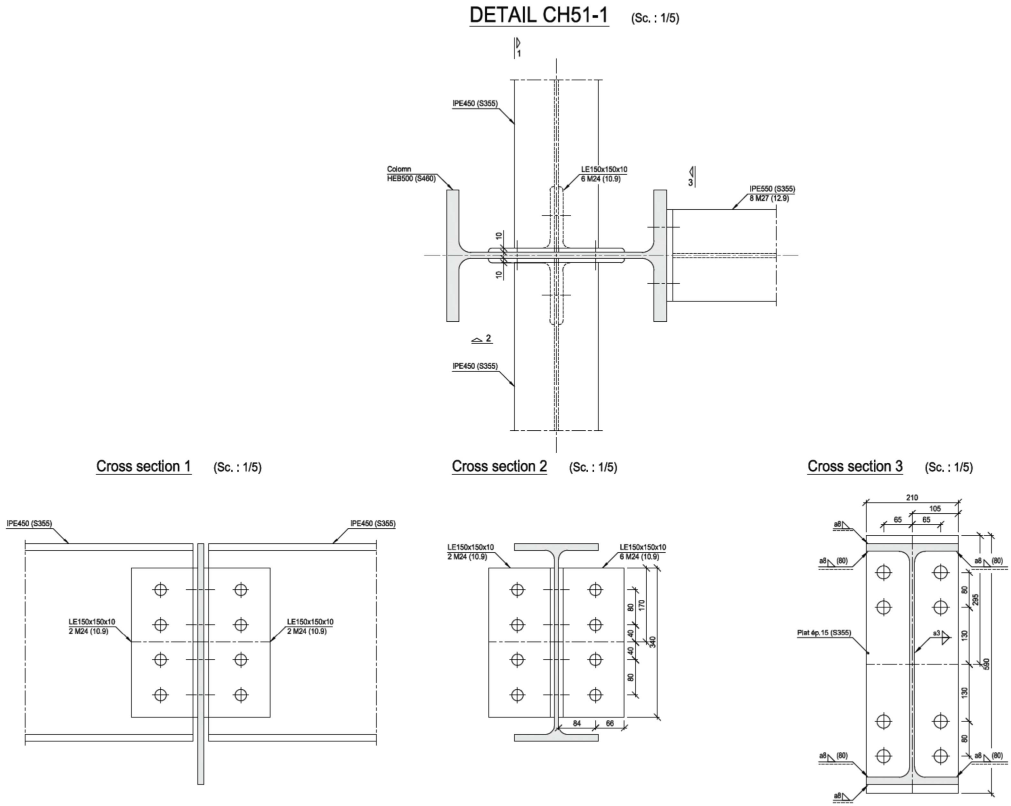

Figure 2 : Main beam and secondary beam to column joint

II.1.2.4. Columns

The columns have a buckling length of 3 meters and are considered in S460 grade in order to minimise their width. It is possible to change the sections of the column on the height of the structure from HEB 550 to HEB 220. The calculation of the rigidity of the joints between column and main beams are made with a HEB 300 column which is the section used for the test and for floors 4 and 5 from the reference car-park.

II.2. Fire scenarios for robustness

Basic idea consists in defining a fire potentially impacting a column in the car park structure. Under fire conditions, this column is deeply affected, and could even fail. According to car park regulation and fire safety engineering practices, worst scenario for column is as follows: four cars are burning around the column and the fire spreading from one car to the others after a short time (12 minutes). An alternative scenario for edge column could include only two cars. In this report, only internal columns of the structures are considered for robustness scenario. Location of the fire could potentially be anywhere at any floor, provided that there are 4 car places around a column (see Figure 3).

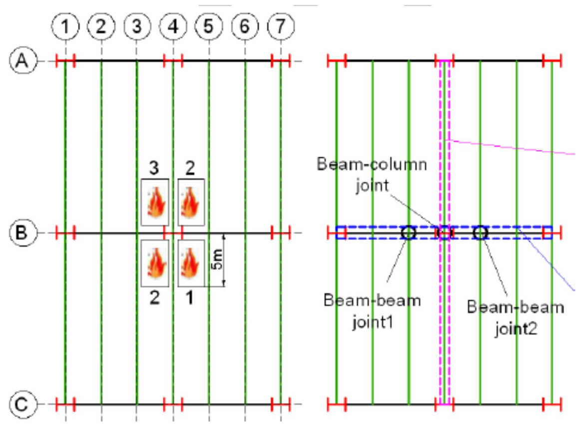

Figure 3. Initial position of fire cars.

Here, for demonstration purpose, only two column locations are studied, one at ground floor and the other under roof floor. First location corresponds to the most loaded column. The second one corresponds to the minimized alternative loading paths from the upper structure, limiting the possibility of structural adaptation to a local failure.

Under each of above fire scenarios; the fire affected column is considered to fail fully and in consequence their resistance disappears totally.

III. Practical design recommendations – Numerical approaches

III.1. Robustness assessment framework

III.1.1. Introduction

Existing codified treatment of structural robustness for extreme loading is based on prescriptive rules. Although some codes already incorporate guidance for the assessment and design of structural robustness, this is not immediately applicable to the fire condition, thus a considerable gap therefore exists between fire resistance and structural robustness research. In line with WP4, this report proposes robustness assessment approaches that offer a practical framework for the consideration car park under localised fire. Two alternative approaches are proposed, namely, a simplified temperature-dependent approach (TDA) and a temperature-independent approach (TIA). These approaches have been developed and verified extensively using sophisticated numerical simulations of the car park structure under localised fire, making use of high performance computing equipment purchased for this purpose. The TDA requires a simplified definition of elevated temperature scenarios, while the TIA corresponds more closely to typical robustness provisions considering unforeseen events, and can be more easily applied in design practice. The reference car park is employed to illustrate the application of the two approaches, where reduced full slab models (Level B) are established in ADAPTIC (Izzuddin, 1991)

III.1.2. Temperature-Dependent Approach (TDA)

An idealised temperature field within the structural model is developed for the simplified TDA, which allows the elevated temperature structural analysis to be performed in a simplified performance-based manner over the temperature domain instead of the time domain as used in WP3. Therefore, the simplified TDA is relatively event-independent, as it does not require details of fire hazard (e.g. the type, the number or sequence of burning cars) but only requires the range of the fire-affected area. The proposed assumptions for the idealised temperature distribution of the reference structure subject to typical localised fires are illustrated in Figure 4.

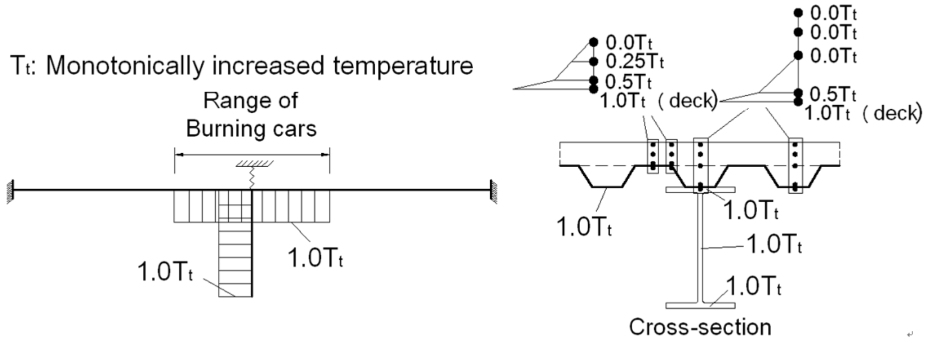

Figure 4. Idealised temperature distribution for simplified TDA

For this simplified temperature distribution, the fire affected area is defined as the area within the range of the burning cars (typically a 7m×10m rectangular area for four burning cars). Due to the high heat conductivity of steel, the temperature in the column is considered to be uniform along the height as well as over the cross-section. The temperatures in the steel beams and the steel decks within the range of burning car areas are considered to be uniform, and the steel beams and the steel decks beyond this fire affected area are assumed to be at ambient temperature. The temperature increase rate for the steel beams and deck is assumed to be the same as that for the column. For concrete, it is assumed that the temperature of the concrete immediately above the steel deck is half of that in the steel deck (which is generally true in the heating phase as observed from the detailed thermal analysis), and it decreases to ambient temperature towards the top face of the slab in a multi-linear manner, as illustrated in Figure 4. Applying the simplified temperature distribution to the structural model of the reference car park, the floor deflection and column axial force with monotonically increasing temperatures are shown in Figure 5 and Figure 6, respectively. Figure 7 gives the shear response of the fire affected joints, where punching shear is deemed to occur when the total shear force transferred by the connections exceeds their overall shear capacity.

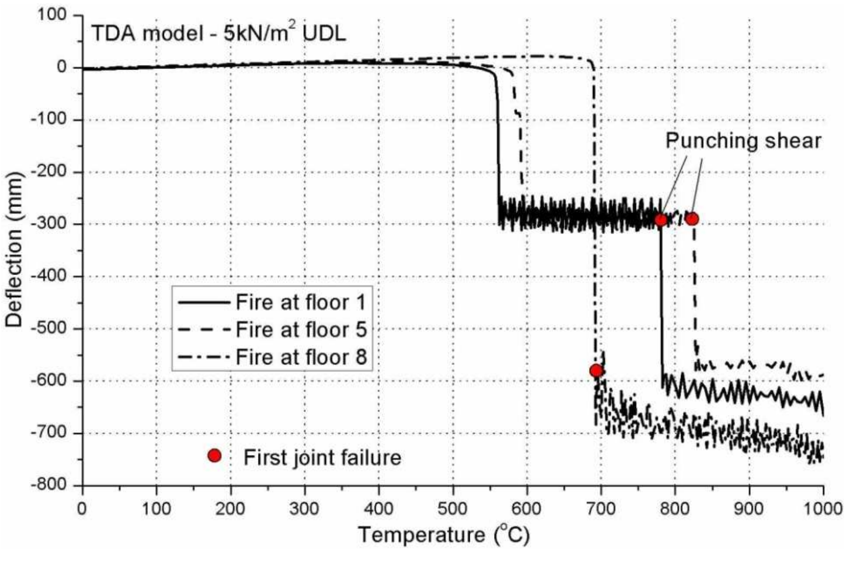

Figure 5. Floor deflection – simplified TDA analysis

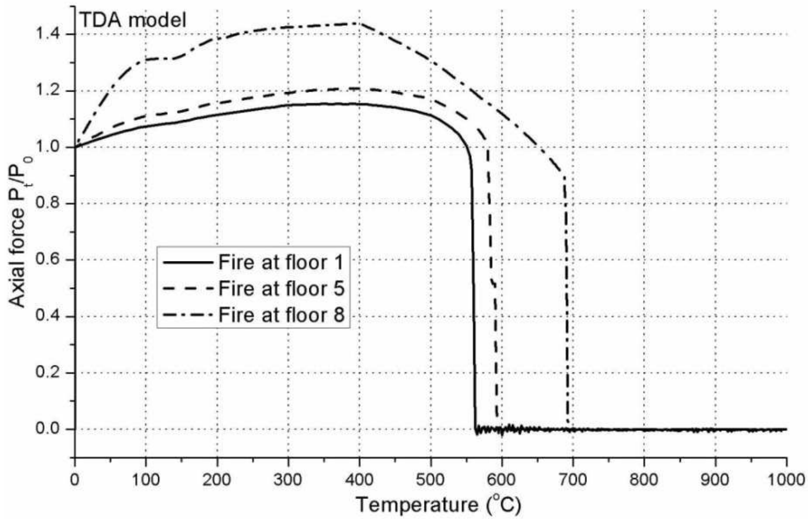

Figure 6. Column axial force – simplified TDA analysis

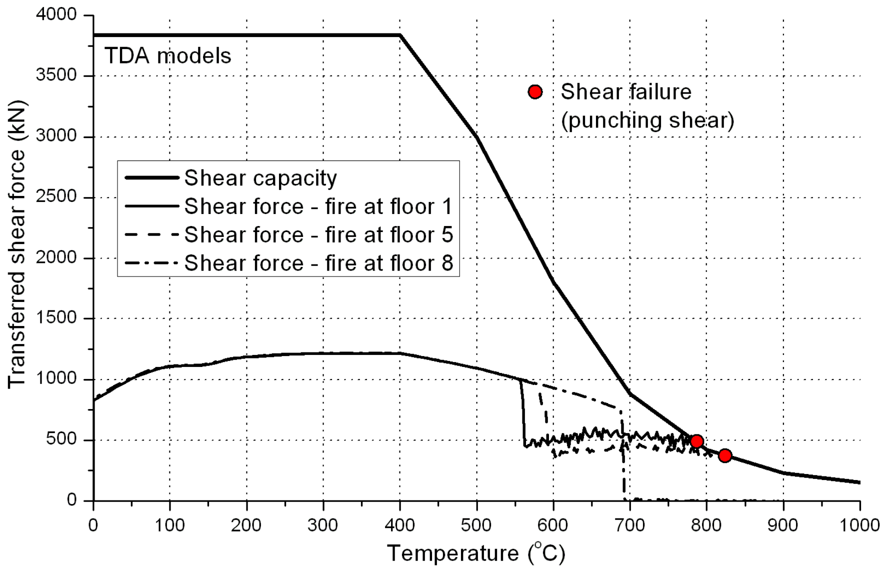

Figure 7. Shear force transferred by fire affected joints – simplified TDA analysis

Table 1 gives the column buckling temperature, the floor deflection after column buckling, the first failure temperature, and the first failure mode for the cases of fire at floor levels 1, 5, and 8 obtained from the real fire analysis (WP3) and simplified TDA analysis. It can be observed that the simplified TDA analysis predicts a similar structural response to that obtained by the real fire analysis. Although the structural performance predicted by the simplified TDA analysis is slightly less conservative (e.g. predict a slight higher critical temperature), all the discrepancies are within a limited and acceptable range. So the simplified TDA analysis can provide a sufficiently accurate approach to evaluate the structural response under localised fires.

Finally, it is noted that the following idealisations are responsible for the differences between the results obtained by the simplified TDA analysis and the detailed thermal and structural analysis: 1) neglect of temperature in the floor beyond the reduced fire affected area, 2) assumption of uniformly distributed temperature within the beams and decks, 3) assumption of identical temperatures in the beam and deck, 4) idealised temperature distribution in concrete, and 5) neglect of unsymmetrical fire load on different sides of column due to different burning times of affected cars. Notwithstanding, these effects are shown to be relatively unimportant when the structure is considered for robustness assessment.

Table 1. Comparison between detailed TDA and simplified TDA analysis

Response	Fire affected floor levels	Real fire analysis (peak temperature = **741ºC**)	Simplified TDA analysis
Column buckling temperature (time)	1	556.1ºC (24m56s)	562.5 ºC
	5	580.9 ºC (25m25s)	590.0 ºC
	8	666.8 ºC (27m10s)	692.5 ºC
Floor deflection after column buckling	1	299.6mm	300.6mm
	5	299.9mm	308.9mm
	8	725.3mm	683.5mm
First joint failure temperature (time)	1	741.0 ºC (30m00s)	780.0 ºC
	5	No first joint failure	825.0 ºC
	8	666.8 ºC (27m10s)	692.5 ºC
First joint failure position/mode	1	Fire affected beam-to-column steel connections in shear (punching shear)	Fire affected beam-to-column steel connections in shear (punching shear)
	5	No first joint failure	Fire affected beam-to-column steel connections in shear (punching shear)
	8	Fire affected major axis beam-to-column joints under sagging moment	Fire affected major axis beam-to-column joints under sagging moment
Progressive collapse triggered after first joint failure?	1	No	No
	5	-	No
	8	No	No

From a robustness perspective, a capacity/demand ratio (CDR) is usually used to indicate the proximity of the structure to a limit state, which is typically expressed in terms of the associated structural resistance compared to the applied loading, where a ratio exceeding a value of 1.0 indicates a safe structure. Clearly, under localised fire conditions, the capacity/demand ratio for a system depends on temperature. In other words, whether a structure can survive under fire depends on the severity of the fire (or the maximum temperature that can be reached). To address this, three peak temperatures are considered in this study for CDR assessment, namely, 500°C, 750°C and 1000°C. These three maximum temperatures represent respectively three typical different severities or probabilities of expected fire, i.e. 'frequent/basic', 'intermediate', and 'rare'. This classification strategy is similar to that used in seismic engineering, where different earthquake occurrence frequencies are employed to deduce different levels of seismic loadings applied on structures. Towards future codification, this strategy can potentially enable a reasonable robustness CDR assessment procedure through applying different pre-determined expected peak temperatures on structures with various functions and significance. Table 2 provides the CDRs for the current structure considering a basic UDL of 5kN/m^2. It is shown that the CDRs exceed 1.0 for all cases, thus indicating sufficient robustness of the reference structure for the basic gravity load.

Table 2. CDR of structure subject to localised fire under UDL (5kN/m^2) – simplified TDA

Fire floor level	Maximum temperature expected (ºC)	UDL capacity (kN/m^2)	CDR
1	frequent (500)	7.00	1.400
	Intermediate (750)	7.00	1.400
	Rare (1000)	6.59	1.318
5	frequent (500)	7.00	1.400
	Intermediate (750)	6.95	1.390
	Rare (1000)	6.76	1.352
8	frequent (500)	12.80	2.560
	Intermediate (750)	5.67	1.134
	Rare (1000)	5.67	1.134

III.1.3. Temperature-Independent Approach (TIA)

While the above discussed simplified TDA has been shown to be capable of providing a reliable performance-based robustness assessment procedure for multi-storey buildings subject to localised fire, the definition of the fire affected area and the maximum expected temperature is still required. Accordingly, the simplified TDA can be deemed only as a 'semi-event-independent' approach. Towards a more practical and comprehensive design approach which is event-insensitive and at the same time performance-based, an alternative robustness assessment approach is proposed in this section, namely, a Temperature-Independent Approach (TIA).

III.1.3.1. Assessment procedure

With the incorporation of the degraded fire affected floor, the TIA does not require thermal analysis and only requires the nonlinear static response of the floor systems under ambient conditions. Employing the energy-based method, potential dynamic effects along with column buckling can be considered in a simplified, yet reliable manner. For a conservative assessment, the assumption of a sudden column loss due to buckling can be accepted in the TIA in order to predict an upper bound of ductility demand. In this case, the additional strain energy dissipated by the buckled column can be ignored, thus leading to a similar assessment procedure to the typical ductility centred approach for sudden column loss, differing only in the requirement of considering a degraded floor system representing the fire affected floor. In view of this, the proposed TIA framework comprises four main steps (three basic and one optional), namely, *nonlinear static floor response*, *modified nonlinear static response (optional)*, *simplified dynamic assessment*, and *ductility assessment*.

- Nonlinear static floor response

The nonlinear static response of a multi-floor TIA system subject to column removal can be expressed by the total gravity load-deflection response. According to the assumption that the upper ambient floors in conjunction with the degraded floor (representing the fire affected floor) resist the gravity load in double span, and considering that the ambient floors and the degraded floor have the same predominant deformation mode, the overall nonlinear static response of the TIA system should be taken as the superposition of all the individual floors (degraded and ambient) above the damaged column, as illustrated in Figure 8. The degraded floor can be presented via removing the fire affected joints and beams.

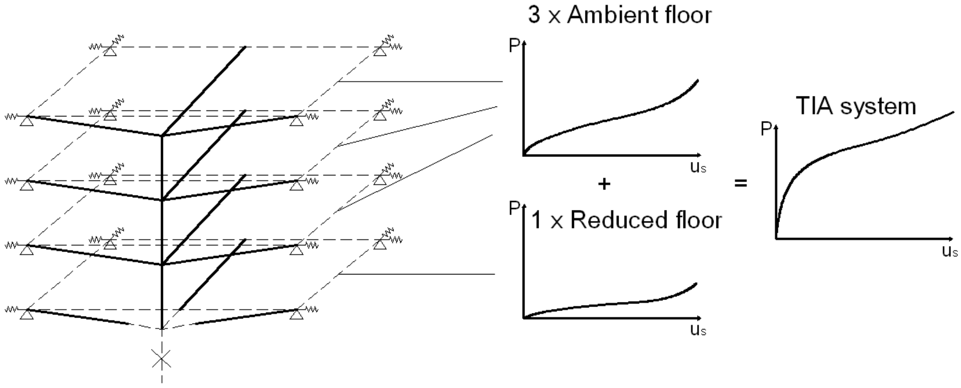

Figure 8. Nonlinear static response of TIA system

The nonlinear static curve can provide a measurement of the energy absorption characteristics of the multi-floor TIA system, which can be expressed as:

$$\delta W = \sum_{j=1}^{n} \delta U_{f,j} \tag{1}$$

where j represents the floor level, $\delta U_{f,j}$ is the incremental internal energy absorbed by one individual floor system, for the incremental external work δW, the relationship between the gravity load and the incremental system deformation can be given in the following equation:

$$\delta W = \sum_{j=1}^{n} \alpha_j . P_j . \delta u_{s,j} \tag{2}$$

Due to the compatibility of the deformations of individual floors:

$$\delta u_s = \delta u_{s,1} = \delta u_{s,2} = ... \tag{3}$$

and considering the same value of the weighting factor $\alpha = 0.25$ for the UDL gravity load distribution, Eq. (1) can be expressed by:

$$\delta W = \alpha . \delta u_s . \sum_{j=1}^{n} P_j = \alpha . \delta u_s . P_{total} = \sum_{j=1}^{n} \delta U_{f,j} \tag{4}$$

where P_{total} is the total gravity load applied on all the floors above the fire affected column. From this equation, the internal strain energy absorbed by all the floors above the fire affected column can be obtained through calculating the area below the $\alpha P_{total} - u_s$ curve.

- Modified nonlinear static response (optional)

The above nonlinear static response $\alpha P_{total} - u_s$ can be directly employed in the third step 'simplified dynamic assessment' in order to acquire an upper bound for the ductility demand of the TIA systems by neglecting the strain energy stored in the buckled column. In this case, a maximum deflection of the TIA system subject to an idealised 'sudden column buckling' process is obtained. However, in order to reflect a more accurate response of the TIA system subject to localised fire, the $\alpha P_{total} - u_s$ curve should be modified with the consideration of the residual column resistance. As discussed before, this is reflected in an additional contribution to the energy distribution:

$$\delta W = \delta U = \sum_{j=1}^{n} \delta U_{f,j} + \delta U_c \tag{5}$$

In this expression, the total incremental strain energy δU is comprised of the incremental strain energy dissipated by the floor systems $\sum_{j=1}^{n} \delta U_{f,j}$ and the incremental strain energy absorbed by the fire affected column δU_c during the buckling process. The overall strain energy absorbed by the column can be obtained through calculating the area under the static response curve of the column under its buckling temperature, as illustrated in Figure 9, where P_i is the maximum load resistance offered by the column under its buckling temperature. In order to predict the buckling temperatures of columns, a simplified numerical method is proposed here which is independent of the axial restraint conditions of the column.

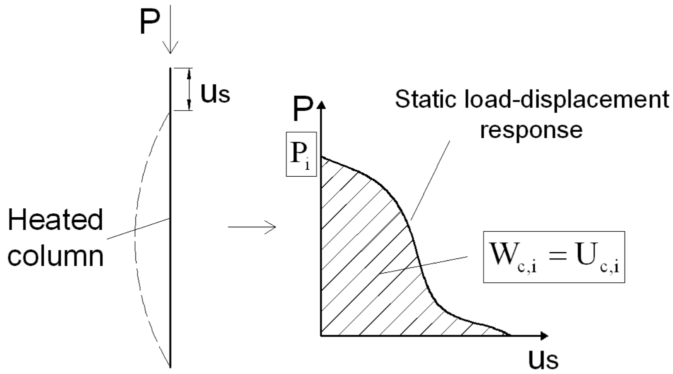

Figure 9. Static response of fire affected column

Firstly, a FE model for the considered heated column at an arbitrary temperature free from axial restraint is established. Afterwards, 'displacement control' can be applied for the column top vertical displacement as a loading scheme to obtain a static load-displacement response. The column temperature is then adjusted until the peak column resistance is identical to P_0, i.e. initial load resisted by the ambient column. This temperature is approximately the column buckling temperature, and the corresponding load-displacement curve is the required curve for calculating the strain energy dissipated by the buckled column under its buckling temperature. This simplified method is based on the fact that one temperature corresponds to only one buckling compressive resistance for a specific column, regardless of its axial restraint conditions; therefore, given a known peak value of buckling compressive resistance P_i, which is approximately taken as the ambient value P_0, the buckling temperature can be easily estimated using this simplified method.

Given the predicted column buckling temperature and the corresponding static load-displacement response of the heated column, the total incremental strain energy of the multi-floor TIA system can be obtained by the sum of $\sum_{j=1}^{n} \delta U_{f,j}$ and δU_c; therefore, the modified nonlinear static response can be taken as the superposition of the two responses, as illustrated in Figure 10.

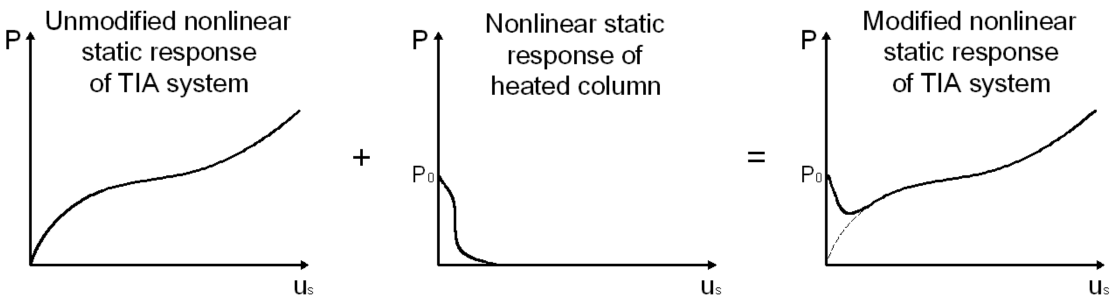

Figure 10. Method of obtaining modified nonlinear static response of TIA system

- Simplified dynamic assessment

Using the modified nonlinear static response of a TIA system under different levels of total gravity load, such as $P_{total,1}$ and $P_{total,2}$, the maximum dynamic response can be obtained from energy balance between the work done by the external load and the internal energy dissipated by the deformed multi-floor TIA substructure and the damaged column. This is illustrated in Figure 11(a) and Figure 11(b), where $u_{d,i}$ is the maximum dynamic deflection based on the unmodified nonlinear static response considering a sudden column loss process, and $u_{r,i}$ is the reduced dynamic deflection based on the modified nonlinear static responses considering the energy dissipated by the column. Energy balance can be used to determine $u_{r,i}$ as follows: $W_i = \alpha.P_{total,i}.u_{r,i} = U_i = \int_0^{u_{r,i}} \alpha.Pdu_s$ (6)

where U_i is the total strain energy absorbed by the floor system and the buckled column, and is equal to the area below the modified nonlinear static curve. Provided that sufficient $\alpha P_{total,i} - u_{r,i}$ points are calculated, a reduced pseudo-static response can be constructed, which depicts the reduced dynamic deflection corresponding to specific values of the gravity load, as shown in Figure 11(c).

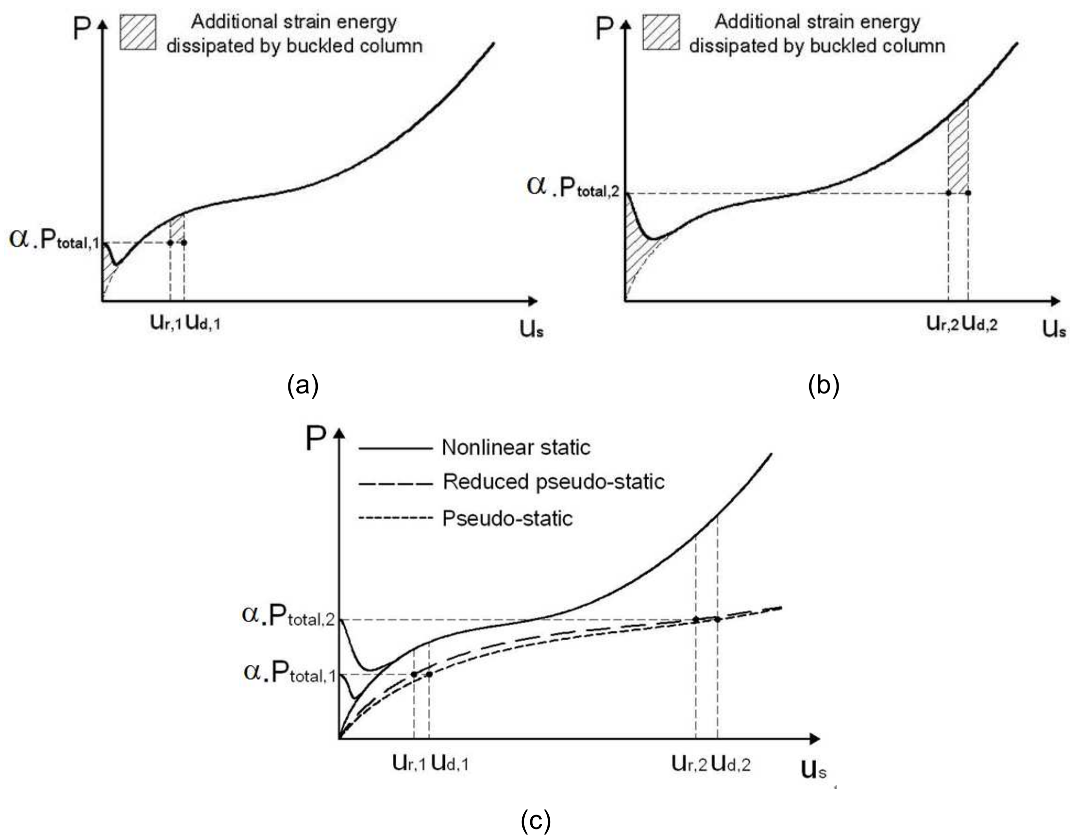

Figure 11. Simplified assessment: (a) $P_{total,1} = \lambda_1.P_0$, (b) $P_{total,2} = \lambda_2.P_0$, (c) Reduced Pseudo-static response

- Ductility assessment

The last stage of the TIA assessment framework compares the obtained ductility demand (i.e. maximum reduced dynamic deflection) to the ductility supply of the considered TIA system. Based on the Robustness Limit State proposing that collapse of any floor, which can lead to impact loading onto the lower floor, is not permitted, the maximum ductility supply of TIA system should be determined with the avoidance of collapse in any of the affected floors, whilst ensuring that the surrounding columns have sufficient resistance to sustain the redistributed load. According to this definition of ductility supply, system failure occurs when the deformation of either the degraded floor or the upper ambient floors first exceeds their respective ductility capacity. In this respect, the failure of any floor system is attributed to the ductility failure of the first surrounding joint on that floor, thus failure criteria are defined in terms of whether the ductility limits of the surrounding joints are exceeded.

III.1.3.2. Application of TIA to reference car park

This section illustrates the application of the proposed TIA, where the reference car park considered previously using the TDA is employed. Progressive collapse assessments are performed at the same three affected floor levels as considered in the TDA, i.e. floor levels 1, 5, and 8. The nonlinear static curves are obtained using the FE models established in ADAPTIC for the degraded floor as well the ambient floor, as shown in Figure 12, where the rotational resistance of the fire affected joints are removed in the degraded floor in the current model. The ductility supplies for the individual ambient floor and the degraded fire affected floor are 610mm and 692mm in deflection, respectively, where failure modes for both floor systems are governed by rupture of rebars in the surrounding major axis beam-to-column joints under hogging moments. By means of superposition, unmodified nonlinear static responses for floor levels 1, 5, and 8 are obtained, as shown in Figure 13.

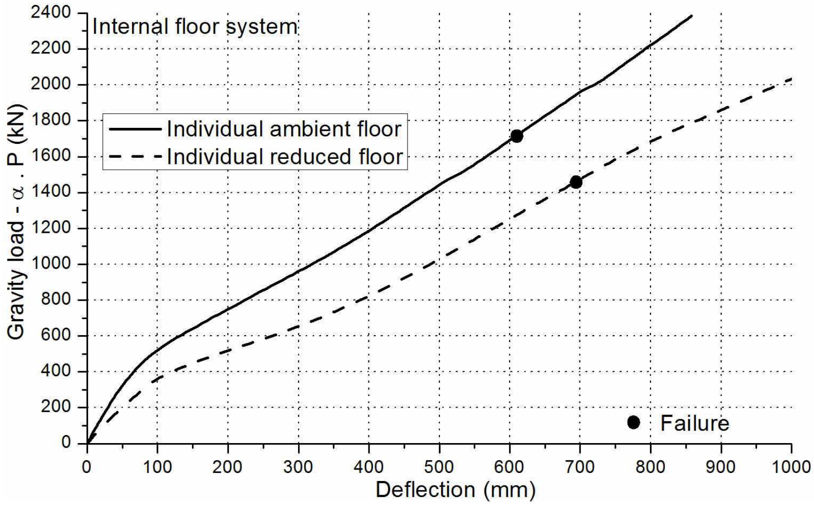

Figure 12. Nonlinear static response of individual floor

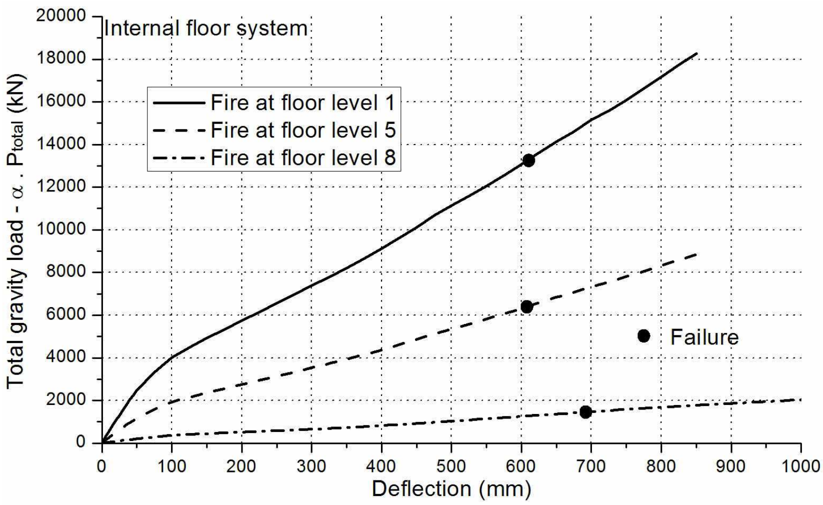

Figure 13. Unmodified nonlinear static response of multi-floor TIA system

Combining the obtained nonlinear static response of the TIA floor systems and the deflected columns, modified nonlinear static curves can be obtained, as shown in figures from Figure 14 to Figure 16 for fire at floor levels 1, 5 and 8, respectively. Based on the principle of energy equivalence, the ductility demands (reduced dynamic deflections) of the reference car park subject to localised fires at floor levels 1, 5, and 8 are obtained as 444.6mm, 479.3mm and 709.9mm, respectively. These results demonstrate increasing ductility demands with the floor level affected by fire, which is due to greater resistance provided by the upper ambient floors when the fire occurs at lower floor levels. Comparing to the ductility supplies, the ductility demands of the structure subject to fires at floor levels 1 and 5 are safely accommodated, which indicates sufficient robustness. On the other hand, for fire at the top floor (level 8), the ductility supply is exceeded by the ductility demand, so a high potential for progressive collapse is indicated for the structure. Table 3 provides the ductility supplies and demands of the structure subject to the three fire affected floors. For comparison purposes, sudden column loss responses which are obtained through the unmodified nonlinear static curves are also given, where larger ductility demands are predicted.

Table 3. Ductility demand and supply of TIA systems

Fire floor level	Reduced dynamic deflection (mm)	Sudden column loss deflection (mm)	Ductility supply (mm)
1	444.6	497.2	610
5	479.3	525.6	610
8	709.9	729.6	692

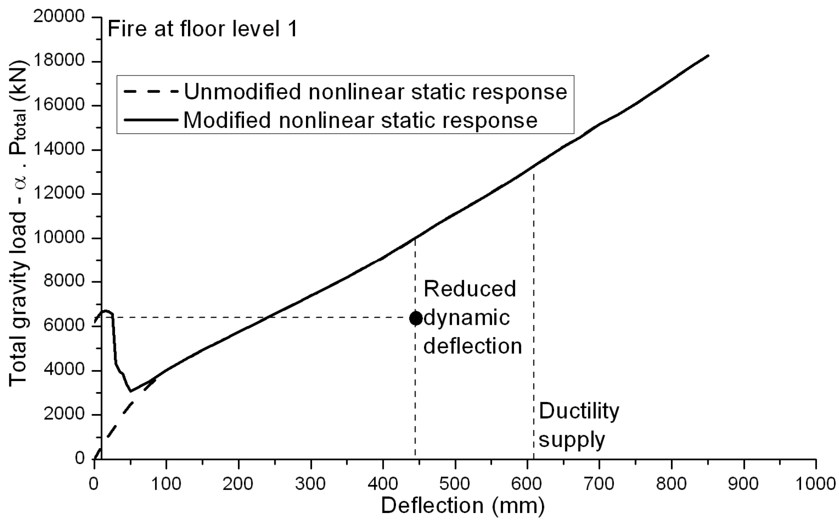

Figure 14. Ductility supply and demand of structure subject to fire at floor level 1

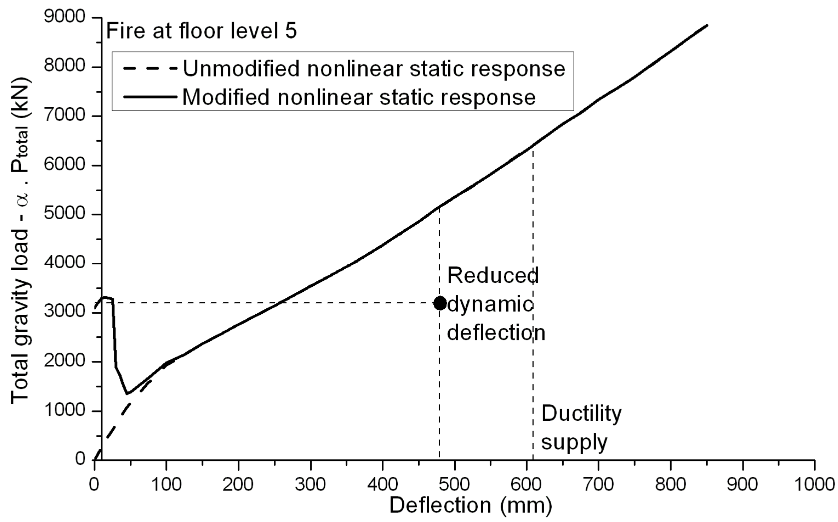

Figure 15. Ductility supply and demand of structure subject to fire at floor level 5

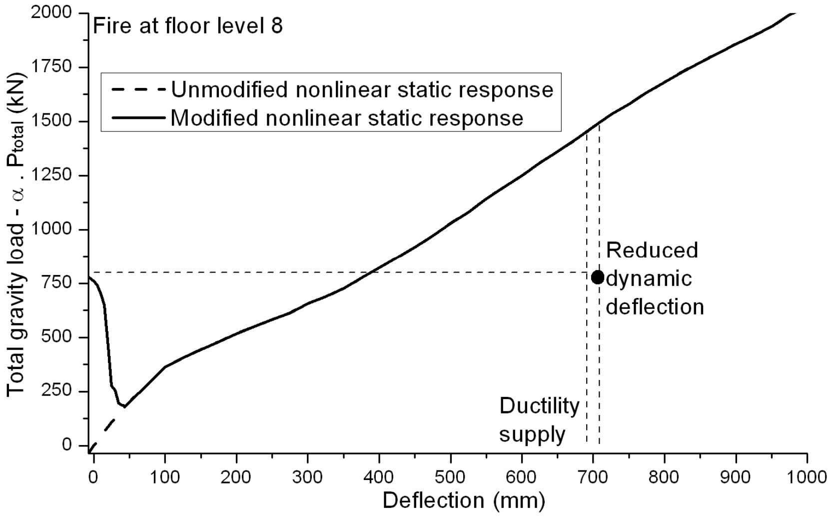

Figure 16. Ductility supply and demand of structure subject to fire at floor level 8

From the perspective of robustness, capacity/demand ratios (CDR) are also used here to indicate the potential of the structure for progressive collapse, which are expressed in terms of the structural resistance at the point of failure compared to the applied loading. Unlike the assessment of CDR in the TDA, the considered CDR for the TIA is independent of temperature. Table 4 provides the CDR's using the TIA for the structure subject to fires at floor levels 1, 5 and 8 with a basic gravity load of $5kN/m^2$. The gravity load capacities are obtained using the modified nonlinear static curves, such that the reduced dynamic deflection is identical to the ductility supply. The CDR's predicted by the simplified TDA (maximum temperature of 750°C) are utilised to compare with those obtained by the TIA in order to verify the reliability of TIA robustness predictions. Table 5 provides the CDR's predicted by both TDA and TIA models.

Table 4. CDR's for reference car park using the TIA

Fire floor level	Gravity load capacity (kN/m^2)	Gravity load applied (kN/m^2)	CDR (Capacity / demand ratio)
1	6.23	5	1.246
5	5.96	5	1.192
8	4.86	5	0.972

Table 5. CDRs for structure under TIA and TDA

Fire floor level	CDR predicted by TDA (max. temperature 750°C)	CDR predicted by TIA	Discrepancy
1	1.400	1.246	11.0%
5	1.390	1.192	14.2%
8	1.134	0.972	14.3%

It can be seen that the CDR's predicted by the TIA are relatively conservative, and this can be attributed to two reasons. Firstly, the strain energy absorbed by the entire TIA system may be underestimated due to the idealisation of the degraded floor system, where the strain energy dissipated by the removed floor components (e.g. fire affected joint) is ignored. Secondly, more energy may be dissipated via compressive arching effects of the fire affected floor along with column buckling, which is underestimated by the ambient degraded floor system. Despite these inaccuracies, the discrepancies of CDR between the TDA and TIA predictions are within 15% on the conservative side, which is acceptable for design application.

III.2. 3D sophisticated model of a composite joint

In this section, advices are given to perform three-dimensional sophisticated models of composite beam-to-column bolted joints subject to variable bending moments and axial loads. The studied joint corresponds to the main beam-to-column joint internal column, for which the column is lost due to a localised fire. It is assumed that the loss of the column can be modelled by statically removing it, and that the column stays perfectly straight at the joint zone (no column rotation).

III.2.1. Elements modelling and contact interactions

In order to save computational time, the symmetry of the joint should be taken into account in the model; one fourth of the joint can be modelled. In that case, the displacements out of the plane of the column web and beam web have to be restrained, assuming no local buckling of the webs; this assumption can be made if evidenced before by experimental tests. If local buckling is considered, half of the joint (half of the column, one composite steel-concrete beam and one end-plate) should be modelled.

Three-dimensional solid elements should be used to model the main joint members. In order to simplify the model and save computational time, the upper and bottom parts of the steel column away from the joint zone should not be modelled; in case the upper part of the column needs to be modelled, computational time can be saved by modelling it using 3D beam elements.

In the FE programs that support 3D modelling, the entire joint can be modelled, included all the small details like the bolt washers or the bolt thread. Usually, bolt head or nut can be modelled by polygon shape, but when a washer is used, the corresponding bolt head or nut can be modelled circular (diameter of the washer), with the additional washer thickness. The bolt threads are not often modelled because of highly time consuming; so failures by stripping of the bolt threads or stripping of the nut threads are not taken into account; the diameter of the bolt can be modelled with a reduced diameter size d_s equivalent to the resistant section A_s. In order to simplify the model and avoid some numerical convergence problems, the clearance around the bolt shank does not need to be modelled and the hole diameter can be equal to the bolt diameter d_s; however, some information could be lost in case of high bolt diameter and consequently of high bolt clearance (the end-plate deformation could be influenced by this clearance).

The width of the concrete or composite steel-concrete slab to be modelled should correspond to the width that includes the steel rebars defined in the composite joint design. Modelling the composite slab as in reality, with the steel sheeting and the real shape of the ribs is possible, but this is really time consuming and not really necessary: if the ribs are perpendicular to the steel beam, only the slab height out of the ribs should be modelled, which include the steel rebars; if the ribs are parallel to the beam, the entire slab thickness should be considered. The steel rebars can be modelled by solid elements, but truss elements can be used to simplify the model.

The welds modelling between the beam and the end-plate are not necessary; in a bolted connection, these welds are designed in such a way that other components failure happen before; the steel beam can be fully connected to the end-plate, with all the degrees of freedom (displacements and rotations) of the beam side constrained to the end-plate ones.

Contact interactions have to be defined between the end-plate and the column flange surfaces, and between each bolt and the column flange and the end-plate surfaces: nut - column flange; bolt head - end-plate; bolt shank - column flange hole; bolt shank - end-plate hole. Contacts should be defined with: i) a normal behaviour defined as hard contact, and for which separation is allowed after contact; ii) a tangential behaviour with a friction coefficient of 0.25 or 0.3 (according to Dai et al., 2010, the effect of using a wide range of friction coefficients on the simulation results is very small). A contact surface is also defined between the concrete slab and the steel column using a normal contact, allowing separation after contact, and the tangential behaviour can be neglected to simplify the FEM simulation.

The interaction between steel beam and concrete slab can be defined, as a first approximation, by a full connection between the two members behaviour, by which all the displacements and rotations degrees of freedom between the slab bottom side and the steel beam top flange are constrained. However, as this full connection does not allow any sliding, once the frame starts deforming, unrealistic high tensile stresses could appear at the contact surface between the concrete slab and the steel beam, which difficult the convergence of the model. These tensile stresses should be avoided; in order to simulate the realistic sliding behaviour, the shear connectors should be modelled. Springs or solid elements can be used to model shear connectors. The advantage of the springs is the time computing saved, but local problems could be encountered with the concentrated stresses at the point where the spring is connected to the concrete. In order to model the normal and tangential behaviours, two springs should be defined (see the composite beam benchmark in Deliverables II, section IV). If shear connectors are modelled in 3D, the real shape of the composite slab with the ribs should be considered, and the computational cost increases much more.

Because the purpose of this study is the joint behaviour, no geometrical imperfections are introduced in the beam and in the column. If one half of the joint is modelled, the local deformations of the column and beam webs can be studied and initial imperfections should be defined. If additional initial imperfections can be measured on the joint before the FEM simulation, they should be reproduced.

In the steel part of the connection, the components that should suffer more deformations and/or failures should be meshed with a thinner mesh in order to well reproduce the behaviour and deformation. The concrete slab and the steel beam should be meshed with small elements at the contact zone with the steel column /end-plate, and coarser mesh along the beam. Bolts should be meshed with element size of around 4 mm, and at least three elements should be defined on the steel plate/column flange thickness in order to avoid hourglass deformations (which happen when reduced integration elements are used).

III.2.2. Material properties

Concrete properties can be defined by Eurocode 2, part 1.1 at ambient temperature, and part 1.2 at elevated temperatures. Structural steel properties at ambient and elevated temperatures are defined in Eurocode 3 part 1.1 and 1.2 respectively; the yield strength and the ultimate tensile strength of bolts are defined in Eurocode 3 part 1.8 (the curve is not defined), and the reduced capacities due to elevated temperatures are defined in Eurocode 3 part 1.2.

If tensile tests of structural steel coupons or bolts are performed at ambient and elevated temperatures, the real properties are known and standardized curves can be defined using the Menegotto-Pinto model for materials of sharp-knee type (Kato at al., 1990) or the Ramberg-Osgood model for materials of round-house type (de Martino et al., 1990).

In the FEM simulations, the nominal stress-strain values (σ_{nom},ε_{nom}) obtained from the standardized curves have to be converted to the true stress-strain measures (σ_{tru},ε_{tru}) for the definition of the uniaxial material response. These quantities are defined with respect to the current length and cross-sectional area of the coupon and are related to the engineering values by means of the following relationships (Malvern, 1969):

$$\sigma_{tru}=\sigma_{nom}(1+\varepsilon_{nom}) \qquad \text{and} \qquad \varepsilon_{tru}=\ln(1+\varepsilon_{nom}) \qquad (1)$$

III.2.3. Thermal and mechanical loadings

A general static analysis can be used, including nonlinear effects of large deformations and displacements; the loading increments size should be well adapted to the thermal and mechanical loading values, but also to the deformations. The static analysis algorithm is really difficult to solve once contact pairs are defined, and an easy way to pass through the first loading step is to pre-load the bolts at the beginning of the analysis; if no pre-loaded bolt is considered, the pre-load value can be quite small. In the static analysis, temperatures of the steel/concrete parts of the joint are directly applied. In case of a localised fire, the heat flux received by the members located at the ceiling level can be calculated by one of the simplified methods presented in Annex C of Eurocode 1 part 1.2: i) Heskestad method, when the flames are not impacting the ceiling, and ii) Hasemi method, when the flames are impacting the ceiling. In a usual open car park building, the height under beam is not very high, and the flames from burning car(s) use to impact the ceiling (Hasemi method). In this method, temperatures along the steel beam can be calculated (uniformed in the section) according to the fire scenario(s) and the rate of heat release of the fire, defined in Jaspart et al. (2008). At the joint, it could be assumed, as a rough approximation, that column, end-plate and bolts are at the same temperature than the steel beam, and the concrete or composite slab is not heated. A more detailed solution, but more time consuming, is to perform a heat transfer analysis in order to define the varying temperatures in the joint components: the air temperature at the joint zone can be calculated using the same Hasemi method, but with a fictitious steel profile with a really high section factor, so that it is heated at the same velocity than the air (Vila Real et al., 2011). Once the thermal analysis is performed, temperatures are used in the static analysis. Another easier way to define thermal loading is to use the ‘block’ temperature model directly applied in the static analysis (see the simplified Temperature-Dependent Approach in § III.1).

In order to increase the sagging bending moment (in case of the loss of the column), vertical displacements of the column base should be increased (displacement control of the column) in order to obtain the increase of the loads, but also the decrease of them once the joint begin to fail.

III.2.4. Boundary conditions

The vertical direction at the beam extremity should be restrained; the beam support can be modelled by a rigid cylinder in contact with the beam, and no friction is applied. The horizontal direction at the beam extremity is free, and the axial restraint to the beam coming from the unaffected part of the building should be modelled by a spring, elastic linear. This spring should be connected at the gravity centre of the composite beam section. The column vertical displacements of the bottom part can be restrained before the column loss, then the column loss is simulated by leaving free the vertical direction; the horizontal directions are restrained all along the column web (if one fourth of the model).

III.2.5. Failure criteria

Under sagging bending moment, the failure modes of the joint should be: i) the concrete crushing in compression; ii) the bolt fracture in tension of the bottom bolt row; iii) the plate in bending. If one half of the joint is modelled, local failures of the column and beam webs can be observed (if initial imperfections are modelled). It is assumed that bolt fracture, or steel cracking, occurs when the ultimate strain ε_u is attained, and concrete crushing is reached once the strain ε_{c1} at peak stress is attained. These values are the nominal values, dependent of the temperature.

IV. Practical design recommendations – Experimental approaches

Based on the feedback reached from the seven experimental tests performed within the present project, this section presents practical recommendations to perform experimental studies of composite beam-to-column joints subject to axial and bending loadings under elevated temperatures. The tested composite frame was subjected to mechanical (bending and axial forces) and thermal loadings (constant temperature equal to 20ºC, 500ºC or 700ºC; or linear increase up to 800ºC); the effect of the axial restraint to the beam was simulated. The two dimension sub-frame was extracted from an actual composite open car park building, keeping the real cross-section dimensions of the beams (IPE 550) and the columns (HEB 300), and using bolts M30, cl 10.9 in the composite connection.

IV.1. Sub-frame dimensions

Testing the real sub-frame in the laboratory, with wide cross-section dimensions, is rather complicated, even with a reduced beam length and column height: i) the equipment of the laboratory should be of large capacity for the measurements and loadings; ii) for the heating, higher furnaces and electrical power are required; iii) restraining the displacements of the sub-frame is complicated, especially under elevated temperatures (the column cannot rotate or the studied joint behaviour is affected); iv) the measured displacements are not so accurate because of the large distances and the difficulties to adjust the position of the point where the displacement is measured; v) difficulties are faced in the assembly and the alignment of the pieces in the plan because of the large weight and size; vi) the work is more dangerous than typical laboratory work because it is performed at high level above the ground; etc. This item presents some tips to reduce these problems: i) increasing the hydraulic jack stroke during the tests (see Deliverables II, section II); ii) using strain gauges to measure the elastic strain and convert it into stress, and then in axial load (in case of a steel profile uniformly in compression or in tension, and which stays in the elastic range of deformation; for example, the total axial restraint to the beam, see following § IV.4); iii) using electrical fire facility instead of furnace to heat the joint (see following § IV.2); iv) restraining the column rotation as far as possible from the rotation point (pin) to be more efficient; v) establishing safety measures for workers, notably the use of harness (in addition to the basic measures).

In the ROBUSTFIRE tests, large sub-frame was tested in a laboratory, no scaling was considered. These experiments allowed to test bolts M30 10.9, to observe new deformations of the steel end-plate between the bolts (the space between the two bolt rows 2 and 3 was 260 mm), and to define properties of such an internal beam-to-column joint under variable M-N-temperatures.

IV.2. Fire testing facilities

Several fire testing facilities are currently used for fire testing sub-frames, and vary according to the heat sources, or to the fact that facilities are opened or closed. Using furnaces (closed facilities) to test beam-to-column internal joint (one column and two beams) is really difficult because of the shape: i) the furnace should be customized on the sub-frame dimensions, ii) it should be able to displace with the joint (for example, downward when the column is lost), and iii) a solution to adapt the thermal isolation of the furnace when the rotation/deformation at the joint is increasing should be found in order to limit the thermal losses. In conclusion, open facilities are required to heat internal joints; they consist of ceramic heating elements or burners that surround the specimen to be heated; they have the advantage of being easily adapted to heating localised areas or long specimens, as well as beam-to-column joints with difficult shapes for which furnaces are not adapted. Individual gas burners can be suspended along the specimen to be heated; the heating rate simulates a natural fire, including the heating and the cooling phases (Santiago, 2008). However, this system is really dangerous, and requires much work to be calibrated. The electrical Flexible Ceramic Pad (FCP) heating elements allow the heating of a localised zone; gradient temperature is possible, although the heating rate is always linear, and ISO or parametrical fire curves cannot be simulated; natural cooling is not reproduced, neither flames similar to those observed in urban fires. These electrical elements are the correct solution to perform tests under constant temperatures; they are flexible and so adaptable to displacements and deformations of the sub-frame; they are protected by rock-wool.

IV.3. Mechanical loadings

Variable loadings are usually applied by hydraulic jacks, who have the ability to control the velocity of the loading, either by the displacement or by the force; however, if the loading leads to the failure of the sub-frame or joint, the displacement control is the more secure way. The loading velocity should not be too high in order to be able to measure well the displacements and deformations of the sub-frame, or to adapt other loadings as the spring axial restraints to the beams (see following § IV.4); however, the total duration of the test under elevated temperatures should also be limited as much as possible in order to limit the creep effects (Kodur et al., 2010). An (or several) "unloading-reloading" should be performed at the beginning of each mechanical loading (whereas the behaviour of the joint is still elastic) in order to better characterize the elastic stiffness of the joint, and to avoid clearances that could lead to wrong displacements measurement.

Constant loadings (under varying temperatures) could be applied by positioning concrete blocks or sandbags along the beams (well maintained at their places); another way is to use the hydraulic jack with force control.

IV.4. Axial restraint to the beam

The effect of the axial restraint to the beam coming from the unaffected part of the building can be taken into account. If total (infinite) axial restraint is desired, the extremity of the beam cannot move in the horizontal direction: the beam extremity should be linked (pinned) to a strong reaction wall. In that case, the axial loading is automatic as no manual external loading have to be applied. Some difficulties may come from the huge axial loads that these axial restraints induce: pins and load cells need to be designed to resist and to measure the reaction loads, respectively. Moreover, if the sub-frame is symmetrical, the axial restraints are applied at the two beams, and the double quantity of the material is necessary. A solution to avoid load cells is to use strain gauges to measure the elastic strain and convert it into stress, and then in axial load. The rotation of the restraint should be measured in order to define the axial load orientation.

If realistic axial restraint behaviour is required (spring restraint), they need to work under compression or tension loads: i) compression loads increase at the beginning of the heating due to the effect of the temperatures (beams expand), and ii) tensile membrane loads increase at the restraints due to the deformations of the sub-frame once the column is lost. Note that the spring restraint should be connected to the gravity centre of the composite beam section. Hydraulic system, with cylinders, can be used to simulate the spring stiffness: for each variation of the horizontal displacement measured at the beams extremities, the load applied by the spring restraint should be manually adapted; an automatic system would be very complicated to define: i) during the heating, sudden deformations could happen because of the beams expansion, which make difficult for the automatic control to adapt the loads, and ii) usually, the behaviour of a symmetric frame in the laboratory is not completely symmetric, and the two axial restraints to the beams should work separately. The real spring stiffness as in the actual building is difficult to simulate in the laboratory due to the limitations of the hydraulic circuit capacities, but also because no displacement of the specimen would be observed at the beams extremities as for the total (infinite) axial restraint (the flexibility of the joint would not be investigated); the axial stiffness value should be adapted to the sub-frame tested (to the dimensions, to the loading and to the expected deformations).

In the ROBUSTFIRE tests, the objective of the axial restraints to the beams was the simulation of axial loads in the joint and the study of the M-N behaviour of the heated joint. However, if the entire sub-frame behaviour is studied, rotational restraints should also be simulated at the beams extremities, as in the experimental test performed in Liège (Demonceau, 2008).

IV.5. Instrumentation

The main requirements of the instrumentation are to measure the temperature, the distribution of internal/reaction forces and the deflected shape of the floor and main structural elements. The instrumentation includes: i) thermocouples to measure steel and concrete temperatures, ii) displacement transducers or wire transducers to measure the displacements and deformations of the specimen and to check the residual displacements of the restraint auxiliary structures (such as footings, frames, etc…),

iii) load cells and pressure transducers to measure reaction loads and pressure in hydraulic cylinders, and iv) strain gauges to measure the elastic strains.

At the heated zone of the sub-frame, loads, displacements and strains cannot be directly measured because current loads cells, displacement transducers and strain gauges are limited to maximum temperature of 60ºC or80ºC; the instrumentation, and therefore the results, are limited to the temperatures. The choice of thermocouples should be done according to the test and the expected maximum temperature. The displacements in the heated zone cannot be directly measured, but a system with wire transducers could be used, using a protected thermocouple to extend the wire transducer inside the heated zone. However, when electrical FCP heating elements are used, the entire heated zone is covered by rock-wool, and it is not easy to let the wire through the thermal isolation. Standard steel strain gauges measure the elastic strains (up to 5%), but under elevated temperatures, they cannot be used. Some special strain gauges are able to measure the strains (up to 1%) at maximum 300ºC, or even 600ºC, but they are very expensive, and very limited. The load cells that measure the reaction loads should be located far from the heated zone in order to avoid any influence of the temperature, and all the reaction loads of the sub-frame should be measured.

Before the tests, preliminary numerical simulations should be performed to estimate the global behaviour of the sub-frames to be tested in the laboratory, and to define the required capacities of the thermocouples, load cells, displacement transducers and hydraulic jack.

IV.6. Control tests

Control tests are performed to define material properties of the steel joint components and concrete slab, in order to able the comparisons between the experimental results and the numerical and/or analytical results. The steel coupons are extracted from the *extra* length of the steel beam and the steel column, and from the *extra* steel plate from which the end-plate was cut. From the hot-rolled steel profiles, the coupons are cut in the longitudinal direction of the flanges (EN ISO 377:1997); web steel properties should also be defined because they could be different due to the reduced thickness. The real tensile behaviour of the bolts can be studied by tensile tests of the entire bolt, but testing bolts M30, cl. 10.9 requires a high capacity loading testing machine, as well as highly resistant grip pieces to connect the bolt to the machine. Nevertheless, the material properties can be acquired by tensile coupon tests. At elevated temperatures, steel properties can be defined by steady-state tests, or transient-state tests. Steady-state tests are usually performed; in these tests, the coupon is heated up to a specific temperature and then loaded to its limit states in tension, under constant displacement speed. These tests are easier than transient tests, but the testing speed should be well defined as it has a strong influence on the strength of steel. In transient-state tests, the load is maintained constant whereas the temperature increases at a given rate. These tests give more realistic results, closer to the Eurocode 3 part 1.2 values: in general, the ultimate strength obtained by a steady-state test is larger than the ones obtained by a transient-state test. However, according to Yang et al. (2006), the difference is smaller when the strain is larger than 1%, and can be ignored when strains corresponding to the ultimate strength of steel are larger than 5%. Usually, three tensile tests of steel web/flange/plate/bolt are performed at ambient temperature, and for each elevated temperature. Minimum three compression tests should be performed on concrete blocks after 7 days, 14 days, 28 days, and then the day of each test in order to confirm the concrete properties (NP EN 206-1 2007).

V. Practical design recommendations – Analytical approaches

V.1. Prediction of the M-N joint resistance at elevated temperatures

Within WP 2, an analytical procedure aiming at predicting the resistance M-N interaction curves of joints was developed and validated through comparisons to the experimental results obtained in Coimbra. The analytical procedure was presented as a contribution to WP 2 dealing with structural elements and, accordingly, is reported (with an example of application) in Deliverable III, Section II.

V.2. Global frame behaviour

The considered car-park structure is supposed to lose one column further to a localised fire. In these simplified analytical approaches, the affected column is supposed to be an internal one (the loss of a perimeter column is not studied herein). Moreover, the column is admitted to be completely and statically removed (no residual bearing capacity – no dynamic effects).

If the lost column is part of the structure upper storey, section V.2.2 of this document should be referred to. In the opposite case, the method suggested in section V.2.1 should be followed.

V.2.1. Internal column – upper storey excepted

V.2.1.1. Assumptions

In order to study the structural response of the frame when submitted to a column loss, an elementary substructure is isolated for sake of simplicity. First, the part made up of the 3D vertical slice above the lost column, called "directly affected part" is extracted. The rest of the structure is called "indirectly affected part".

When the column is removed, a beam plastic mechanism forms in the directly affected part and, due to the large displacements induced, tension loads develop in the beams of the directly affected part. These loads are applied to the indirectly affected part which provides a sort of lateral "support" to these tension forces. The stiffness of the indirectly affected part against these forces is very high thanks to the bracing systems in both planes and the slabs acting as diaphragms and ensuring the formation of a compression ring. The indirectly affected part can thus reasonably be assumed as fully restrained at its extremities when isolated (as far as the horizontal displacement is concerned) (Figure 17). In this approach, the directly affected part is studied as a mesh of composite beams: only a given effective width of slab is considered in both directions (collaborating with the steel profile) and the rest of the slab is neglected.

The beams of the directly affected part lower level are at elevated temperature because they are subjected to fire. Their stiffness is much decreased and thus much lower than the stiffness of the ambient temperature upper beams. Consequently, the contribution of the lower "hot" beams to sustain the column removal will be much smaller than the contribution of the other storeys. That is why the fire-affected level is neglected in the simplified approach: only the "cold" floors of the directly affected part are taken into account (Figure 17). As all these floors are the same and have the same infinite restraint at their extremities (fixed supports), they will all contribute identically to sustain the column loss.

Finally, an elementary substructure such as represented in 2D in Figure 17 is studied: it is made up of the beams of only one floor with the joints at their extremities (two double-beams perpendicular to each other define the 3D substructure). If the initial compression load in the column (before it fails) is N_0 the structure will be considered as robust if the above-defined 3D substructure is able to sustain a force $P = N_0/n_{cold}$, where n_{cold} is the number of cold floors in the directly affected part (i.e. the number of floors in the directly affected part minus one).

Besides, in the considered case, the partial-strength joints at the beam ends are such that their *M-N* resistance curve is entirely included within the beam *M-N* plastic resistance curve. So no yielding will appear in the beams and the joint resistance and deformability will be crucial.

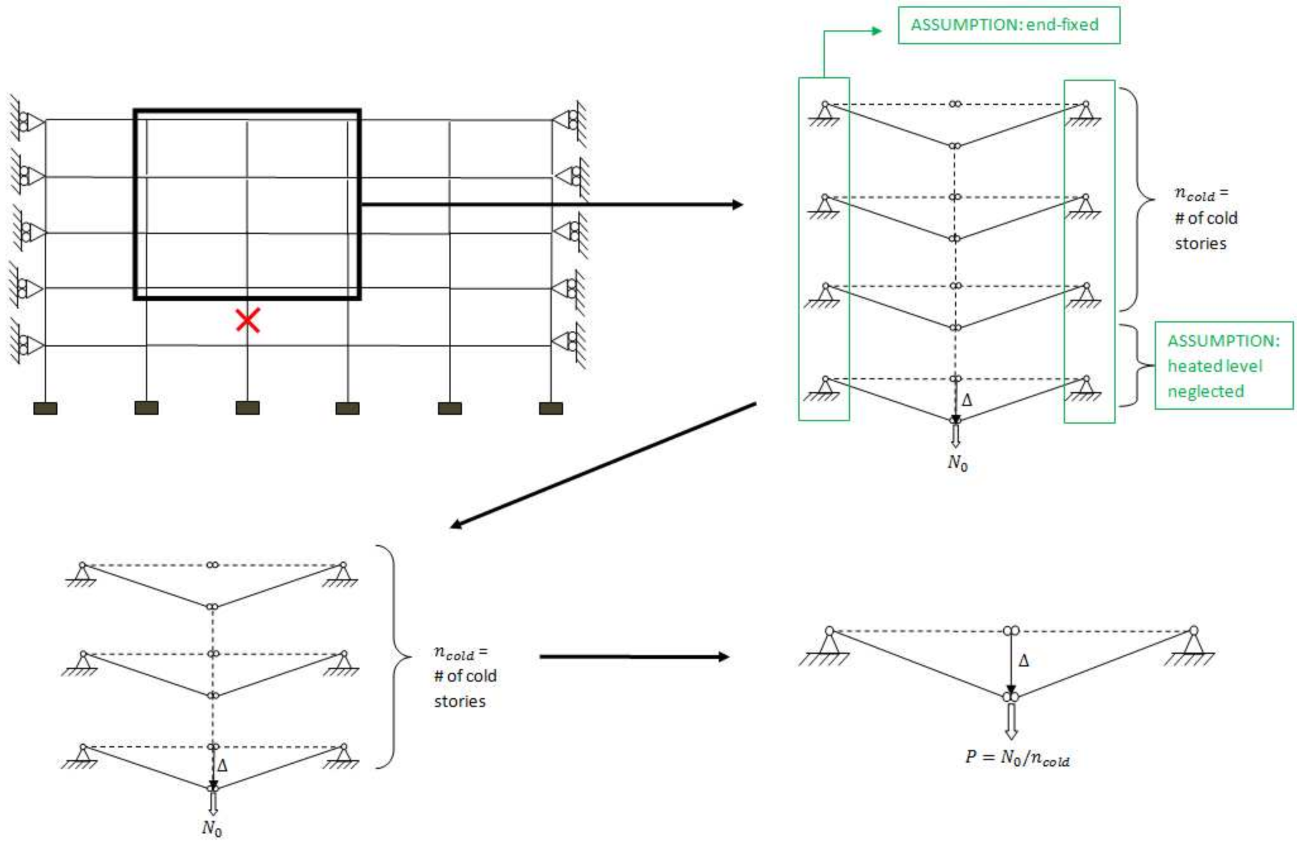

Figure 17. Simplifications for the case study

V.2.1.2. Input data

- n_{cold}, the number of cold stories above the lost column
- N_0, which is the compression in the lost column before it fails
- L_{0x} and L_{0y}, which are the initial lengths of the primary and secondary beams of the 3D-frame (x is for the primary frame, y for the secondary one)
- $M - N$ interaction laws, both in hogging and sagging, and for the two perpendicular directions.
  For the secondary frame, the joints are assumed to be hinges.
  For the primary frame, the joints are partial-strength joints so that their *M-N* resistance curve is entirely included within the beam *M-N* plastic resistance curve. So the $M - N$ interaction law to be considered is the joints one, not the beam cross section one.
  More information on how to analytically determine these M-N curves for the joints can be found in Deliverable III, Section II.
- $\delta_N - N$ laws, for both hinges in hogging and hinges in sagging, and for the two perpendicular directions.
  Indeed, neglecting the beam elastic elongation beside the yielded joint elongations, the lengths L_x and L_y, which are the lengths of the beams when submitted to membrane forces, may be expressed as follows:

$$L_x = L_{0x} + \delta_{Nx,SAG}(N_x) + \delta_{Nx,HOG}(N_x)$$
$$L_y = L_{0y} + \delta_{Ny,SAG}(N_y) + \delta_{Ny,HOG}(N_y)$$

  where the δ_N are the joint elongations in line with the beam axis under the given combination of forces *M*+*N*, with *M* linked to *N* via the plastic resistance law. Indeed, each joint is yielded and "moves" along its *M-N* resistance curve starting from *N*=0 and increasing progressively (in tension).

So this relation δ_N (*N*) for a joint needs to be determined. The procedure is still under investigation and it has appeared to be more complicated than initially thought. For this reason, it is not possible yet to provide an easy analytical method to determine such a δ_N (*N*) relation. These laws are for now assumed to be linear (as highlighted through numerical simulations), so that $K_N * \delta_N = N$. The development of an analytical procedure for the prediction of this law constitutes a perspective to the present project.

The numerical values for these K_N parameters are the following:

- For primary beams joints: $K_{Nx,HOG} = K_{Nx,SAG} = 20\,000$ kN/m
- For secondary beams joints: $K_{Ny,HOG} = K_{Ny,SAG} = 15\,000$ kN/m

V.2.1.3. Analytical models and solving procedure

For the substructure defined in V.2.1.1, several equations can be written (forces equilibrium, compatibility equations ...). This complete system of coupled equations can be found in Deliverable V, Annex C.

The input data's of this system of equations are the ones described in V.2.1.2.

The solving procedure is the following:

- choose a value of Δ (the vertical displacement at the top of the lost column (Figure 17))

- for this value of Δ, solve the system of equations described in Deliverable V, Annex C

- compare the obtained value of P with the value of N_0/n_{cold}:

  - if $P < N_0/n_{cold}$, try with a higher value of Δ
  - if $P > N_0/n_{cold}$, the value of the displacement corresponding to the column removal is smaller than the chosen Δ
  - if $P = N_0/n_{cold}$, the considered value of Δ is the one corresponding to the column loss

- when the chosen Δ is such that $P = N_0/n_{cold}$, check

  - ductility conditions: can the joints sustain the rotations?,...
  - resistance conditions: cant the joints (in primary and secondary frames) sustain the tensions forces N_x et N_y?,...

In the annexe of the present deliverable (X.2) is presented a Matlab-code that solves the system of equations described in Deliverable V, Annex C. This Matlab-code allows finding the curve $P - \Delta$ and the evolution of the tension forces N_x and N_y.

V.2.2. Internal column – upper storey

V.2.2.1. Assumptions

In this part, it will be assumed that a localised fire occurring near a supporting column just below a composite slab will lead to the inefficiency of the heated beams (primary and secondary) and to the inefficiency of the heated steel sheet of the composite slab.

Also, it is assumed that the unidirectional concrete ribs of the composite slabs are not significantly influencing the behaviour of the slab when significant membrane effects are developing i.e. it is assumed that only the upper part of the slab is contributing to the slab resistance.

Accordingly, the behaviour of the composite slab can be investigated through the study of a 3D uniform slab, uniformly loaded and submitted to the loss of one of its supporting column, assuming that this slab remains at ambient temperature. The objective is to investigate if the response of the slab further to its support loss can be predicted through analytical methods, taking the membrane effects into account.

V.2.2.2. Input data

The bold symbols in Table 6 are the input data of the analytical method.

Table 6. Input data's

Symbol	Units	Meaning
$\boldsymbol{a}$	m	Long span of the slab
$\boldsymbol{b}$	m	Short span of the slab
α	$-$	Aspect ratio $$\alpha = \frac{a}{b} > 1$$
η	$-$	Plastic mechanism parameter $$\eta = \frac{1}{2\alpha^2}\left(\sqrt{3\alpha^2+1}-1\right)$$
$\boldsymbol{d}$	m	Effective thickness of the slab
$\boldsymbol{A_s}$	m^2/m	Steel area per unit width of the slab $(A_{sx} = A_{sy} = A_s)$ Here, has described previously, $A_s = \frac{1000}{150}.\frac{\pi.10^2}{4} = 523.6\ mm^2/m$
$\boldsymbol{f_y}$	N/m^2	Yield strength of the reinforcement
$\boldsymbol{f_u}$	N/m^2	Ultimate strength of the reinforcement
T_y	N/m	$T_y = A_s * f_y$
T_u	N/m	$T_u = A_s * f_u$
$\boldsymbol{E_2}$	N/m^2	Hardening modulus of the reinforcement
$\boldsymbol{\sigma_b}$	N/m^2	Bond strength per unit width per unit length of slab
ε_u	$-$	Ultimate strain of the reinforcement $$\varepsilon_u = \frac{f_u - f_y}{E_2}$$
$\boldsymbol{f_c}$	N/m^2	Compression strength of the concrete

Slab plan dimensions (a, b)

A plan view of the car park defined in paragraph II.1 is represented in Figure 18.

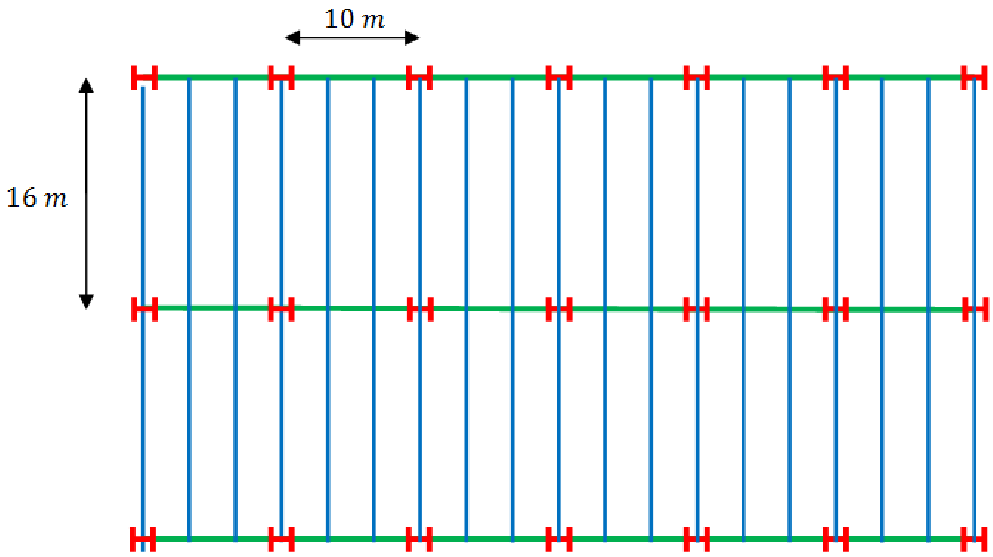

Figure 18. Plan view of the car park

From this figure, the dimensions of the slab panel to be considered can be deduced:

$$a = 2 * 16 = 32\ m$$

$$b = 2 * 10 = 20\ m$$

Slab cross section (d, A_s)

The slab cross section is given in Figure 19. As previously mentioned, the heated steel sheet of the composite slab can be neglected. Moreover, it has been shown (in Robustfire Report "Benchmark study for floor slabs") that the influence of the ribs on the slab membrane response was negligible, so the slab cross section can be simplified into a uniform thickness cross section (Figure 20).

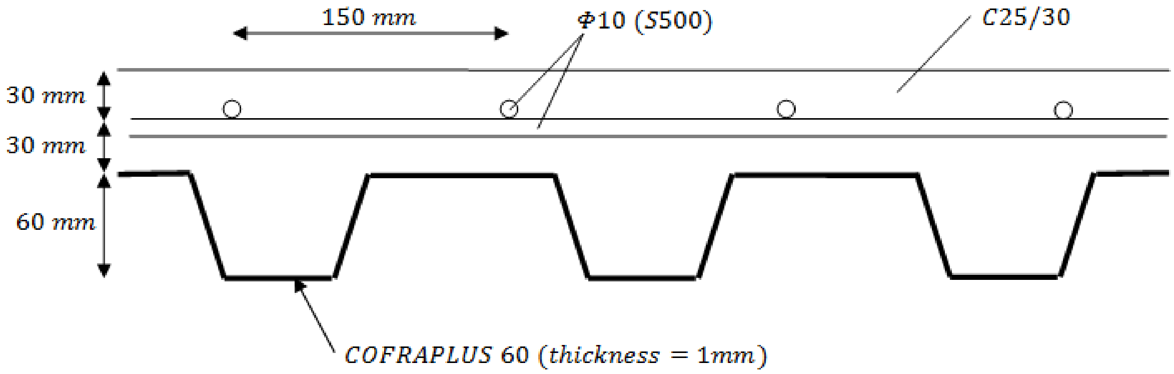

Figure 19. Real slab cross section

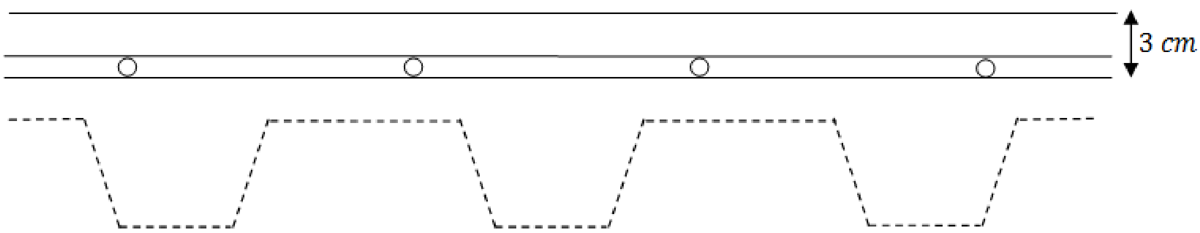

Figure 20. Simplified slab cross section

Material properties (f_y, f_u, E_2, σ_b, f_c)

Some of the slab constituent materials properties (f_y, f_c) are given in paragraph II.1 (or in Figure 19).

Some others (f_u, E_2, σ_b) can be found in the Eurocodes, and additional explanations about the latter can be found in Deliverable V, Annex A.

V.2.2.3.   Analytical models and solving procedure

The analytical models used to solve this problem can be found in Deliverable V Annex A. The solving procedure is the following:

- compute the limit vertical displacement in the centre of the slab $U_{c,limit}$ for which the slabs fails

- compute the value of the uniform load $q_{limit}$for which this maximal displacement $U_{c,limit}$ is reached

- compare this value of q_{limit} with the value of the uniformly distributed load acting on the slab q. If $q < q_{limit}$ than the slab can sustain the loss of the column. If $q > q_{limit}$, than the slab has to be improved to reach $q = q_{limit}$.

VI. Critical appraisal from the “practice-oriented” partners

Most of the presented design recommendations result in the proposal of design procedures of different natures (numerical, experimental or analytical), for different part of the structure (structural members, joints or the structure as a all) and with different level of sophistications.

The most practical ones are for sure the simplified analytical approaches as the latter may be applied using tools available in any design offices. It is the reason why the “practice-oriented” partners have mainly focused their work on the applicability of the approach allowing predicting the global frame response, in particular by applying the latter to the reference building as presented in § VIII.

This approach is funded on two main assumptions:

- the development of membrane forces in the slab is neglected for a column loss which does not occur at the top level;
- the fire effects are not explicitly taken into account (indeed, the elements directly affected by the fire are neglected).

The assumptions on which the simplified analytical model for robustness check is based lead to a safe prediction of the structural response for the considered scenario, i.e. the loss of a column further to a localised fire. The conservative character of the procedure can obviously be seen as a source of inefficiency, as soon as the economy of the project is concerned. In reality, it is presently “the price to pay” to keep “easy-to-apply” analytical procedures. The designer who would like to predict more “accurately” the response of the structures would have then to use the more “sophisticated” numerical approaches (§ VII).

VII. “Sophisticated” FEM approaches – Application of the Robustfire methodology to the reference building

The applicability of the “sophisticated” FEM approaches (developed within WP3) to the reference building have been investigated but these investigations have already been reported as demonstrative example in WP 3, and are detailed in Deliverable V, Section III. Accordingly, this contribution will not be repeated herein.

VIII. Analytical approaches – Application of the design recommendations to the reference building

VIII.1. Methodology aspects

Basically, two levels of analysis can be applied. One is called “complex model”, based on FEM analysis, with several levels of refinement. The other is called “simplified method” and relies on analytical analysis. The details for this model are given in the present document, in § III.1. Following paragraphs illustrate an application on the basis of simple approach which is considered to be more practical for ordinary design engineers.

Directly impacted zone and indirectly impacted zones are analysed separately. This approach uses a simple grillage model for the directly impacted zone, the surrounding elements at ambient temperature are considered as boundary condition (supports) of the grillage. Like in the complex model, it is necessary to calculate properties of the springs that represent the indirectly impacted zone.

In theory, the impacted zone can be studied with analytical formulas. Two levels of refinement are proposed:

1. To consider the remaining load bearing capacity of elements exposed to fire, by reducing their capacity according to their level of heating. It requires assessing properly the behaviour of joints in high temperatures conditions.
2. To simply ignore the elements exposed to fire, considering that they failed. This leads to temperature independent analyses.

The following illustrates the application of simplified method for the case study. This method could be applied without difficulties by common design offices.

VIII.2. Substructure

As models for the distribution of temperature in joints are not yet available, a 3D model where a column and the heated beams and floor are removed is studied, according to Deliverable V, Annex C (and according to the internal report “Simplified approach”). This temperature independent analysis is supposed to be solved mainly analytically, with the help of simple simulations to determine rigidity.

Main steps are:

1. extract sub structure (beams) and calculate tension force due to the loss of the down column,
2. indirectly affected zone supposed infinitely stiff due to the ring of compression,
3. define the join MN curves,
4. calculate the structural response of the affected part, modeled with beams and springs and verify the joint capacity.

Due to the fact that in the transverse direction, the structures have only two bays, it seems that the anchorage of the sub structure in the indirectly affected part is only efficient in the longitudinal direction. In the transverse direction, anchorage is neglected. It comes that 2D model could be a satisfactory modelling (see Figure 21). More precise approach requires more insight in the membrane effect of the slab, which probably contributes to stiffness of supports of the substructure in the transverse direction.

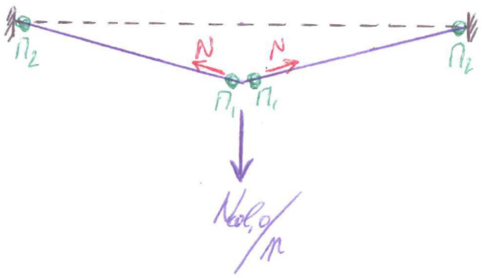

Figure 21. Elementary substructure – 2D view

VIII.3. Application of the models

VIII.3.1. Verification of Robustness – Loss of a column other than a column at the top floor

In this section we have considered that the fire takes place in ground floor and for this reason this floor is not taken into account. We have verified the robustness of the non-affected structure by the fire.

For a vertical displacement *u* (see Figure 22) in the head of a column, at the connection level, the rotation could be expressed in function of this displacement as follow:

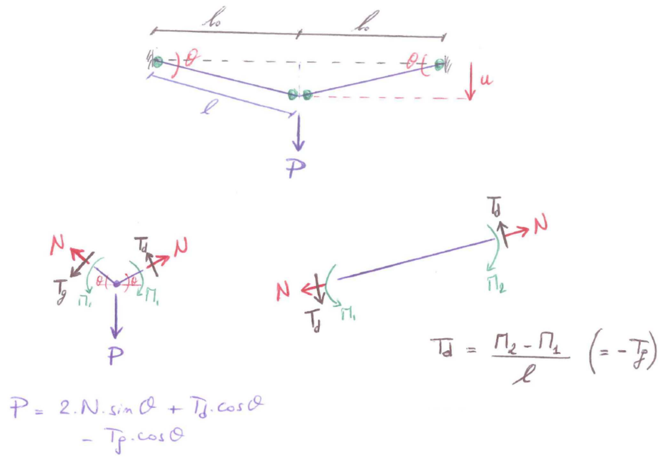

Figure 22. Deformed structure.

$$\theta_x = \arctan\left(\frac{u}{l_{0,x}}\right) \quad (2.3.1) \qquad \text{and} \qquad \theta_y = \arctan\left(\frac{u}{l_{0,y}}\right) \quad (2.3.2)$$

$$l_x \cdot \cos\theta_x = l_{0,x} \quad (2.3.3) \qquad \text{and} \qquad l_y \cdot \cos\theta_y = l_{0,y} \quad (2.3.4)$$

$$l_x = l_{0,x} + \delta_{Nx,1}\left(N_x\right) + \delta_{Nx,2}\left(N_x\right) \quad (2.3.5) \qquad \text{and} \qquad l_y = l_{0,y} + \delta_{Ny,1}\left(N_y\right) + \delta_{Ny,2}\left(N_y\right) \quad (2.3.6)$$

The equilibrium equation in head connection point (in 3D) leads to the following relation:

$$P = 2 \cdot N_x \cdot \sin\theta_x + 2 \cdot \frac{M_{x,2} - M_{x,1}}{l_x} \cdot \cos\theta_x + 2 \cdot N_y \cdot \sin\theta_y + 2 \cdot \frac{M_{y,2} - M_{y,1}}{l_y} \cdot \cos\theta_y \qquad (2.3.7)$$

In this last relation the indices *x* and *y* refer to the two main vertical planes of the structure.

VIII.3.1.1. Data for case study

For our case study the following parameters are known:

- $l_{o,x1} = l_{o,x2} = l_{0,x}$ = 10 m and $l_{o,y1} = l_{o,y2} = l_{0,y}$ = 16 m,
- Principal beam is IPE 550 with a steel grade of S355,
- Secondary beam is IPE 450 with a steel grade of S355,

- Column HEB 550, HEB 400, HEB 300 and HEB 220 with a steel grade of S460 (see Annex A of this document (X.1) for more details).

The sizes and the properties of bolts and end plates are designed by GREISCH in pre-dimensioning of the reference's car park report. The entire design of the reference's car park can be found in the present Deliverable VI, in Annex A, §X.1.

Furthermore it is necessary to know the following parameters:

- N_x, N_y, M_x and M_y are defined by MN diagrams,
- For primary beams joints: $K_{Nx,1} = K_{Nx,2} = 20000$ kN/m,
- For secondary beams joints: $K_{Ny,1} = K_{Ny,2} = 15000$ kN/m,

The $N - \delta_N$ laws cannot be, at this stage of the developments, determined analytically. They are assumed to be linear (as highlighted through numerical simulations), so that $K_N * \delta_N = N$. The development of an analytical procedure for the prediction of this law constitutes a perspective to the present project. The values of K_N given here above are realistic values of the parameters, taken form (Demonceau, 2008).

As stated above, it is considered that the fire takes place in ground floor and for this reason this floor directly affected by fire (first level) is not taken into account. The check of the robustness considers only the non-affected structure by the fire that is from second floor to eighth floor.

VIII.3.1.2. MN diagrams for studied car park

The MN diagrams of main beam joints are defined according to the method explained in the internal report "Simplified approach" (and in Deliverable V, Annex C). The figures 2.3 to 2.6 give the resultant MN diagram of 4 main beam-to-column joints of studied structure.

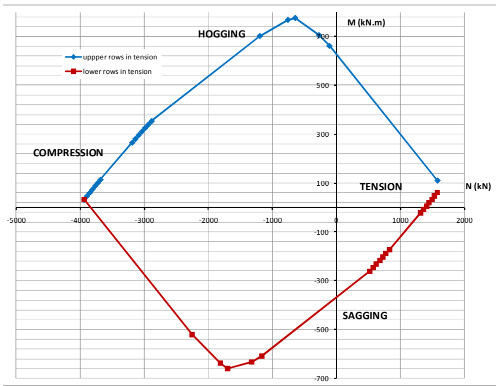

Figure 23. MN diagram for HEB500 column.

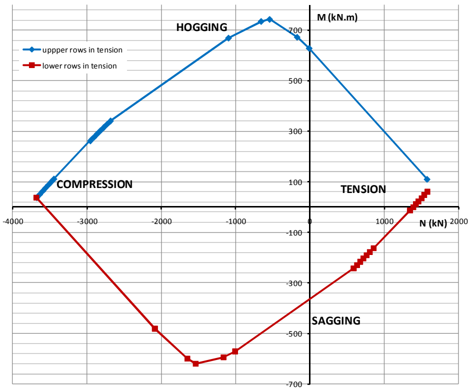

Figure 24. MN diagram for HEB400 column.

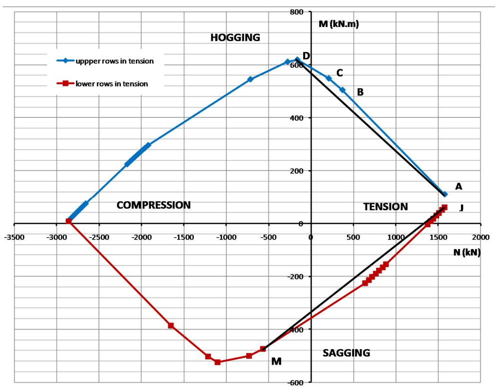

Figure 25. MN diagram for HEB300 column

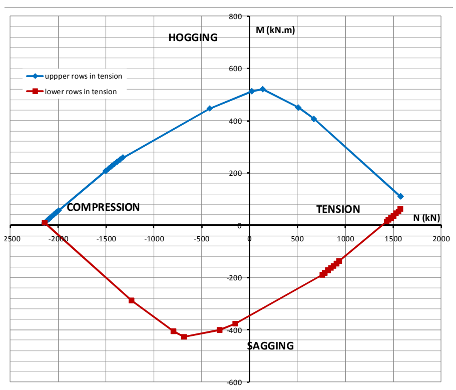

Figure 26. MN diagram for HEB220 column.

These diagrams allows to know that the maximum tensile resistance of all main beam joints for the studied case is $N_{x,max}$ =1577 kN.

With respect to secondary beam to column joints, as they are designed as pined ones, they will not have any moment resistance. But the maximum tensile resistance of these joints is limited to 468 kN.

VIII.3.1.3. Determination of maximal vertical displacement of connection point of each floor

In the case where $l_{o,x1}$=$l_{o,x2}$ $= l_{o,x}$ and $l_{o,y1}$=$l_{o,y2}$ $= l_{o,y}$ the equation 2.3.5 and 2.3.6 could be written as:

$l_x = l_{o,x} + 2 \quad \delta_{Nx} = l_{o,x} + 2 \quad \dfrac{N_x}{K_{Nx}}$ and $\qquad l_y = l_{o,y} + 2 \quad \delta_{Ny} = l_{o,y} + 2 \quad \dfrac{N_y}{K_{Ny}}$.

Using these two last equations and the equations 2.3.1 to 2.3.4, the maximal vertical displacement of the connection point (column point) could be defined in function of $N_{y,max}$ =468 kN, $N_{x,max}$ =1577 kN, K_{Nx}= 20000 kN/m and K_{Ny}=15000 kN/m given previously.

The maximum vertical displacement will be limited by the tensile force developed in two perpendicular beam to column joints (main and secondary beams respectively), which cannot exceed the maximum tensile resistance of these joints.

VIII.3.1.4. Determination of bearing capacity of the connection of each level and robustness verification

The applied load taken into account for the design of the car park structure is defined by following relation: $A = G + 0.7 * 0.8 * Q$. The two coefficients affecting the term Qcorrespond to the coefficient Ψ_2 (EN1990, Annex A1) coming from the accidental combination load case, and to a coefficient α_n (EN 1991-1-1, §6.3.1.2 (11)), which is a reduction factor for a column supporting a large surface.

G: takes into account the dead load of concrete slab (2145 N/m^2) and steel structure (400 N/m^2) and Q=2500 N/m^2.

The bearing capacity of all steel beams connected to lost column can be obtained using the formula 2.3.7. In this formula: if the vertical displacement at column point is defined, N_x, l_x, l_y, θ_x, θ_y are known and, M_y equals to zero because the secondary beams are supposed to have hinged connection. Concerning $M_{x,1}$ and $M_{x,2}$, it is necessary to define them. In order to simplify the calculation, it is suggested to use the linear relations derived from accurate MN diagram (see Figure 25) in order to get their values directly.

If one observes the four MN diagrams given in figures from Figure 23 to Figure 26, it can be easily concluded that MN curves are nearly linear. Consequently it is proposed to consider that from the point A to C or from the point J to M the MN curves are perfectly straight.

In fact, for robustness calculations, only the points located at the tension side will be used. In consequence, the second point over the MN curves in our case for the hogging moment could be B, C or D. The result will be more precise if the accurate values based on all points between lines AB (C.) and JM are used. However, the advantage of actual approach resides on its efficiency.

With this assumption, it is possible to define the $M_{x,1}$ (sagging moment) and $M_{x,2}$ (hogging moment) with the following relations:

$$M_{x,1} = (\frac{M_J - M_M}{N_J - N_M}).(N_x - N_M) + M_M \quad \text{and} \qquad M_{x,2} = (\frac{M_A - M_D}{N_A - N_D}).(N_x - N_D) + M_D$$

Finlay, the bearing capacity is defined by the simplified relation:

$$P = 2 \cdot N_x \cdot \sin\theta_x + 2 \cdot \frac{M_{x,2} - M_{x,1}}{l_x} \cdot \cos\theta_x + 2 \cdot N_y \cdot \sin\theta_y$$

For all levels over the whole height of the structure with four different column sections, the MN diagrams are given respectively in figures from Figure 23 to Figure 26, the maximum load-bearing capacities obtained from above calculation procedure are:

- floor with column in HEB550: P = 469.8 kN,
- floor with column in HEB400: P = 469.7 kN,
- floor with column in HEB300: P = 462.9 kN,
- floor with column in HEB220: P = 456.0 kN,

The total applied load to the bottom of the column of the structure is:

$P_{applied}$(tot)=619.2 x 8=4953.6 kN.

The total bearing capacity of the structure once the column fails at ground level is:

P_{res}(tot)= 469.8+469.7x2+462.9x2+456x2=3247 kN

$P_{res}/P_{applied}$=0.655

Consequently it is necessary to modify the connection parameters proposed by the pre-dimensioning report of the car park structure.

VIII.3.2. Verification of robustness – Loss of a column at the top floor

As explained in simplified approach report provided by this project, in case of a fire in the upper storey, the column of this storey fails. The robustness of the top floor has to be provided by the rectangular slab given in Figure 27.

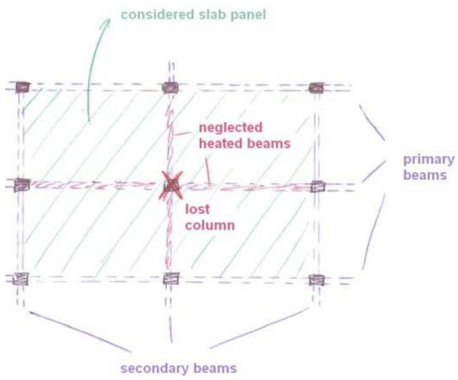

Figure 27. Slab considered for robustness of th top floor.

The mechancial load taken into account is calculated as shown in §VIII.3.1.4. The robustness of this floor is ensured if following two criteria (defined in Deliverable V, Annex A) are met:

- 1st or CM criterion: not full depth crack in the centre of the slab,
- 2nd or IM criterion: not full depth crack at the intersections of diagonal yield-lines.

For CM and IM criteria the failure happens when the reinforcement crossing the cracks reaches its ultimate strength f_u . At this moment the deflection at failure is U_{fc} .

In order to have a robust floor, its load bearing capacity must to be higher than applied load. This point is defined by the interaction point of the limit deflection line and the bearing capacity curve (see Figure 28 and Figure 29).

For the car park structure dealt with in this study, the basic mesh of the top slab is:

- reinforcement spacing 200 mm,
- reinforcement diameter 8 mm

With these dimensions, none of the two criteria given above is met. In order to satisfy these criteria, the following mesh must be employed:

- reinforcement spacing 100 mm,
- reinforcement diameter 15 mm (this values is used just as an example for the optimization of CM and IM criteria).

Figure 28 and Figure 29 represent the results for the CM and IM criterion.

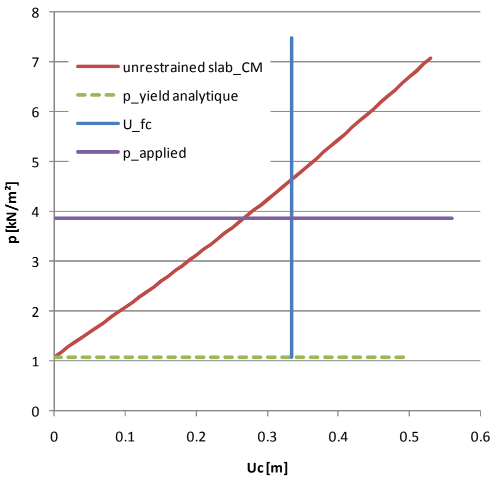

Figure 28. Result of CM criterion for a reinforcement mesh Ø15 by 100.

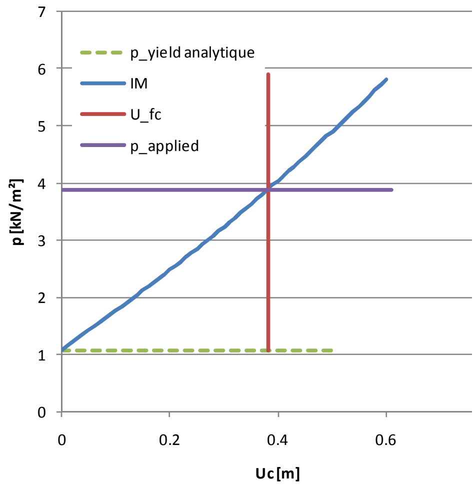

Figure 29. Result of IM criterion for a reinforcement mesh Ø15 by 100

VIII.4. Conclusions

The proposed design procedures have been applied to the "actual" reference building.

It has been demonstrated within the present Section that the simplified analytical approach can be easily applied to the reference building. Only one parameter, the axial stiffness of a yielded joint, cannot yet be computed through an analytical procedure, what constitutes a perspective of development for the future (investigations already in progress).

Through the application of the simplified analytical approach, it is demonstrated that the robustness of the reference building is not sufficient for the considered scenarios. Accordingly, the designer would have to select one of the following possibilities: (i) improvement of the resistance of the joints (in bending and/or under axial loads) and of the slab at the top level or (ii) to use a more sophisticated approach using FEM, to take into account, for instance, the membrane effects developing in the slabs (effects neglected within the analytical approach).

IX. Conclusions

The possible progressive collapse of steel-concrete composite car parks under a localised fire resulting from the burning of cars is one of the key aspects to deal with nowadays. The absence of appropriate reply to this request is likely to limit the market for such very well appreciated structural solutions.

The project so aimed to investigate these aspects and derive design procedures and recommendations for the mitigation of the risk of progressive collapse.

The problem is rather complex as it implies to address the numerous following aspects:

- The scenarios to be considered (one car, more cars, located where, …)
- The distribution of temperatures in the air and the evaluation of the temperatures in the affected columns and the surrounding beams, slab and connections.
- The reduction of bearing resistance of the column.
- The local response of the beams, slab and joints when the bearing resistance of the column decreases and the progressive development of membrane forces in the floors.
- The global stability of the whole frame further to a local destruction of a part of the structure.

In order to achieve the goals of the project and to structure the work amongst the partnership, the following strategy has been set up further to an initial state-of-the art of the available knowledge:

- Derivation of all structural requirements for car park structures (dimensions, layout, loads, fabrication/construction/ erection constraints, realistic fire scenarios, …)

- Design of a reference structure under normal loading and in accordance with Eurocodes.
- Evaluation of the distribution of temperatures in the structure and in the constitutive structural elements during the exceptional event.
- Individual study of the main structural elements at room and elevated temperatures (columns, beams, connections, floor) through experimental and/or numerical investigations.
- Derivation of analytical approaches for the prediction of the individual response of the above-mentioned structural elements.
- Development of various numerical procedures for the evaluation of the stability and the resistance of the structure further to the event (sophisticated models with different levels of sophistication).
- Derivation of a simplified event-independent and Eurocode compatible approach for the evaluation of the robustness of the structure (simplified model).
- Application of the simplified model to the reference structure by the "practice-oriented" partners and feed back to the "scientific partners".
- Drafting of design guidelines.

Within the present deliverable, the developed design recommendations and their critical appraisal were presented. In particular, the proposed recommendations were applied to the designed reference car park.

The main conclusion of the presented developments is certainly the fact that the simplified model is based on series of assumptions which allows, at the end, and at it was requested by the contract, to check the robustness of the car park through a "scenario-independent" approach, but with a non-excessive but actual level of conservatism that could be criticised. In fact, this conservatism has to be seen as the "price-to-pay" to limit the investment of a design office in terms of calculation costs.

Should the conservative character of the simplified model be considered as excessive, then more sophisticated models as presented in the present deliverable should be preferred. In the project, much information is made available to practitioners who would prefer to follow a numerical approach: choice of the model, distribution of temperatures, substructure to be studied, loads and boundary conditions to apply.

X. Annexes

X.1. Annex A: Design of a reference structure

Table of contents

I. Introduction

In order to lead tests and studies of this research on the basis of a common structure used in our countries, a standard structure of an open car-park has been designed. This structure will be called in all the documents "the reference structure".

The geometry of the designed car-park must be the most general possible in order to cover the greatest number of existing structures. After discussion with the partners of research, the structure selected is described on Figure 1. Except for the columns, whole the elements have a composite resistance. Thus, the slab is composite and the beams are connected to this one, but are not coated with concrete. The metal beams will be sections I of nuance of S355 steel, while the metal columns will be sections H of nuance of S460 steel in order to reduce their obstruction. It is thus about a car-park having internal columns laid out every 10 m, the beams have a range of 16 m and are spaced of 3,333 m which is the range of the slab.

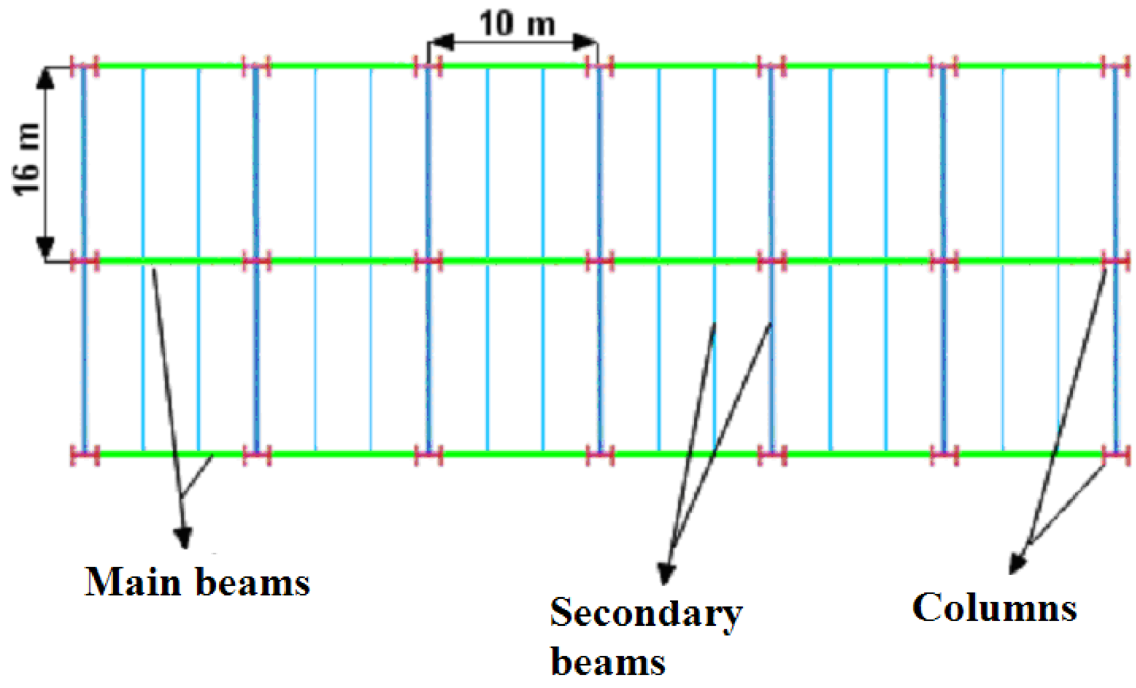

Figure 1 : structure description (plan view)

The height of the stages is fixed at 3 m, which makes a total height of the building equal to 24 m. Moreover, no roof is envisaged on the last stage, this one also being used as level of parking and the selected metal sections will be the same ones on the whole of the structure.

All plans of this reference structure can be found in the "Annex 1 : Reference structure plans" hereafter and are organised as follow:

- CH01 = Plan view
- CH02 = Slab reinforcement
- CH11 = Longitudinal section
- CH21 = Transverse section
- CH51 = Assembling detail

The structure will be braced, wind-bracing being carried out using the ramps approach built out of concrete laid out on each side of the building and fixed at the small frontages. These slopes as well will allow a blocking of horizontal displacements in the longitudinal direction as transverse the building, thanks to the diaphragm effect of the slab which will transmit the horizontal efforts of the frontages towards the components of stability. This aspect is essential in the concept of the stability of the building because it will enable us to consider that the whole of the building is with fixed nodes.

The bending moments in the columns due to side displacements can thus be neglected and the columns can only become deformed between floors. Thus, we can model the structure in the following way:

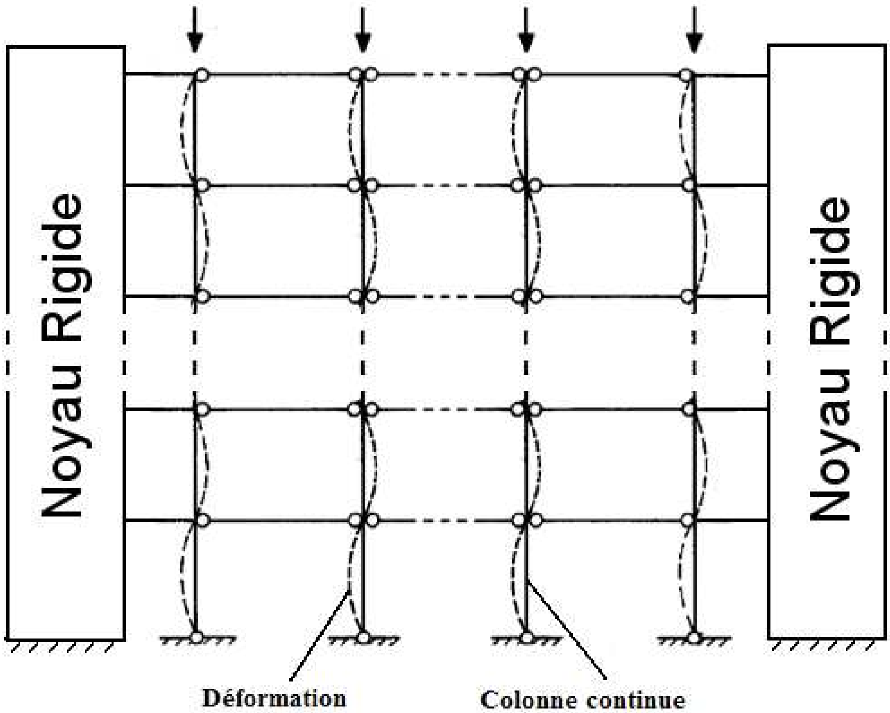

Figure 2 : Longitudinal bracing of the structure thanks to the ramps approach (Elevation of the building)

II. Loadings

Self weight of the structure [$\gamma_{ELU} = 1 \,;\, 1.35$] :

Composite slab (see annex 1)……………………………………………..214.5 kg/m²

Secondary beams (IPE 450)…………………………………………………77.5 kg/m

Main beams (IPE 550)……………………………………………………..105.0 kg/m

Column (HEB 220 to HEB 550 – see Figure 3)………………..…….71.5 kg/m to 199 kg/m

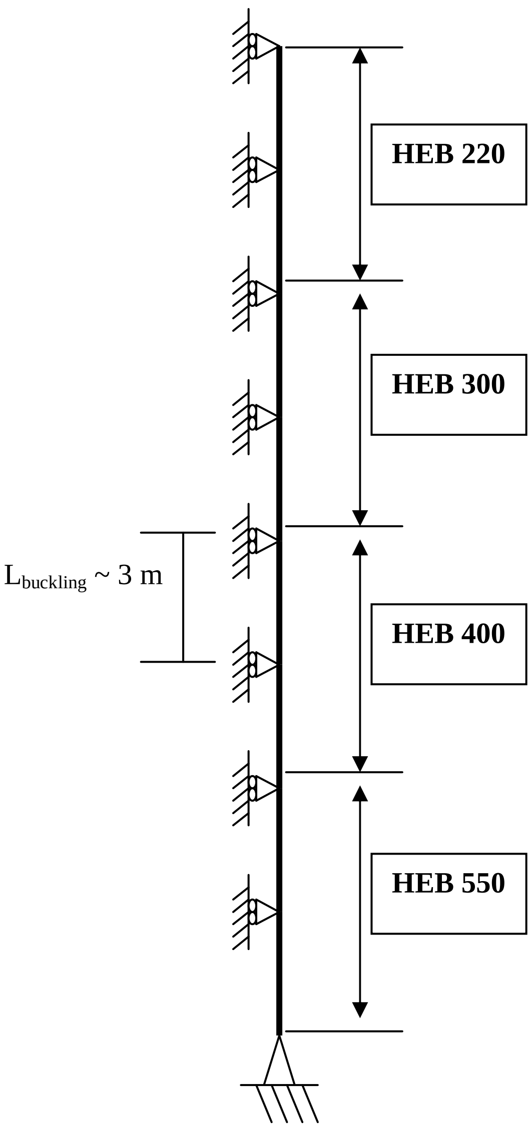

Figure 3 : Column description

Variable load [$\gamma_{ELU} = 0 \,;\, 1.5$] :

Vehicles load, etc……………………………………………………………250 kg/m²

III. Material properties

Concrete [γ_{ELU} = 1.5] : C25/30 → f_{ck} = 25 Mpa, E = 31476 Mpa

Steel [γ_{ELU} = 1.0]

- Hollow rib : S350 → $f_{y,hr}$ = 350 Mpa, E = 210000 Mpa
- Secondary and main beams :S355 → $f_{y,s1}$ = 355 Mpa, E = 210000 Mpa
- Column : S460 → $f_{y,s2}$ = 460 Mpa, E = 210000 Mpa

Rebars [γ_{ELU} = 1.15] : S500 → $f_{y,r}$ = 500 Mpa, E = 200000 Mpa

IV. Composite slab dimensionning

The composite slab is of type COFRAPLUS 60, made up of a ribbed metal sheet of 1 mm of thickness which represents the lower reinforcement in the longitudinal direction of the slab, but also the formwork of this one during the casting of the concrete; this sheet thus has a double function. The thickness of this slab is of 120 mm which is relatively weak. The choice of the thickness of the sheet was limited primarily by its deflection during the construction phase.

The analysis of the slab will be made on a segment of 1 m depth and 3.333 m span.

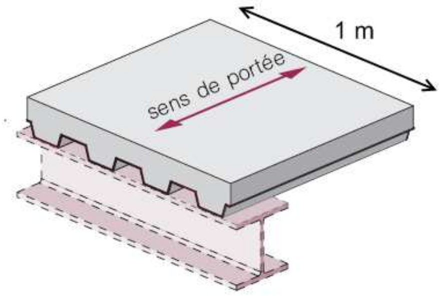

Figure 4 : composite slab

During the construction phase and the service state, the sheet and the composite slab will be verified for the ULS and SLS.

IV.1. Properties of the hollow rib slab

The ribbed metal sheet of type Cofraplus 60 is a ribbed profile notched laterally, intended for the construction of concrete slabs, it avoids the dismantling of the formwork, reduces the floor weigth and saves a line of reinforcement.

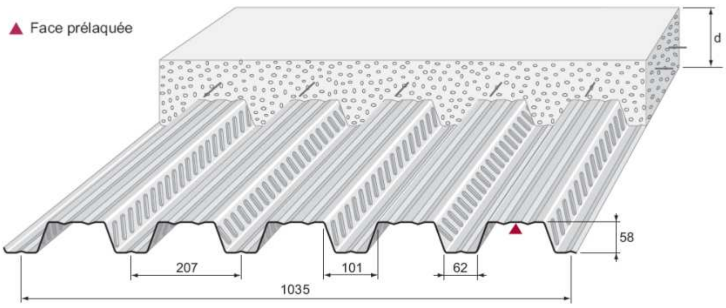

Figure 5 : COFRAPLUS 60

The self weight of the metal sheet and the concrete weight have to be taken into account.

Metal sheet weight (gp)	0.1137 kN/m²
Concrete weight (gb)	2.03 kN/m²

IV.2. Construction phase : Dimensioning of the metal sheet

During the construction phase, only the metal sheet will undertake the loads applied. Thus, in the majority of the cases, it is this situation which will be most constraining for this one.

To facilitate the setting in of sheets and the casting of the concrete above, it is advised to take sheets of the greatest possible number of spans. This will also reduce the deflection thanks to the hyperstaticity. We will take sheets consequently having a length of 3 spans (10 m) in order to symmetrically distribute them on the whole of the floors. For recall, no stirrups will be used during the construction phase.

Moreover, we will check the pounding effect, the bending and shear resistance of sheet as well as the deflection obtained.

IV.2.1. Pounding effect

The pounding effect is characteristic of the composite constructions. This effect leads to take into account an accumulation of the freshly-mixed concrete in the middle of the span, due to a relatively important deflection of sheets under self-weights.

Thus, a concrete overload must be taken into account when the deflection under self-weights of the sheet and the concrete exceeds 1/10 the total height of the slab.

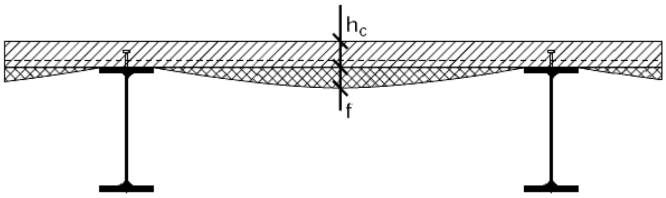

Figure 6 : Effet de mare

The maximal deflection on three uniformly loaded spans is :

$$\delta \text{ max} = 6{,}8\ 10^{-3}.ql^4/EI = 0{,}0115 \text{ m} < h/10 = 0{,}012 \text{ m}$$

No pounding effect has to be taken into account. This conclusion will also be valid for the dimensioning of the main and secondary beams if an initial deflection is given to these beams.

IV.2.2. ELU verification of the hollow rib

The variable load during construction must be applied where it has the most unfavourable effects. The same has to be done with the self weight of concrete, indeed although it constitutes a permanent load, during its casting this one can have a variable distribution on the floor. The sheet is regarded as being continuous on 3 spans.

The bending moments are :

$$M_{Ed,max} \text{ - span} = 4{,}43 \text{ kNm}$$

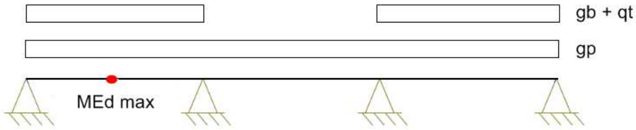

Figure 7 : Load case for the span bending moment

$$M_{Ed,min} \text{ - support} = -5{,}18 \text{ kNm}$$

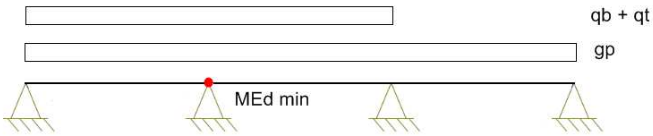

Figure 8 : Load case for the support bending moment

The resistant bending moment of the metal sheet is calculated following the class 4 section of eurocode 3, this is thus the effective bending inertia that is applied.

$$M_{c,Rd} = \frac{W_{eff,min} f_y}{\gamma_{M0}}$$

$M_{c,Rd} = 6{,}85$ kNm > $M_{Ed,min}$

The shear on the support is equal to :

$V_{Ed,max} = 8$ kN

The resistant shear is calculated considering that only the web of the metal sheet is operating :

$$V_{pl,Rd} = \frac{A_v\left(\frac{f_y}{\sqrt{3}}\right)}{\gamma_{M0}}$$

$V_{pl,Rd} = 94$ kN > $V_{Ed,max}$

IV.2.3. ELS verification of the hollow rib

Among characteristics provided by the manufacturer, a maximum deflection of sheets under self-weight of the concrete during the casting exist. Moreover, this one is limited to L/240

δ max = 11,5 mm < L/240 = 14 mm

IV.3. Service phase : Dimensioning of the slab

IV.3.1. ELU verification of the composite slab

To avoid a too great number of rebars in the composite slab, it is allowed by the Eurocode (see 9.4.2(5) of EN 1994-1-1) to calculate a continuous slab as an isostatic one. The only condition is that a minimum rebars section has to be placed in the slab.

The maximum bending moment in sagging is thus equal to :

$M_{Ed,max} = 9.5$ kNm / m

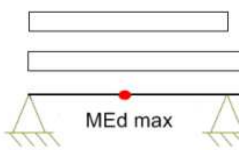

Figure 9. Loading and maximum bending moment for the slab

The plastic sagging resistant bending moment of the composite slab is calculated using the plastic distribution of stresses shown hereafter:

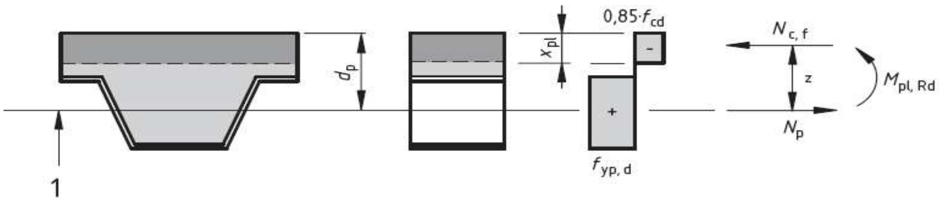

Figure 10. Bending resistance moment for the slab – stress distribution

$M_{pl,Rd} = N_{c,f}\, z = N_p\, z$

$N_{c,f} = 0{,}85.fcd.$

$N_{c,f} = 0.85\, f_{cd}\, x_{pl}\, b_p$

$N_p = A_p\, f_{yp}$

Thus,

x_{pl}	34,4 mm
z	69,5 mm
$M_{pl,Rd}$	28 kNm > $M_{Ed,max}$

Concerning the vertical shear, the maximal shear force is equal to :

$V_{Ed,max} = 11$ kN

The resistant shear can be calculated in accordance with the vertical shear strength of the elements without shear rebars[1] :

$$V_{Rd,c} = [C_{Rd,c} k (100 \rho_l f_{ck})^{\frac{1}{3}} + k_1 \sigma_{cp}] b_w d$$

Thus,

$V_{Rd,c} = 29$ kN > $V_{Ed,max}$

Finally, the punching resistance of the slab for a concentrated load equal to the axle load (V_{Ed}=γ_q.Q_k/2) has to be verified. The critical perimeter under this load has to be determinate :

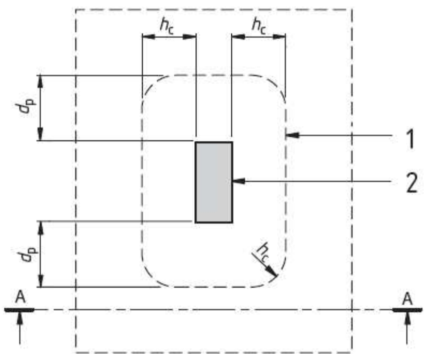

Figure 11 : Critical perimeter for the punching of slab

1 Critical perimeter cp

2 Loaded ares

[1] EN 1992-1-1, 6.2.2

- Critical perimeter (c_p) = 886 mm
- Shear stress in the slab ($v_{Ed} = V_{Ed}/c_p.d_p$) = 0,15 N/mm²

The punching resistance of the slab can be calculated by the following equation[2] which take into account the fact there is no shear rebars :

$$V_{Rd,c} = C_{Rd,c} k(100\rho_l f_{ck})^{1/3} + k_1\sigma_{cp} \geq (V_{min} + k_1\sigma_{cp})$$

Thus,

$V_{Rd,c}$ = 0,884 N/mm² > v_{Ed}

IV.3.2. ELS verification of the slab

The purpose of this paragraph will be to check the control of the cracking of the concrete but also the value of the deflection.

The opening of the cracks must be limited to Wmax whose value recommended for a class of exposure XC4 is of 0,3 mm. Actually, that causes to limit the maximum constraint (σs) in the bars of reinforcements right after cracking and also their spacing according to a diameter of bar chooses on the following table:

Contrainte de l'acier [2] [MPa]	Diamètre maximal des barres [mm]		
	w_k=0,4 mm	w_k=0,3 mm	w_k=0,2 mm
160	40	32	25
200	32	25	16
240	20	16	12
280	16	12	8
320	12	10	6
360	10	8	5
400	8	6	4
450	6	5	-

Table 1 : Maximum diameter of rebars in order to limit cracking

Following the Eurocode[3], when stirrups are not used and that the calculation of the slab is made as if it was some isostatic spans, the anti-cracking rebars located up to the ribs must have a minimum area equal to 0,2 % of the area of the concrete located up to these ribs :

$A_{s,min}$ = 124 mm²/m

Moreover, the spacing between the rebars must not be greater than two times the height of the slab, i.e. 240 mm.

A basic mesh of Φ8 mm spaced by 200 mm is ok (A_s = 250 mm²/m).

The deflection of the composite slab must be checked, thus the manufacturer imposes a limit of active deflection in service of L/350. In addition, a maximum deflection exists for the visual comfort of the users which is L/300. We will take into account the creep of the concrete under permanent loads.

The equivalent moment of inertia (for a steel equivalent section) will be taken equal to the average value determined in cracked section and uncracked section. The coefficients of equivalence for the concrete are 6,8 for the short term and 21,7 for the long term:

[2] EN 1992-1-1, 6.4.4
[3] EN 1994-1-1, 9.8.1 (2)

	Short term	Long term
Uncracked section inertia	1221,9 cm^4	816,8 cm^4
Cracked section inertia	651,3 cm^4	581,9 cm^4
Mean inertia	936,6 cm^4	699,4 cm^4

Service active deflection[4] (w_3) :

$1{,}7 \text{ mm} < L/350 = 9{,}5 \text{ mm}$

Visual comfort[5] ($w_1+w_2+w_3 = w_{max}$) :

$11{,}5 + 0{,}3 + 1{,}1 = 12{,}9 \text{ mm} > L/300 = 11{,}11 \text{ mm}$

Since it is about a car-park, we will tolerate a deflection a little bit more important than the limiting deflection for visual comfort → OK

[4] Rare actions combination
[5] Frequent actions combination

V. Composite beams dimensioning

Attention has to be taken because of the modification of the statical scheme of these beams during their life. Indeed, during and just after concreting of the slab, only the “steel” joint is able to carry loads. Whether once the concrete is able to carry loads, the rebars will also contribute to the stiffness and resistance of the joint.

This point is taken into account to evaluate the solicitations in the composite beams in the 3D model developed for the project. This model is shown on Figure 12. A pinned connection is considered for the column feet.

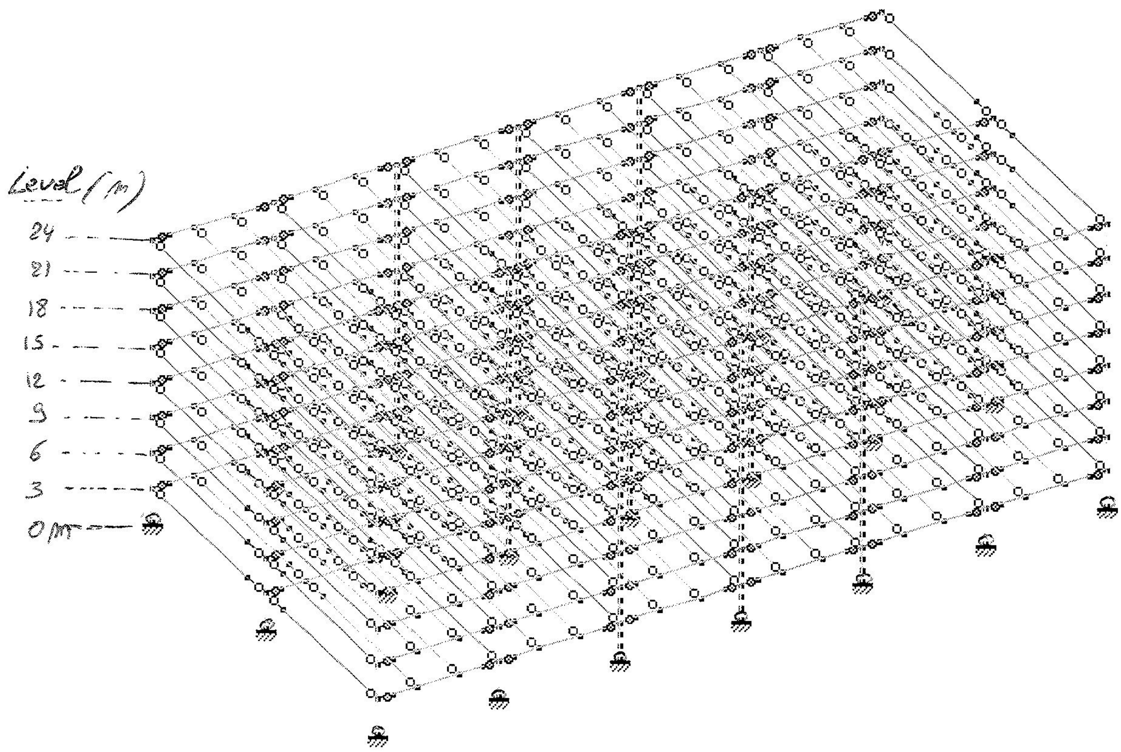

Figure 12 : 3D model

V.1. Mechanical properties used in the 3D model

The static schemes that are considered in relationship with the load case considered are described on Figure 13 and Figure 14.

Figure 13 shows that a rigid joint connection is used for the main beam to column joint with the rigidity equal to S_{j2} for the self-weight loads (steel section only) and S_{j3} for the variable loads (composite section). The calculation of these joints rigidity is described in Annex 3 : Calculation of the main beam to column joint. For this study, the rigidity has only been evaluated for the connection with a column of type HEB300 which will be the column used in the test and which is the column calculated for floor 4 and 5 of the reference structure.

The configuration of this connection is shown in plans CH02 and CH51.

For the variable loads, the composite mechanical properties of the main beam section are considered in hogging in the center of the beam and in sagging (cracked slab) for the sides of the beam (on 1.3 meter). For the self-weight loads, only the steel mechanical properties of the main beam (IPE550) are used.

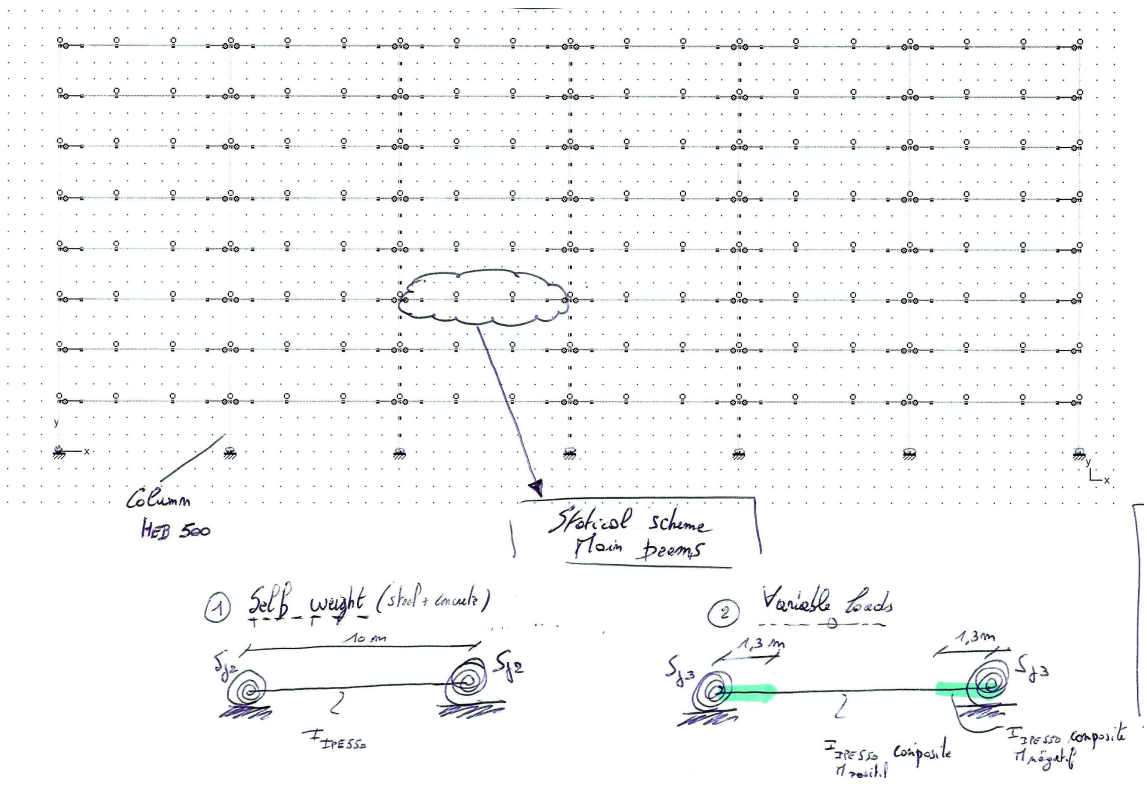

Figure 13 : Statical scheme - main beams

Figure 14 shows that a pinned connection is used for the secondary beam to column joint and for the secondary beam to main beam joint. The steel connection is only realised on the web of the beam which can be considered as an hinge. For the variable load, the rigidity of the connection coming from the slab will not be considered because if only one span is loaded, the rebars in the slab are not able to carry loads. A pinned connection can also be considered for the variable load. For the beam mechanical properties, only the steel mechanical properties (IPE450) are considered for the self-weight whether the composite properties of the secondary beams (hogging) are considered for the variable loads.

The configuration of this connection is shown in the plan CH02 and CH51.

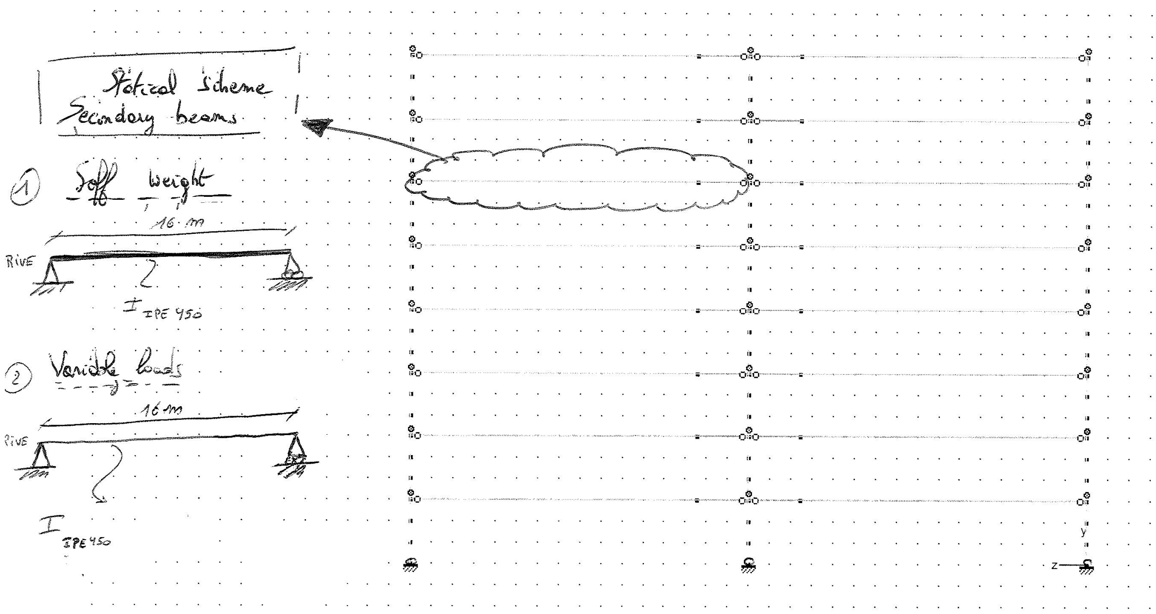

Figure 14 : Statical scheme - secondary beams

The mechanical properties of these composite beams are described hereafter.

Beam profile

Type	IPE 550
hb [mm]	550
bb [mm]	210
twb [mm]	11.1
tfb [mm]	17.2
rb [mm]	24
Ab [cm²]	134.4
Iyb [cm^4]	67120
Wpl,yb [cm³]	2787
Izb [cm^4]	2668
Wpl,zb [cm³]	400.5
d [mm]	467.6

Slab properties

General	
beff,- [mm]	1875
beff,+ [mm]	2500
h [mm]	670
hc [mm]	85
hp [mm]	35
Hollow rib properties	
Ribs	Paral. To the profile
Ip [mm^4]	7.45E+05
b0 [mm]	81.5
yg [mm]	33.3
Ahr [mm²/m]	1391
Studs	
Calculations?	YES
ds [mm]	19.05
hs [mm]	100
fu,s [mm]	450
Nr	1
Constr. mode	Studs welded through the hol. Rib
Hol. rib Thick.	<= 1mm

Longitudinal rebars	
Layer 1 (upper)	
As1 [mm²/m]	653.3
Cover [mm]	25
Layer 2 (lower)	
As2 [mm²/m]	0
Cover [mm]	0
Transverse rebars	
Layer 1 (upper)	
As3 [mm²/m]	250
Cover [mm]	35
Layer 2 (lower)	
As4 [mm²/m]	0
Cover [mm]	0

Mechanical properties

Profile steel	S355
Hollow rib	S355
Concrete	C25/30
Rebars	S500
Security coefficient	
Type	Eurocode
γs	1
γc	1.5
γr	1.15
γhr	1
γstud	1.25

Mechanical property details

Profile steel	
fy,s [Mpa]	355
Es [Mpa]	210000
Hollow rib	
fy,hr [Mpa]	350
Ehr [Mpa]	210000
Concrete	
fy,c [Mpa]	25
τc [Mpa]	0.3
Ec [Mpa]	31476
Rebars	
fy,r [Mpa]	500
Er [Mpa]	200000

Computation Results

Mechanical properties		
Bending moments	Mpl,rd,- [kNm]	1168.5
	Mpl,rd,+ [kNm]	1535.0
Shear force	Vpl,rd [kN]	1482.4
Transversal rebars	Vrd [kN/m]	217.4
Stud property	Prd [kN]	74.7

Geometrical properties		
Hogging zone = M-	Aeq [mm²]	14665.0
	yg [mm]	305.9
	Ie [mm^4]	824893937.9
	Class section	1
Sagging zone = M+	Aeq [mm²]	45290.7
	yg [mm]	522.9
	Ie [mm^4]	1864807814.9
	Class section	1

Figure 15 : Main beams properties

Beam profile	
Type	IPE 450
hb [mm]	450
bb [mm]	190
twb [mm]	9.4
tfb [mm]	14.6
rb [mm]	21
Ab [cm²]	98.82
Iyb [cm^4]	33740
Wpl,yb [cm³]	1702
Izb [cm^4]	1676
Wpl,zb [cm³]	276.4
d [mm]	378.8

Slab properties			
General		*Longitudinal rebars*	
beff,- [mm]	2500	*Layer 1 (upper)*	
beff,+ [mm]	3333	As1 [mm²/m]	250
h [mm]	570	Cover [mm]	25
hc [mm]	62	*Layer 2 (lower)*	
hp [mm]	58	As2 [mm²/m]	0
Hollow rib properties		Cover [mm]	0
Ribs	Perp. To the profile	*Transverse rebars*	
Ip [mm^4]	7.45E+05	*Layer 1 (upper)*	
b0 [mm]	81.5	As3 [mm²/m]	250
yg [mm]	33.3	Cover [mm]	35
Ahr [mm²/m]	1391	*Layer 2 (lower)*	
Studs		As4 [mm²/m]	0
Calculations?	YES	Cover [mm]	0
ds [mm]	19.05		
hs [mm]	100		
fu,s [mm]	450		
Nr	1		
Constr. mode	Studs welded through the hol. Rib		
Hol. rib Thick.	<= 1mm		

Mechanical properties	
Profile steel	S355
Hollow rib	S355
Concrete	C25/30
Rebars	S500
Security coefficient	
Type	Eurocode
γs	1
γc	1.5
γr	1.15
γhr	1
γstud	1.25

Mechanical property details	
Profile steel	
fy,s [Mpa]	355
Es [Mpa]	210000
Hollow rib	
fy,hr [Mpa]	350
Ehr [Mpa]	210000
Concrete	
fy,c [Mpa]	25
τc [Mpa]	0.3
Ec [Mpa]	31476
Rebars	
fy,r [Mpa]	500
Er [Mpa]	200000

Computation Results

Mechanical properties		
Bending moments	Mpl,rd,- [kNm]	685.6
	Mpl,rd,+ [kNm]	1048.6
Shear force	Vpl,rd [kN]	1042.1
Transversal rebars	Vrd [kN/m]	1191.1
Stud property	Prd [kN]	53.2

Geometrical properties		
Hogging zone = M-	Aeq [mm²]	10507.0
	yg [mm]	244.0
	Ie [mm^4]	397593014.2
	Class section	1
Sagging zone = M+	Aeq [mm²]	40855.3
	yg [mm]	471.3
	Ie [mm^4]	1088752922.6
	Class section	1

Figure 16 : Secondary beams properties

The following table can be used to summarise all these data concerning the resistance and rigidity of joints :

	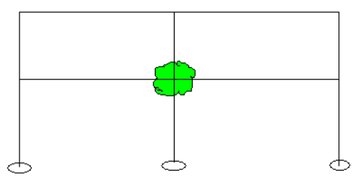		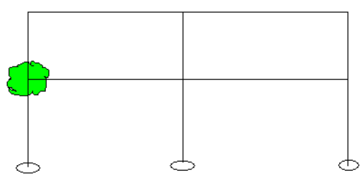	
	Steel	Composite	Steel	Composite
Main beams	M_{rd} = 313.4 kNm $S_{j2,ini}$ = 98813 kNm/rad (= 2*S_{j2})	M_{rd} = 580 kNm $S_{j3,ini}$ = 182111 kNm/rad (= 2*S_{j2})	M_{rd} = 304.5 kNm $S_{j2,ini}$ = 58781 kNm/rad (= 2*S_{j2})	M_{rd} = 472 kNm $S_{j3,ini}$ = 71559 kNm/rad (= 2*S_{j2})
Secondary beams	M_{rd} = 0 kNm $S_{j2,ini}$ = 0 kNm/rad (= 2*S_{j2})	M_{rd} = 0 kNm $S_{j3,ini}$ = 0 kNm/rad (= 2*S_{j2})	M_{rd} = 0 kNm $S_{j2,ini}$ = 0 kNm/rad (= 2*S_{j2})	M_{rd} = 0 kNm $S_{j3,ini}$ = 0 kNm/rad (= 2*S_{j2})

Tableau 2 : Joints mechanical properties (with HEB 300 column)

V.2. Solicitations of beams

The resultant bending moment diagram are shown in the following figures (the values already take into account the security factor for the ULS) :

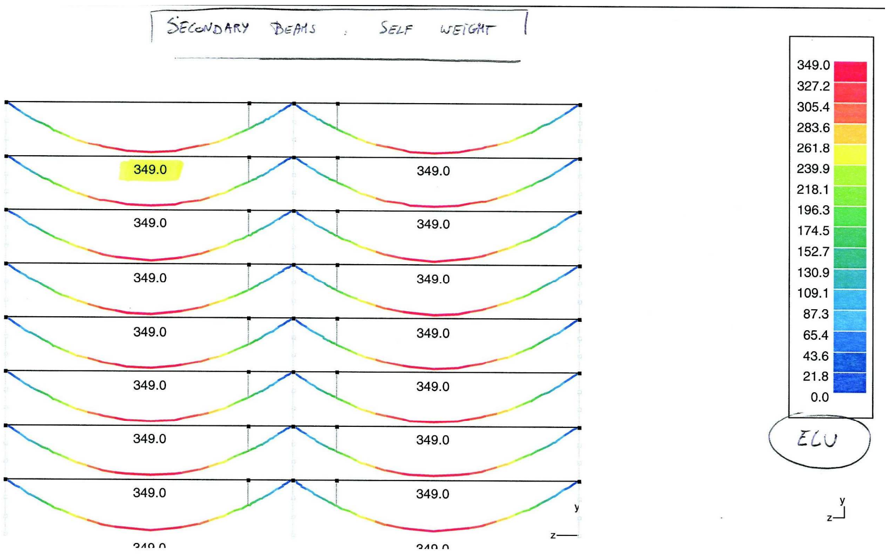

Figure 17 : Bending moment : secondary beam, self weight

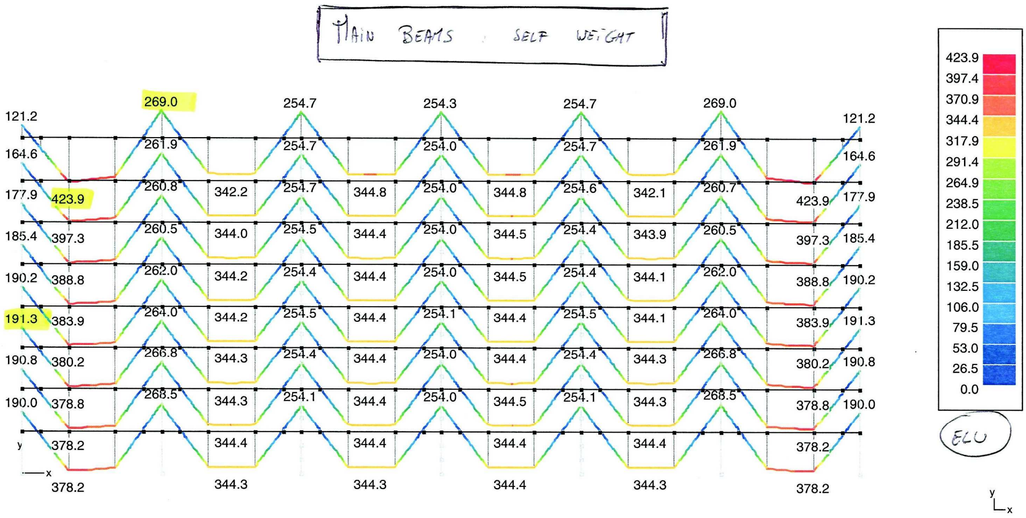

Figure 18 : Bending moment - Main beam – Self-weight

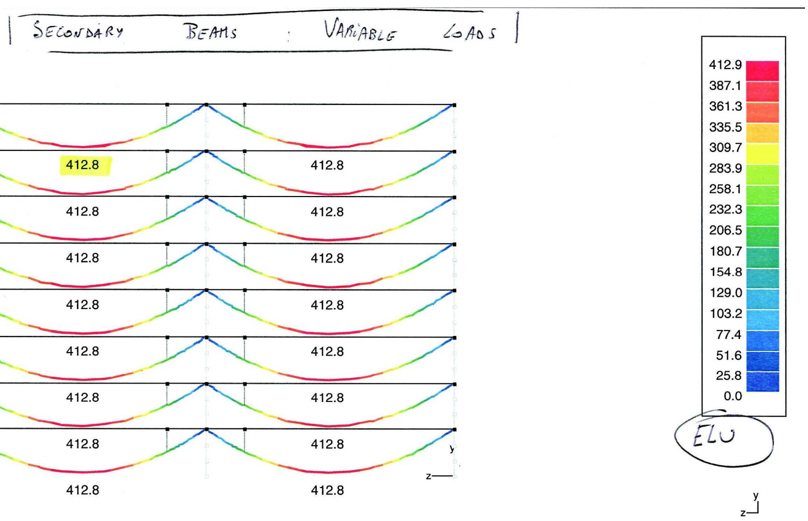

Figure 19 : Bending moment – Secondary beams – Variable loads

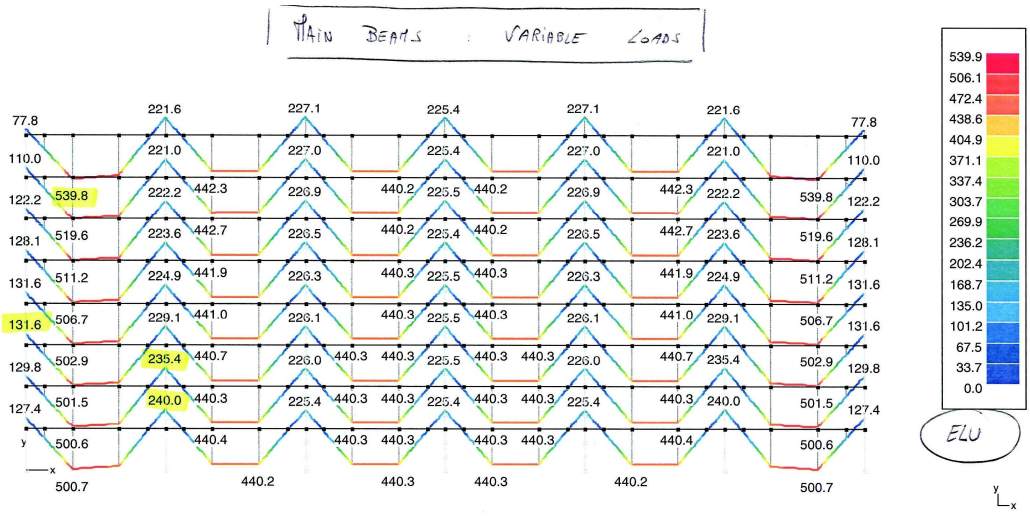

Figure 20 : Bending moment – Main beams – Variable loads

V.3. *ULS verification*

a. Main beams

M_{sd+} = 423.9 + 539.8 = 964 kNm < 1535 kNm

M_{sd-} = 269 + 240 = 509 kNm < 1296 kNm (beam verification)

< 580 kNm (joint verification)

V_{sd} = 408 kN < 1482 / 2 kN (beam verification – no M-V interaction)

< 513 kN (joint verification)

b. Secondary beams

M_{sd+} = 349 + 412.8 = 762 kNm < 1048 kNm

V_{sd} = 209 kN < 1042 / 2 kN (beam verification – no M-V interaction)

< 452 kN (joint verification)

V.4. *SLS verification*

The following deflections are calculated :

Deflection (mm)	Main beam	Secondary beam
Self weight	131	28
Variable loads	48	14
Precamber	-130	-25
TOTAL	**49**	**17**

Those deflections are lower than L/300 and are acceptable.

VI. Columns dimensioning

Steel grade = S460 ; buckling curve = b curve

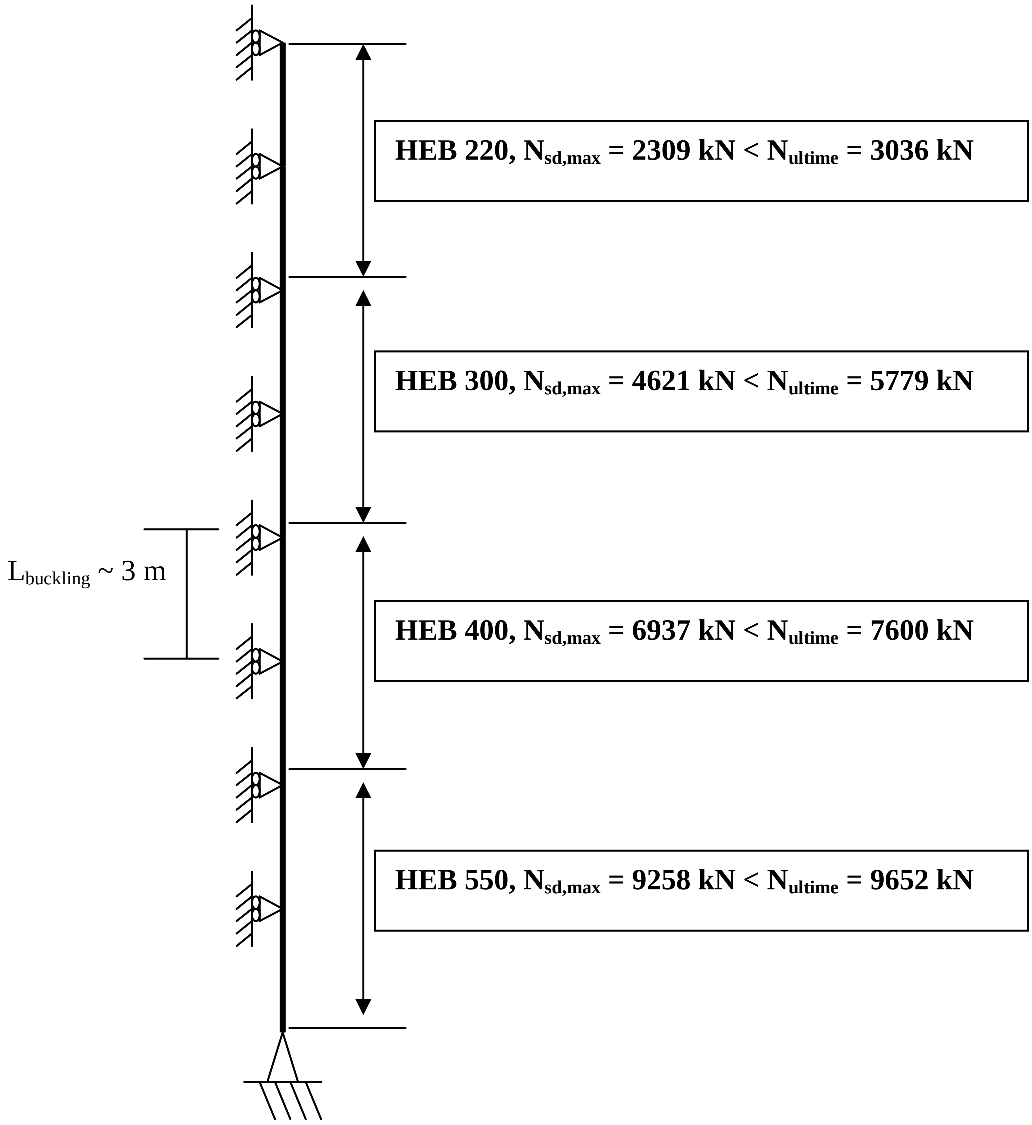

VII. Annex 1 : Reference structure plans

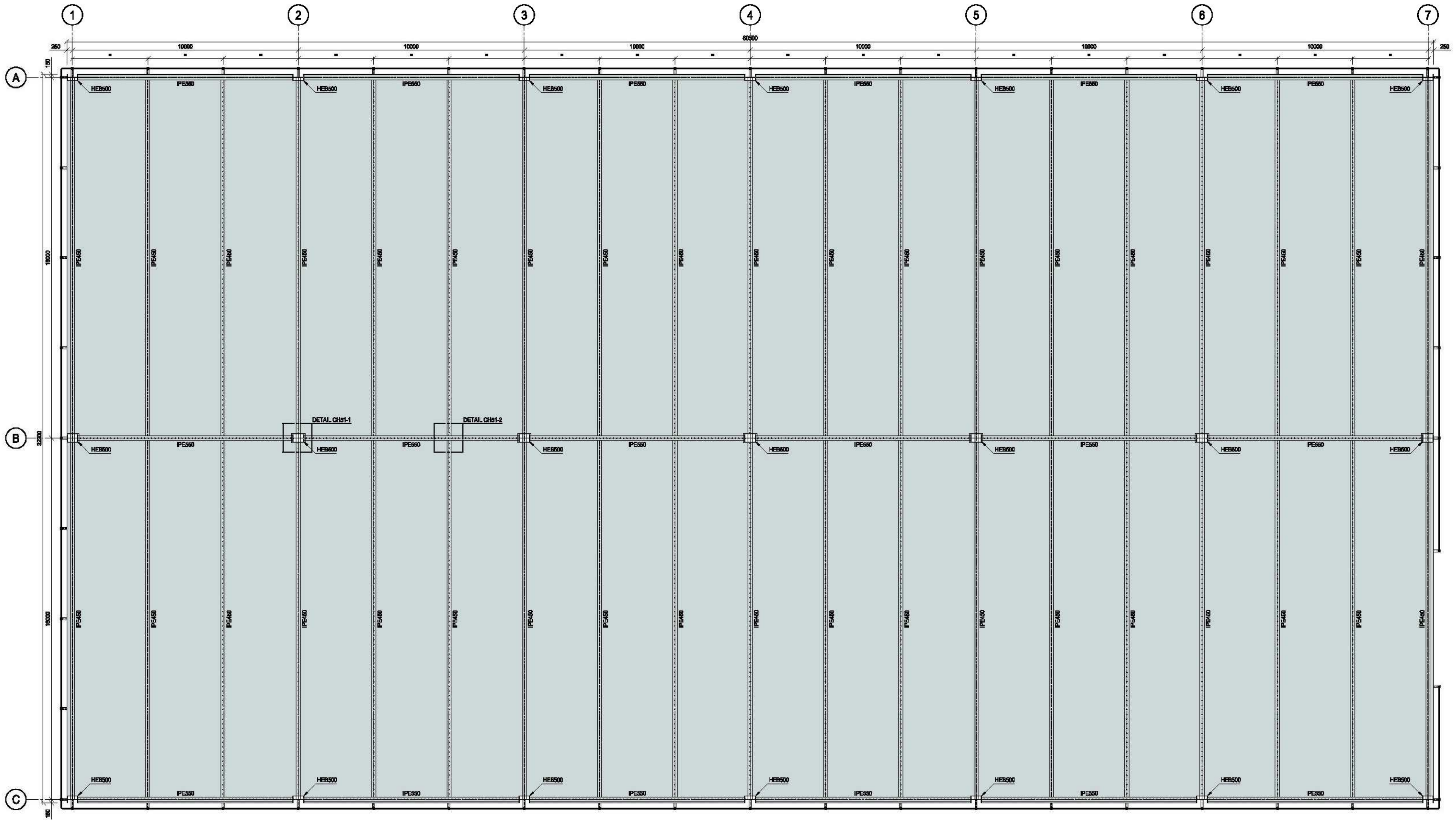

Remarks

- Steel grade :
  - Main and secondary beams : S355
  - Columns : S460
  - Rebars : S500
- Concrete grade :
  - C 25/30
- Metal stud :
  - ¾" - H=100mm

UNIVERSITE de Liège

greisch

bureau d'études greisch, stabilité
allée des noisetiers 25 à 4031 Liège (Belgique)
tél +32 (0)4 366 16 16 - fax +32 (0)4 366 16 18 - bureau@greisch.com

ROBUSTFIRE PROJECT

ROBUSTNESS OF CAR PARKS AGAINST LOCALISED FIRE

PLAN VIEW

index	modification	drafter	auditor	date
-	First diffusion	MD	FGE	03.09.09

issuer	stage	scale	file	folder	
Greisch	project	1/75	4144-PR-P-CH01_HEB500	4144	CH01-0

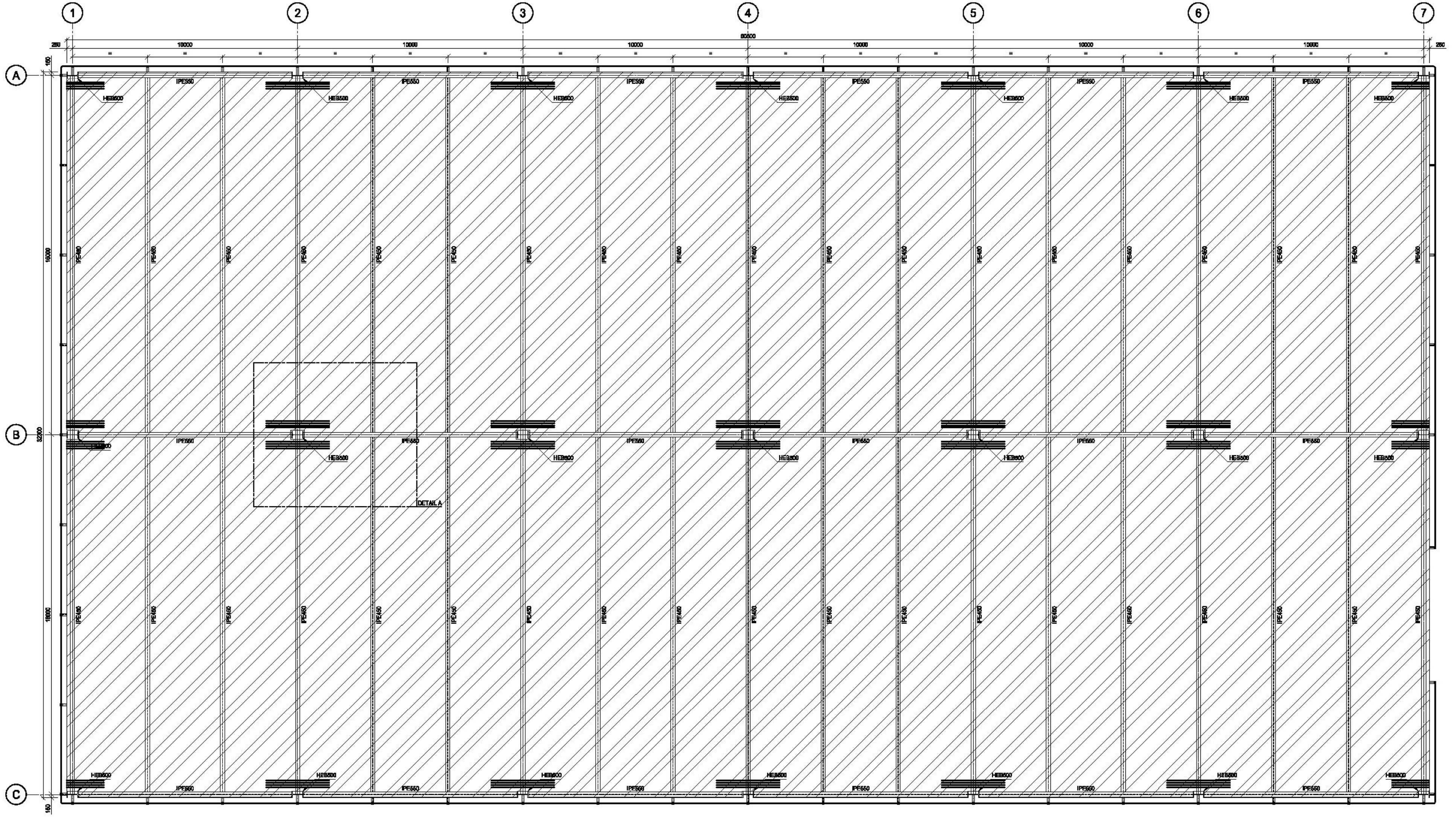

Detail A (Sc. : 1/25)

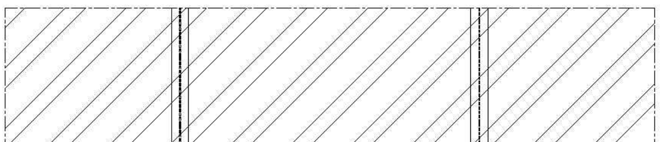

Cross-section A-A (Sc. : 1/10)

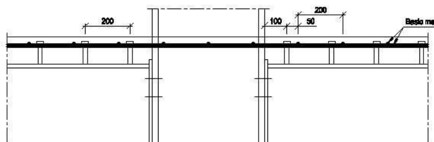

Cross-section B-B (Sc. : 1/10)

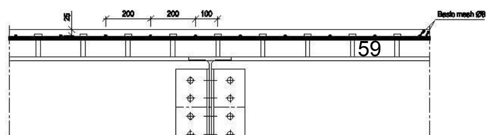

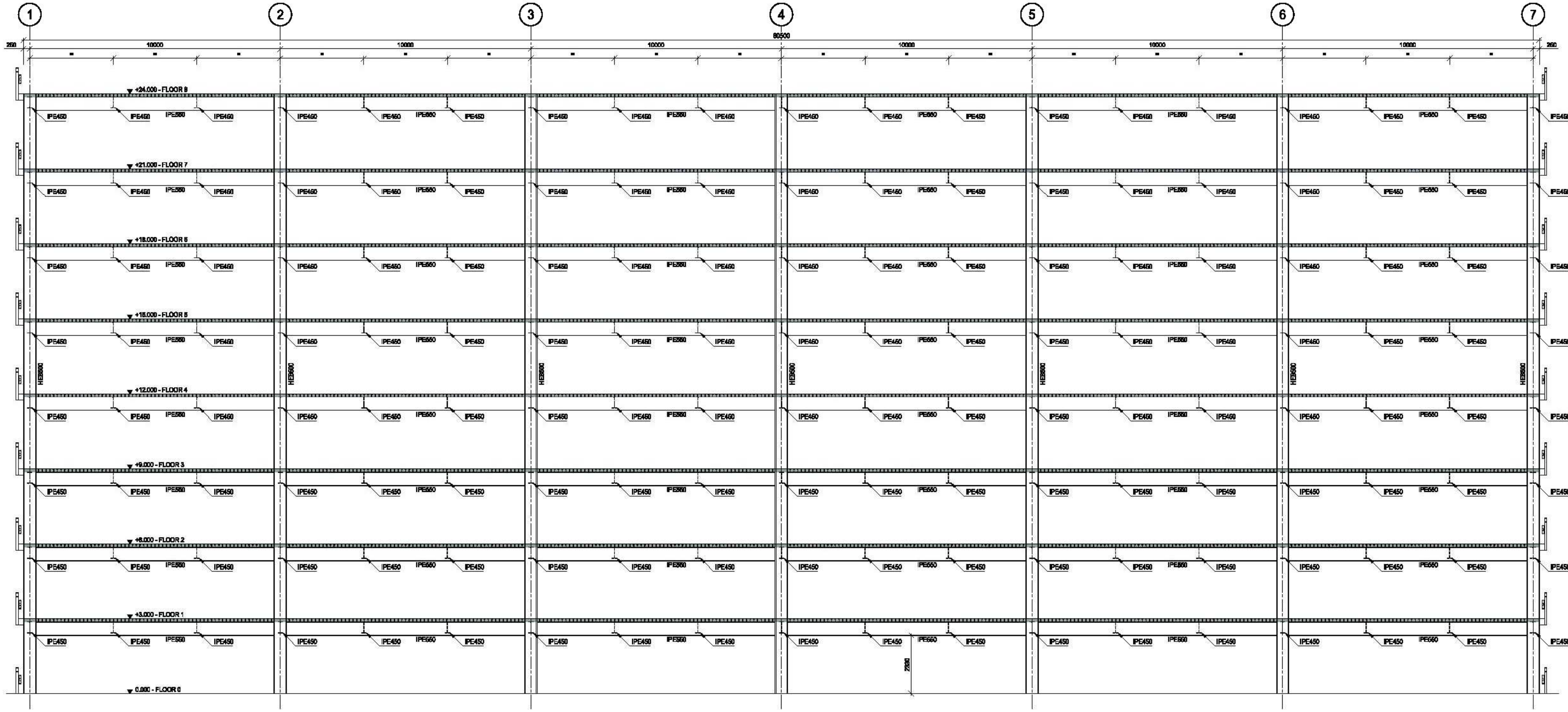

Main beam (Sc. : 1/10)

1 centered metal stud on the cross section
(Sc. : 1/10)

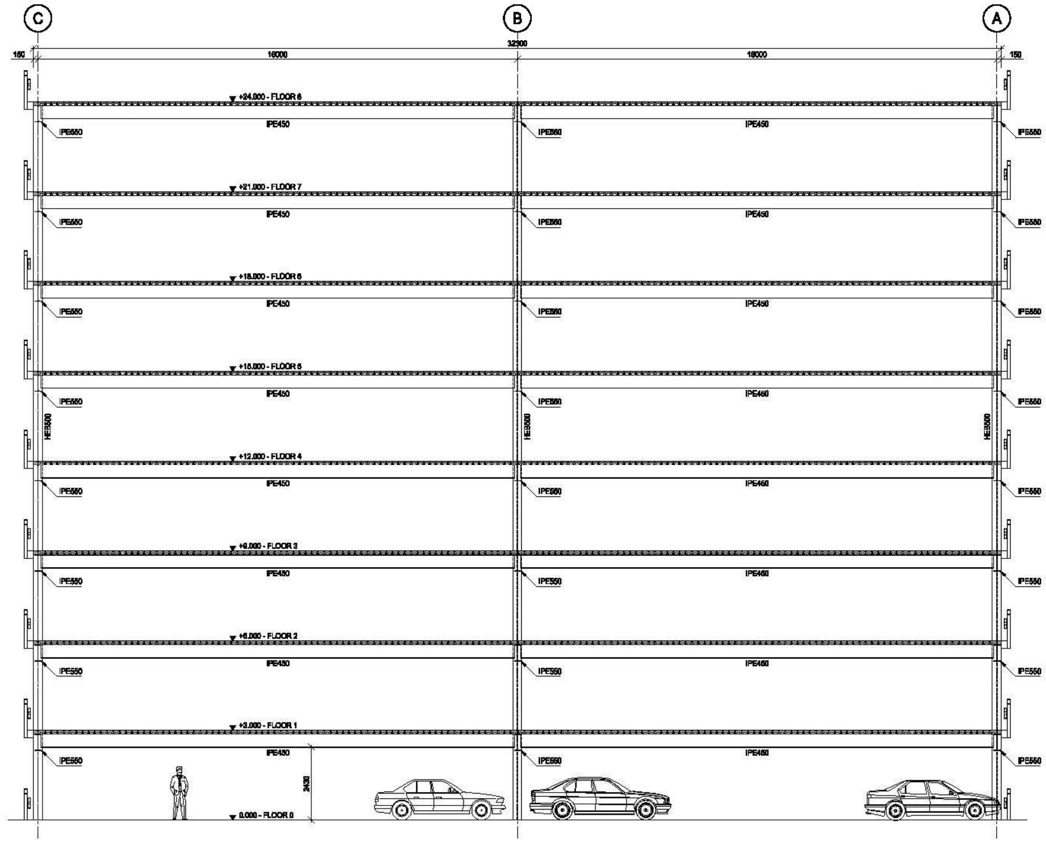

1 centered metal stud on the cross section

(Sc. : 1/10)

Secondary beam (Sc. : 1/10)

Assembled on main beams

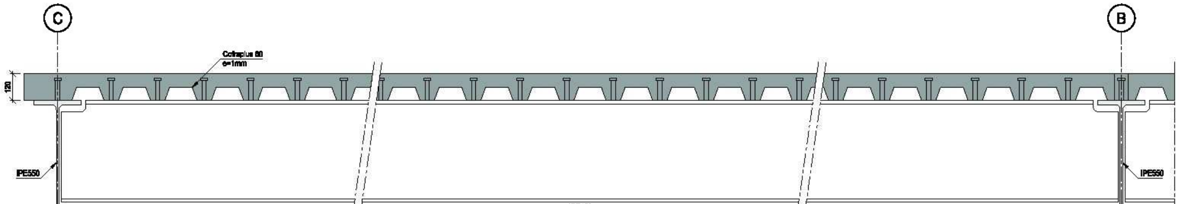

DETAIL CH51-1 (Sc. : 1/5)

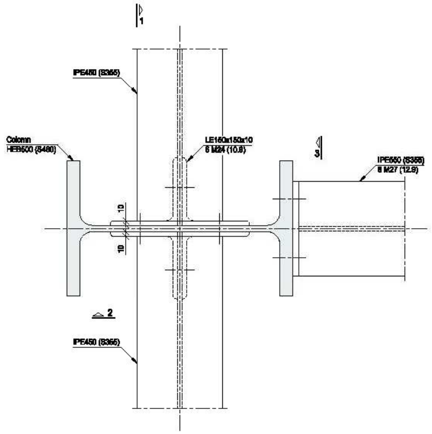

DETAIL CH51-2 (Sc. : 1/5)

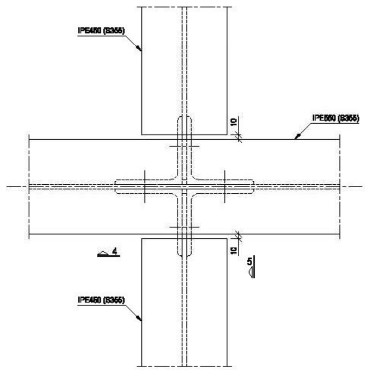

Cross section 1 (Sc. : 1/5)

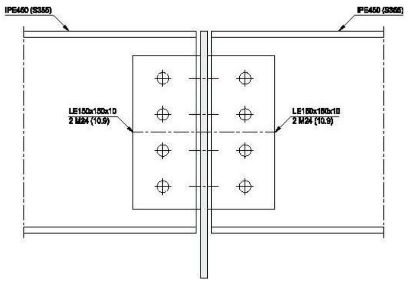

Cross section 2 (Sc. : 1/5)

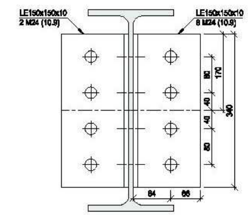

Cross section 3 (Sc. : 1/5)

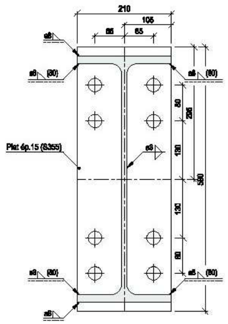

Cross section 4 (Sc. : 1/5)

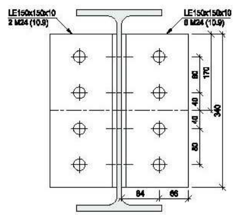

Cross section 5 (Sc. : 1/5)

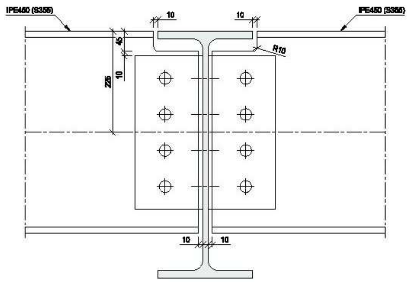

VIII. Annex 2 : Geometrical characteristics of the hollow rib

Arval Haironville-Pab

PLANCHERS COLLABORANTS **COFRAPLUS 60**

CARACTÉRISTIQUES GÉOMÉTRIQUES

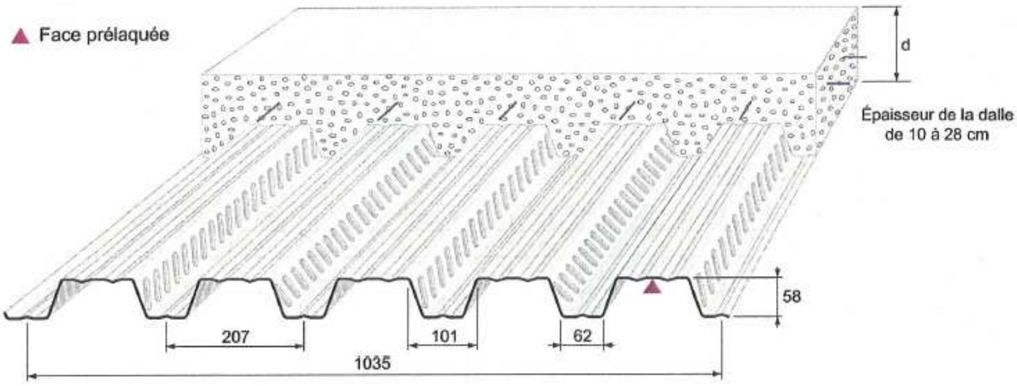

APPLICATIONS

Cofraplus 60 est un profil nervuré cranté latéralement destiné à la construction de dalles béton.
Cofraplus 60 évite le décoffrage, allège le plancher et économise une nappe d'armatures.

Cofraplus 60 est spécialement conçu pour les ouvrages à surchages modérées et portées moyennes.
Les planchers sur vide sanitaire doivent être visitables et ventilés.

DÉFINITIONS / NORMES

Identification de l'acier

- Norme NF EN 10326 : "bandes et tôles en acier de construction revêtues en continu par immersion à chaud".
- Norme XP 34-301 : "Tôles et bandes d'acier de construction galvanisées prélaquées ou revêtues d'un film organique calandré, destinées au bâtiment".
- Norme EN 10169-3 : "Produits plats en acier revêtus en continu de matières organiques (prélaqués) - partie 3 : produits pour applications intérieures dans le bâtiment".
- Acier : S350 GD selon norme NF EN 10326.

Coffrage

Cofraplus 60 sert de coffrage porteur, entre solives dans la pose sans étai, ou entre files d'étais et solives.
Sa légèreté facilite la manipulation d'éléments de grand format livrés à longueur jusqu'à 15 mètres.

Armature

Le crantage latéral scelle le profil autour des nervures moulées en sous-face de la dalle béton des planchers.
Comme armature, Cofraplus 60, en épaisseur 0,75 mm apporte 10,29 cm²/ml ou 13,91 cm²/ml d'acier en épaisseur 1,00 mm dans le sens porteur du plancher.

Revêtement

- galvanisé Z 275.
- galvanisé prélaqué :
  - Intérieur 12 :
    - catégorie II selon XP 34-301
    - catégorie CPI2 selon EN 10169-3
  - Haiplus® 25 :
    - catégorie IIIa selon XP 34-301
    - catégorie CPI3 selon EN 10169-3
- Autres revêtements : sur consultation.

Réglementation

- Avis Technique 3/03-390 et 3/03-390* 01 Add.

Versions

Trois versions sont disponibles :

- La version standard est appelée **COFRAPLUS 60**.

- La version spécialement adaptée pour utilisation en système poutre mixte avec connecteurs de types Hilti ou Nelson posés au travers du bac sur chantier est appelée **COFRAPLUS 60 C** : fabrication spécifique sur demande.

COFRAPLUS 60 C
(version connecteur fond de nervure)

- COFRAPLUS 60 peut être réalisé avec préperçage pour le passage des goujons soudés en atelier. Cette version est appelée **COFRAPLUS 60 P** :
Étude et fabrication sur demande.
(jusqu'à une épaisseur de 1,00 mm).

COFRAPLUS 60 P
(le plan de perçage est à fournir)

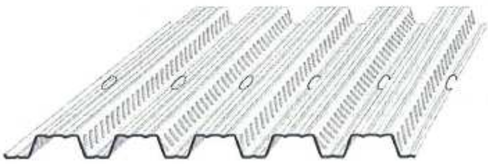

3

CARACTÉRISTIQUES TECHNIQUES DU PLANCHER VERSION STANDARD

Caractéristiques utiles du profil

Épaisseur nominale de la tôle e		mm	0,75	0,88	1,00	1,25
Poids au mètre carré utile		daN/m²	8,53	10,00	11,37	14,22
Section active d'acier :	A	cm²/ml	10,29	12,17	13,91	17,57
Inertie propre du profil :	i	cm⁴/ml	55,12	65,21	74,53	93,94
Position fibre neutre :	v_i	cm	3,33	3,33	3,33	3,33
Module d'inertie :	I/v_i	cm³/ml	16,55	19,58	22,38	28,20

Consommation nominale de béton

Épaisseur d	cm	10	11	12	13	14	15	16	18	20	24	28
Litrage	l/m²	65	75	85	95	105	115	125	145	165	205	245
Poids théorique du béton seul*	daN/m²	155	179	203	227	251	275	299	347	395	491	587

* Pour obtenir le poids total de la dalle il faut ajouter le poids du béton dû à la flèche ainsi que le poids du profil.
Poids volumique du béton 2400 daN/m³.

Caractéristiques utiles en travée de la dalle

Épaisseur d	cm	10	11	12	13	14	15	16	18	20	24	28
Pour e = 0,75 mm distance $d-v_i$	cm	6,67	7,67	8,67	9,67	10,67	11,67	12,67	14,67	16,67	20,67	24,67
Distance x	cm	3,25	3,56	3,90	4,13	4,40	4,65	4,90	5,36	5,79	6,59	7,31
I_{15}	cm⁴/m	252	329	421	527	649	786	938	1289	1705	2731	4024
z	cm	5,59	6,48	7,39	8,29	9,20	10,12	11,04	12,88	14,74	18,47	22,23
Épaisseur d	**cm**	**10**	**11**	**12**	**13**	**14**	**15**	**16**	**18**	**20**	**24**	**28**
Pour e = 1,00 mm distance $d-v_i$	cm	6,67	7,67	8,67	9,67	10,67	11,67	12,67	14,67	16,67	20,67	24,67
Distance x	cm	3,59	3,94	4,28	4,60	4,90	5,20	5,48	6,01	6,51	7,43	8,27
I_{15}	cm⁴/m	309	404	517	648	799	969	1159	1600	2123	3424	5073
z	cm	5,47	6,36	7,24	8,14	9,04	9,94	10,84	12,67	14,50	18,19	21,91

Notation

- d : épaisseur de la dalle, nervure du bac incluse
- v_i : distance de l'axe neutre du bac à sa fibre inférieure
- x : distance de l'axe neutre de la dalle à sa fibre supérieure
- I_{15} : inertie mixte équivalente en acier correspondant à $E_a/E_b = 15$
- z : bras de levier conventionnel ($d-v_i$ - x/3)

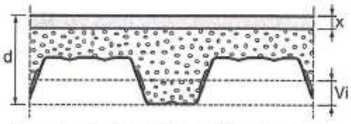

Les valeurs de "m" et de "k" sont données dans le système d'unités : longueur en cm, force en daN.

Cisaillement admissible entre tôle et béton

$\tau = T / 100 . z \leq m . \rho \, d/L + k$

avec

ρ = rapport de la section de la tôle à la section utile de béton (hauteur $d-v_i$)

L = portée de calcul en cm

	Résistance	Glissement Charge statique	Glissement Charge dynamique
m	3238	1775	1420
k	0,1286	0,5302	0,4242

Résistance au feu

CF : degré coupe-feu du plancher brut.
Une épaisseur minimale est requise pour le respect du critère de température en face non exposée.

CF demandé	60'	90'	120'	180'
d mini en cm	11	12	15	18

En l'absence d'armatures spécifiques, les planchers Cofraplus sont CF 30'. Pour des CF supérieurs, la résistance du plancher pour le délai requis d'exposition au feu doit être justifiée par la prise en compte des seules armatures enrobées dans le béton.

Isolation acoustique

Le comportement acoustique du plancher brut correspond à la loi de masse. (valeurs calculées par modélisation)

Épais. d en cm	10	11	12	13	14	15	20	24	28
Rw (C;Ctr)	44 (-1;-3)	45 (-1;-4)	46 (-1;-4)	47 (-1;-4)	48 (-1;-5)	48 (-1;-4)	52 (-2;-6)	54 (-1;-7)	56 (-1;-7)

IX. Annex 3 : Calculation of the main beam to column joint

41

23-10-2008

Design of the joint between the IPE550 S355 beam and the HEB300 S460 column

②

Loads to be supported during the ~~the~~ at "composite" state:

These loads will depend of the joint properties and the joint properties will depend of the loads to be supported

⇒ in a first step, it is assumed that the designed joint will have to support the loads computed when designing ~~the sol~~ previously the solution with the HEB 500 column, i.e.:

$$\begin{cases} M_{Ed} = 1550 \text{ kNm} \\ V_{Ed} = 441 \text{ kN} \end{cases}$$

1e configuration étudiée ⇒ cf. feuille suivante

Propriétés:

- $\ast$ Rangée 1 : $F_{Rd,1} = 339,3$ kN (EPB - mode 2) – $k_{eff,1} = 1,63$ mm
- $\ast$ Rangée 2 : $F_{Rd,2} = 211,86$ kN (EPB - group 1-2 - mode 1) – $k_{eff,2} = 1,47$ mm
- $\ast$ Rangée 3 : $F_{Rd,3} = 325,69$ kN (EPB - individual - mode 2) – $k_{eff,3} = 1,47$ mm
- $\ast$ Rangée 4 : $F_{Rd,4} = 205,25$ kN (EPB - group 1-4 - mode 1) – $k_{eff,4} = 1,63$ mm

$\underline{1082,2 \text{ kN}}$ ≈

~~Let system~~:

Resistance of the component in compression:

↳ $F_{Rd,c} = \underline{1174,4 \text{ kN}}$ ≈ ⇒ CWC $k_c = \underline{10,82 \text{ mm}}$ ≈

We can see that the sum of the resistance of the components in tension is close to the resistance in compression of the column web

42

23-10-2008

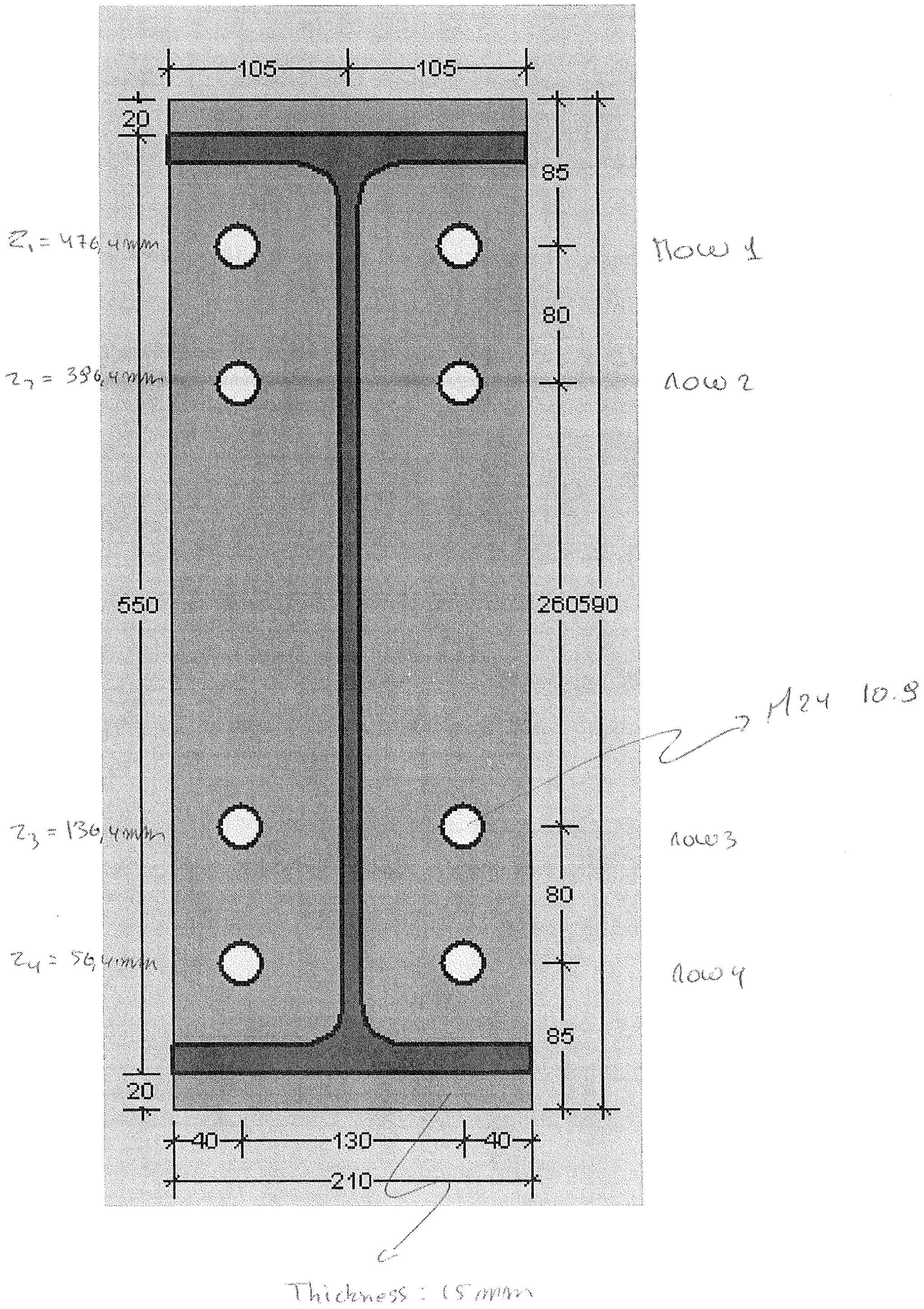

105
105
20
85
80
550
260590
80
85
20
40
130
40
210
z_1 = 476,4mm
z_2 = 396,4mm
z_3 = 136,4mm
z_4 = 56,4mm
row 1
row 2
row 3
row 4
M24 10.9
Thickness : 15mm

43

23-10-2003

(5)

=> If we add component in tension which is the component "rebars in tension" => the resistance of the CWC will be reached => The resistance of the composite joint will be governed by this component.

The bending moment to be transmitted is 550 kNm.
Let assume that only the two first bolt rows will contribute to the bending resistance of the joint:

$$550\,kNm = F_{Rd,1} \cdot z_1 + F_{Rd,2} \cdot z_2 + F_{arm} \cdot z_{arm}$$

$$= 338,3 \cdot 0,4764 + 211,86 \cdot 0,3964 + F_{arm} \cdot 0,6314$$

$$z_{arm} = 550 - \frac{17,2}{2} + 120 - 30$$

↳ rebars covering

↳ total thickness of the slab

$$\Rightarrow F_{arm} = 482\,kN$$

Let assume that we will place a total of 10 S500 rebars at the joint level (i.e 5 each side of the column)

$$\Rightarrow 482\,kN = \frac{\pi d^2}{4} \cdot 10 \cdot \frac{f_{ys}}{\gamma_s}$$

$f_{ys} \to 500$, $\gamma_s \to 1,15$

$$d \geq 11,8\,mm \Rightarrow 12\,mm$$

=> 10 ϕ12mm rebars will be placed

$$\Rightarrow F_{arm} = 491,7\,kN$$

$$\Rightarrow F_{Rd,1} + F_{Rd,2} + F_{arm} = 1043\,kN$$

$$\Rightarrow F_c - 1043\,kN = 1174,4 - 1043 = 131,4$$

to be elastically distributed between rows 3 & 4

(44)

23-10-2009

(4)

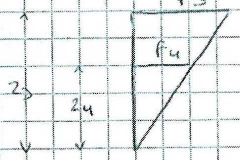

$F_4 = 131{,}4 - F_3$

$\frac{F_4}{z_4} = \frac{F_3}{z_3} \Rightarrow F_3 = \frac{F_4 \cdot z_3}{z_4}$

$F_4 = 131{,}4 - \frac{F_4\, z_3}{z_4}$

$\Downarrow$

$F_4\left(1 + \frac{z_3}{z_4}\right) = 131{,}4$

$\Rightarrow F_4 = 38{,}44\ kN$

$\Rightarrow F_3 = 92{,}96\ kN$

$\Rightarrow M_{Rd,joint} = 338{,}3 \cdot 0{,}4764 + 211{,}86 \cdot 0{,}3964 + 491{,}7 \cdot 0{,}6314 + 92{,}96 \cdot 0{,}1364$
$+ 38{,}44 \cdot 0{,}0564$
$= 571\ kNm$

$t_p \leq 0{,}36 \cdot d_{bolt} \sqrt{f_{ub}/f_{yp}} = 14{,}5\ mm$
$\hookrightarrow$ OK!

Ductility criteria:

$A_s \leq \frac{1{,}1 \cdot (0{,}85 \cdot f_{ck}/\gamma_c) \cdot b_c \cdot d_{eff}}{\beta\,(f_{sk}/\gamma_s)}$
$\hookrightarrow 0$ $= \infty$

$A_s \geq 0{,}004 \cdot d_{eff} \cdot (h_{eff} \cdot b_c) = 235{,}6\ mm^2$
$\hookrightarrow 60 \cdot 2 \cdot 61{,}25 \quad \hookrightarrow 0{,}3$ $\Rightarrow$ OK!

Stiffness:

$k_{arm} = k_{st} \cdot k_n$

$k_{st} = \frac{A_s}{h_c\left(\frac{1+\beta}{2} + K_\beta\right)} \cdot \frac{E_s}{E_a} = \frac{10\,\pi \frac{d^2}{4}}{300 \cdot 0{,}5} \cdot \frac{200\,000}{210\,000} = 7{,}2\ mm$

- $\beta = 0$
- $K_\beta = 0$ for $\beta = 0$
- $h_c = 300\ mm$

$k_n = \frac{1}{1 + \frac{E_s \cdot k_{st}}{K_{sc}}}$

- $K_{sc} = \frac{N \cdot k_{sc}}{\nu - \left(\frac{\nu - 1}{1+\xi}\right)\frac{h_{s}}{d_s}}$ $\Rightarrow \xi = \frac{E_a \cdot I_a}{d_s^2\, E_s\, A_s} = \frac{210\,000 \cdot 67\,120\,000}{365^2 \cdot 200\,000 \cdot 10\,\pi \frac{144}{4}}$

$\hookrightarrow \frac{350}{2} + 120 + 30 = 365\ mm$

$\Rightarrow \xi = 4{,}7$

$\Rightarrow \nu = \sqrt{\frac{(1+\xi)\, N \cdot k_{sc} \cdot l \cdot d_s^2}{E_a \cdot I_a}}$

45

23-10-2009

5

$k_{sc} = \frac{0,7\, P_{Rk}}{1,5}$

$= 100$ kN/mm (assumption

$D = 0,15 \cdot 10000 = 1500$ mm

$N = \frac{1500}{150} = 10$

↳ spacing of the stud

$\Rightarrow \nu = \sqrt{\frac{(1+4,7)\cdot 10 \cdot 100000 \cdot 1500 \cdot 365^2}{210000 \cdot 67120\,0000}} = 2,84$

$\Rightarrow K_{sc} = \frac{10 \cdot 100000}{\left(2,84 - \left(\frac{2,84-1}{1+4,7}\right)\cdot \frac{631,4}{365}\right)} = 438291,2$

$\Rightarrow k_1 = \frac{1}{1 + \frac{200\,000 \cdot 7,2}{438291,2}} = 0,23$

$\Rightarrow k_{a\,mm} = 7,2 \cdot 0,3 = 1,68$ mm

$\Rightarrow z_{eq} = \frac{1,68 \cdot 631,4^2 + 1,63(476,4^2 + 56,4^2) + 1,47(396,4^2 + 136,4^2)}{1,68 \cdot 631,4 + 1,63(476,4 + 56,4) + 1,47(396,4 + 136,4)}$

$= 480,46$ mm

$\Rightarrow k_{eq} = \frac{1,68 \cdot 631,4 + 1,63(476,4 + 56,4) + 1,47(396,4 + 136,4)}{480,46} = 5,65$ m

$\Rightarrow S_{j,ini} = \frac{E_a \cdot z_{eq}^2}{\frac{1}{k_{eq}} + \frac{1}{k_i}} = \frac{210\,000 \cdot 480,46^2}{\frac{1}{5,65} + \frac{1}{10,82}} = 179839$ kNm/rad

$\Rightarrow$ Comparation with OSSA2D

$\Rightarrow 9,59$ kN/m

$\Rightarrow I = 0,00074636\ m^4$ (composite beam) hogging

$\Rightarrow I = 0,0013672\ m^4$ (composite beam sagging)

$\frac{S_{j,ini}}{2} = 89919,5$ kNm/rad

$\Rightarrow M_{Ed} = 540$ kNm $\Rightarrow$ ok!

$V_{Ed} = 441,01$ kN

46

23-10-2008

6

It can be seen that, according to the computation mode with Cos, the joint resistance in shear is not satisfactory ($V_{Rd} = 322{,}7$ kN)

↳ However, the situation when the joint works as a composite one, is different

Indeed, in the latter, only the two first bolt rows are contributing significantly to the bending resistance of the joint.

↳ It is assumed that these bolt rows are fully contributing to the shear resistance

$\Rightarrow V_{Rd} = 2 \cdot 282{,}4$ kN $= \underline{564{,}8 \text{ kN}} \Rightarrow$ ok!

Even if this solution work, it is "dangerous" from a "ductilness" point of view

A solution would be to use $\boxed{\text{M30 10.9}}$ bolts instead of M24 10.9 ones

		F_{Rd}	δ
$\Rightarrow$	row 1 :	437,85 kN (EPB - mode 1)	1,72 mm
	row 2 :	113,99 kN (EPB - Group 1-2 - mode 1)	1,54 mm
	row 3 :	370,48 kN (EPB - Group 1-3 - mode 1)	1,54 mm
	row 4 :	161,1 kN (EPB - Group 1-4 - mode 1)	1,72 mm

$F_c = 175{,}38$ kN

$V_{Rd} = 512{,}91$ kN $\Rightarrow$ ok!

$M_{Ed} = 560$ kNm

$\Rightarrow 560 \text{ kNm} = 437{,}85 \text{ kN} * 0{,}4764 + 113{,}98 \cdot 0{,}3964 + F_{arm} \cdot z_{arm}$

$\Rightarrow F_{arm} = 484{,}98$ kN

$\Rightarrow 10\ \phi 12$ as previous design

(47)

23-10-2008

(7)

$\Rightarrow F_{3rm} = 491{,}7\ kN$

$\Rightarrow F_{Rd,1} + F_{Rd,2} + F_{3rm} = 1037\ kN$

$\Rightarrow F_t - 1037\ kN = 139\ kN$

$\Rightarrow F_4 = 40{,}7\ kN \quad \Rightarrow F_3 = 98{,}3\ kN$

$\Rightarrow M_{Rd} = 491{,}7 \cdot 0{,}6314 + 437{,}85 \cdot 0{,}4764 + 113{,}99 \cdot 0{,}3864 + 98{,}3 \cdot 0{,}1364$
$+ 40{,}7 \cdot 0{,}0564$
$= 579{,}9\ kNm \Rightarrow ok$

k_{3rm} is the same $\Rightarrow k_{3rm} = 1{,}68\ mm$

$\Rightarrow z_{eq} = 477{,}62\ mm \Rightarrow k_{eq} = 5{,}9\ mm$

$\Rightarrow S_{j,ini} = 182111{,}32\ kNm/rad$

$\Rightarrow$ new $M_{Ed} = 560\ kNm \Rightarrow$ ok!

Also, with this solution the criteria of ductility for the end plate thickness is fully contemplated:

$t_p \leq 0{,}36\, d \sqrt{\frac{f_{ub}}{f_y}} = 17{,}5\ mm$

At the construction stage:

$126{,}81 \cdot 1{,}35 = 184{,}7\ kN$

$\Rightarrow 1{,}05 \cdot 1{,}35 = 1{,}42\ kN/m$

email F. Gens 22/10/2008

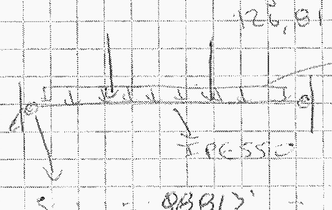

Fresso

$S_{j,ini} = \frac{98813}{2} = 49406{,}5\ kNm/rad$ (CoP)

$V_{Ed} = 191{,}6\ kN < 503{,}9\ kN$ (CoP) $\Rightarrow$ ok!

$\Rightarrow M_{Ed} = 269\ kNm < 313{,}4\ kNm$ (CoP) $\Rightarrow$ ok!

48

23-10-2008

B

Single-sided joint configuration with M30 10.9 bolts

At construction stage:

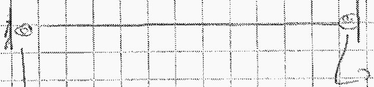

$\hookrightarrow \frac{S_{j,ini}}{2}$ double-sided

$\hookrightarrow \frac{S_{j,ini}}{2}$ single-sided

$\hookrightarrow = \cancel{}\,28\,390$ kNm/rad

$$\Rightarrow \begin{cases} V_{Ed} = 183{,}3 \text{ kN} \\ M_{Ed} = 2\cancel{1}6 \text{ kNm} \end{cases}$$

$\Rightarrow$ OK with resistance computed with COP

At composite stage:

Ductility criteria for the rebars:

$$A_s \leq \frac{1{,}1 \cdot 0{,}85\,(f_{ck}/\gamma_c) \cdot b_c \cdot d_{eff}}{\beta\,(f_{sk}/\gamma_s)} = \frac{1{,}1 \cdot 0{,}85 \cdot \frac{25}{1{,}5} \cdot 300 \cdot 62}{1\left(\frac{500}{1{,}15}\right)}$$

A_s ↓ 1131 mm^2 $= 666{,}7 \text{ mm}^2$

$\Rightarrow$ It is not possible to use the same amount of rebars than for the double sided joint if this criteria has to be respected

$\Rightarrow$ We will define the amount of rebars to respect this criteria

$\Rightarrow$ ~~6~~ $\phi 12$ mm (3 each side of the column)

$\Rightarrow$ 679 mm^2 $\Rightarrow$ OK!

$\rightarrow F_{slab} = 679\,\frac{f_{sk}}{\gamma_s} = 295$ kN

$F_c = 1133{,}65$ kN

$$\begin{cases} \text{row } 1 \rightarrow F_{Rd,1} = 437{,}37 \text{ kN (EPB)} \\ \text{row } 2 \Rightarrow F_{Rd,2} = 113{,}89 \text{ kN (EPB)} \\ \text{row } 3 \Rightarrow F_{Rd,3} = 370{,}46 \text{ kN (EPB)} \\ \text{row } 4 \Rightarrow F_{Rd,4} = 7{,}26 \text{ kN (WPSi)} \end{cases}$$

(49)

23-10-2008
(6)

$F_{2nm} + F_{Rd,1} + F_{Rd,2} = 946,4\ kN$

$F_c - 846,4 = 287,23\ kN$

=> elastic distributi. between rows 3 & 4

=> $F_4 = 84\ kN \Rightarrow F_3 = 203\ kN$

$\Rightarrow M_{Rd} = 288 \cdot 0,6314 + 437,37 \cdot 0,4764 + 113,88 \cdot 0,3864 + 203 \cdot 0,1264$
$+ 84 \cdot 0,0564$
$= \underline{472,24\ kNm}$

Stiffness of the joint

row 1 : $k_1 = 1,72$ mm
row 2 : $k_2 = 1,54$ mm
row 3 : $k_3 = 1,54$ mm
row 4 : $k_4 = 1,72$ mm
$k_c = 10,8$ mm
$k_{shear} = 4,7$ mm

$k_{anm} = k_{st} \cdot k_n$

k_{st} :

$A_s = 675\ mm^2$

$\beta = 1$

$K_\beta = \beta \cdot (4,3 \cdot \beta^2 - 8,9\beta + 7,2) = 2,6$

$\Rightarrow k_{st} = 0,6$ mm

k_n :

$\xi = 7,8$
$\nu = 3,5$
$K_{sc} = 329654,9$

$\Rightarrow k_{n} = 0,73$

$\Rightarrow k_{anm} = 0,44$ mm

50

23-10-2008

10

$\Rightarrow z_{eq} = 417{,}9\ mm \Rightarrow k_{eq} = 4{,}82\ mm$

$$\Rightarrow S_{j,ini} = \frac{210000\,(417{,}9)^2}{\frac{1}{4{,}82} + \frac{1}{10{,}83} + \frac{1}{4{,}7}}$$

$= 71559{,}34\ kNm/rad$

$\Rightarrow$ Analysis of the beam

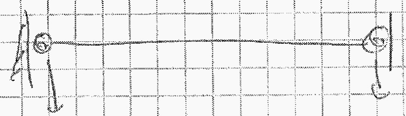

$\frac{71559{,}34}{2}$ $\qquad \frac{182111{,}32}{2} = 91056\ kNm/rad$

$= 35779{,}67\ kNm/rad$

$\Rightarrow M_{Ed} = 326{,}9\ kNm < 472{,}24\ kNm$

$\Rightarrow$ ok!

23-10-2009
(II)

Proposed solution:

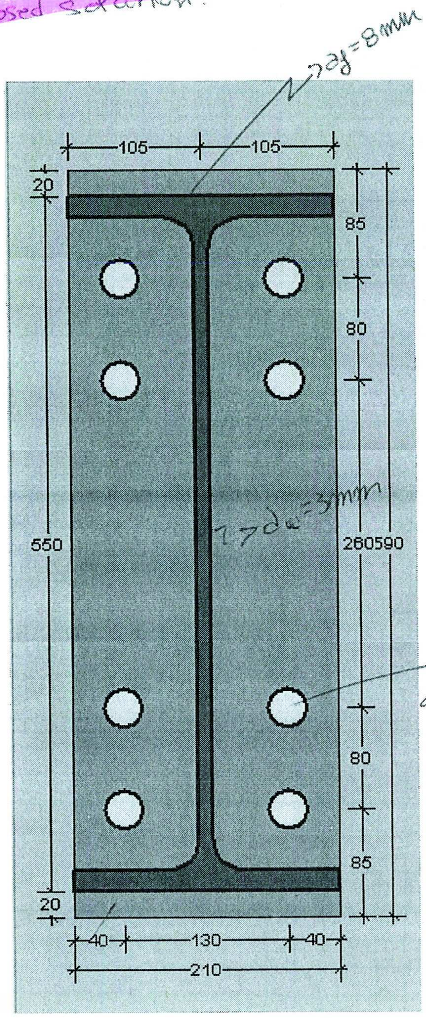

thickness: 15mm

Summary:

double-sided joint: 10 ϕ12mm S500

$M_{Rd} = 578,8$ kNm
$V_{Rd} = 512,8$ kN
$S_{j,ini} = 182111$ kNm/rad

Collapse mode: column web in compression

Single-sided joint: 6 ϕ12mm S500

$M_{Rd} = 472,24$ kNm
$V_{Rd} = 512,8$ kN
$S_{j,ini} = 71558,54$ kNm/rad

Collapse mode: column web in shear

Remark: another solution with 5 bolt rows with
M27 10.8 bolts could also work
The latter has not been designed in details

52

23-10-2009

Annex 1: double-sided joint with M30 10.9 bolts

CoP computation

Calcul d'assemblage de bâtiment suivant l'Eurocode 3 - Annexe J révisée

1. DONNéES

1.1 DONNéES DU PROJET

projet ....:	ROBUSTFIRE
structure ....:	Reference Structure
assemblage ....:	HEB300 S460 - IPE550 S355
identitif. de l'assemblage ..:	Main joint - double-sided with M27 M30
ingénieur ....:	JF Demonceau
date ....:	23/10/2009
procédure de calcul ....:	analyse plastique / vérification plastique du noeud
atmosphère ....:	non corrosive
système structural ....:	contreventé

1.2 principales données de l'assemblage

poutre :	IPE 550, S 355
colonne :	HE 300 B, S460 (MATéRIEL
plat d'about non débordan	590 X 210 X 15, S 355

1.3 caractéristiques mécaniques

	limite élastique N/mm²	résistance ultime N/mm²
âme de la poutre .....:	355.00	510.00
semelle de la poutre .:	355.00	510.00
âme de la colonne ....:	460.00	530.00
semelle de la colonne :	460.00	530.00
plat d'about ....:	355.00	510.00
boulons en traction ..:	900.00	1000.00

1.4 caractéristiques géométriques

1.4.1 poutre : IPE 550, S 355

hauteur ....:	550.00	mm
largeur ....:	210.00	mm
épaisseur de semelle ....:	17.20	mm
épaisseur d'âme ....:	11.10	mm
rayon de gorge ....:	24.00	mm
inertie ....:	67116.52	cm4
aire ....:	134.42	cm²
longueur de la poutre connectée à la colonne ....:	10000.00	mm
inclinaison de la poutre ....:	0.00	°

1.4.2 colonne : HE 300 B, S460 (MATéRIEL

hauteur ....:	300.00	mm
largeur ....:	300.00	mm
épaisseur de semelle ....:	19.00	mm
épaisseur d'âme ....:	11.00	mm

rayon de gorge ....:	27.00	mm
inertie ....:	25165.68	cm4
aire ....:	149.08	cm²

1.4.3 plat d'about 590 X 210 X 15, S 355

distance verticale entre la semelle de la poutre et le bord du plat d'about ....:	20.00	mm
distance verticale entre les boulons et le bord du plat d'about ....:	85.00	mm
distance verticale entre les rangée de boulons 1 et 2 ....:	80.00	mm
distance verticale entre les rangée de boulons 2 et 3 ....:	260.00	mm
distance verticale entre les rangée de boulons 3 et 4 ....:	80.00	mm
distance horizontale entre les boulons ....:	130.00	mm
distance horizontale entre les boulons et le bord du plat d'about ....:	40.00	mm

1.4.4 boulons en traction 10.9

section résistante ....:	561.00	mm²
diamètre du fût ....:	30.00	mm
diamètre des trous ....:	33.00	mm
épaisseur de la tête de boulon ....:	19.00	mm
épaisseur de l'écrou ....:	24.00	mm
épaisseur totale des rondelles par boulon ....:	10.00	mm
diamètre des rondelles ....:	56.00	mm

1.5 facteurs de sécurité

gamma M0 ....:	1.00
gamma M1 ....:	1.00
gamma Mb ....:	1.25
gamma Mw ....:	1.25

1.6 Résultat de l'optimisation des soudures

épaisseurs minimales des soudures pour la procédure de calcul choisie de la structure et des noeuds
(soudures calculées pour développer la pleine capacité du noeud)

épaisseur de la soudure assemblant la semelle de la poutre ..:	7.5	mm
épaisseur de la soudure assemblant l'âme de la poutre ....:	3.0	mm

2. PROPRIéTéS DU NOEUD SOUS MOMENT POSITIF

2.1 CALCUL DES COMPOSANTES

2.1.1 âme de la colonne en compression

largeur effective .... (Form. J.20) :	l1	=	298.39	mm
	l2	=	292.80	mm
	=> beff	=	292.80	mm
coefficient d'interaction .... (Table J.5) :	RHO	=	1.00	
contrainte de compression longitudinale dans l'âme adjacente au rayon de gorge ....:	Sigma	=	0.00	N/mm²

```
facteur de réduction .............. ( Form. J.22 ) : kwc      =        1.00

résistance : ( Form. J.17 )
   * voilement de l'âme :
     élancement ..................................: LAMBDA =        0.98
     résistance ..................................: Fc2    =     1481.55 kN

résistance .......................................: FcwcRd =     1175.38 kN

coefficient de raideur ............ ( Form. J.40 ) : k2     =       10.84 mm
```

2.1.2 semelle de la colonne en flexion

```
paramètres géométriques ............ ( Fig. J.25 ) : e     =       85.00 mm
======================                                emin  =       40.00 mm
                                                      m     =       37.90 mm
                                                      n     =       40.00 mm
                                                      ew    =       14.00 mm
```

2.1.2.1 longueur effective du T équivalent (Tables J.6 - J.7)

```
1) boulons pris individuellement

   * mécanismes circulaires :
       2 Pi m ....................................: l      =      238.13 mm
   * autres mécanismes :
       4 m + 1.25 e ..............................: l      =      257.85 mm

   pour toutes les rangées de boulons :
   * mécanismes circulaires ......................: leff   =      238.13 mm
   * autres mécanismes ...........................: leff   =      257.85 mm

2) boulons appartenant d'un groupe

   groupe entre rangées de boulons n°
```

groupe entre rangées de boulons n°	mécanismes circulaires (mm)	autres mécanismes (mm)
1 - 2	398.13	337.8
1 - 3	918.13	597.8
1 - 4	1078.13	677.8
2 - 3	758.13	517.8
2 - 4	918.13	597.8
3 - 4	398.13	337.8

2.1.2.2 résistance

```
( J.3.5.4.2 )
résistance d'un boulon ............ ( Table 6.5.3 ) : BtRd   =      403.92 kN

1) boulons pris individuellement
   ----------------------------

*  rangée de boulons n° 1

   contrainte compression longitudinale semelle ....: Sigma  =        0.00 N/mm²
   facteur de réduction ............ ( Form. J.29 ) : kfc    =        1.00

   mode de ruine du T équivalent ( J.3.2.1 )

   résistance plastique du T équivalent ( Form. J.7 )
      plastification semelle .......................: Mpl1Rd =     9886.08 Nm
      ruine boulon et plastification semelle .......: Mpl2Rd =    10704.64 Nm
```

```
mode 1: plastification semelle ..................: F1Rd   =     1043.39 kN
mode 2: ruine boulons et plastification semelle .: F2Rd   =      689.64 kN
mode 3: ruine boulons ...........................: F3Rd   =      807.84 kN
        ( Form. J.4 - J.5 - J.6 )

résistance ..................................: FtRd(1)    =      689.64 kN

* rangée de boulons n° 2

contrainte compression longitudinale semelle ....: Sigma  =        0.00 N/mm²
facteur de réduction ........... ( Form. J.29 ) : kfc     =        1.00

mode de ruine du T équivalent ( J.3.2.1 )

résistance plastique du T équivalent ( Form. J.7 )
   plastification semelle .......................: Mpl1Rd =     9886.08 Nm
   ruine boulon et plastification semelle .......: Mpl2Rd =    10704.64 Nm

mode 1: plastification semelle ..................: F1Rd   =     1043.39 kN
mode 2: ruine boulons et plastification semelle .: F2Rd   =      689.64 kN
mode 3: ruine boulons ...........................: F3Rd   =      807.84 kN
        ( Form. J.4 - J.5 - J.6 )

résistance ..................................: FtRd(2)    =      689.64 kN

* rangée de boulons n° 3

contrainte compression longitudinale semelle ....: Sigma  =        0.00 N/mm²
facteur de réduction ........... ( Form. J.29 ) : kfc     =        1.00

mode de ruine du T équivalent ( J.3.2.1 )

résistance plastique du T équivalent ( Form. J.7 )
   plastification semelle .......................: Mpl1Rd =     9886.08 Nm
   ruine boulon et plastification semelle .......: Mpl2Rd =    10704.64 Nm

mode 1: plastification semelle ..................: F1Rd   =     1043.39 kN
mode 2: ruine boulons et plastification semelle .: F2Rd   =      689.64 kN
mode 3: ruine boulons ...........................: F3Rd   =      807.84 kN
        ( Form. J.4 - J.5 - J.6 )

résistance ..................................: FtRd(3)    =      689.64 kN

* rangée de boulons n° 4

contrainte compression longitudinale semelle ....: Sigma  =        0.00 N/mm²
facteur de réduction ........... ( Form. J.29 ) : kfc     =        1.00

mode de ruine du T équivalent ( J.3.2.1 )

résistance plastique du T équivalent ( Form. J.7 )
   plastification semelle .......................: Mpl1Rd =     9886.08 Nm
   ruine boulon et plastification semelle .......: Mpl2Rd =    10704.64 Nm

mode 1: plastification semelle ..................: F1Rd   =     1043.39 kN
mode 2: ruine boulons et plastification semelle .: F2Rd   =      689.64 kN
mode 3: ruine boulons ...........................: F3Rd   =      807.84 kN
        ( Form. J.4 - J.5 - J.6 )

résistance ..................................: FtRd(4)    =      689.64 kN

2) boulons appartenant d'un groupe
```

```
------------------------------

*  groupe entre rangées de boulons n° 1 et n° 2

   contrainte compression longitudinale semelle ....: Sigma   =       0.00 N/mm²
   facteur de réduction ........... ( Form. J.29 ) : kfc      =       1.00

   mode de ruine du T équivalent ( J.3.2.1 )

   résistance plastique du T équivalent ( Form. J.7 )
      plastification semelle ......................: Mpl1Rd =    14025.84 Nm
      ruine boulon et plastification semelle .......: Mpl2Rd =    14025.84 Nm

   mode 1: plastification semelle .................: F1Rd     =    1480.30 kN
   mode 2: ruine boulons et plastification semelle .: F2Rd    =    1189.72 kN
   mode 3: ruine boulons ..........................: F3Rd     =    1615.68 kN
   résistance .................................: FtRd(1,2)=       1189.72 kN

*  groupe entre rangées de boulons n° 1 et n° 3

   contrainte compression longitudinale semelle ....: Sigma   =       0.00 N/mm²
   facteur de réduction ........... ( Form. J.29 ) : kfc      =       1.00

   mode de ruine du T équivalent ( J.3.2.1 )

   résistance plastique du T équivalent ( Form. J.7 )
      plastification semelle ......................: Mpl1Rd =    24819.74 Nm
      ruine boulon et plastification semelle .......: Mpl2Rd =    24819.74 Nm

   mode 1: plastification semelle .................: F1Rd     =    2619.50 kN
   mode 2: ruine boulons et plastification semelle .: F2Rd    =    1881.65 kN
   mode 3: ruine boulons ..........................: F3Rd     =    2423.52 kN
   résistance .................................: FtRd(1,3)=       1881.65 kN

*  groupe entre rangées de boulons n° 1 et n° 4

   contrainte compression longitudinale semelle ....: Sigma   =       0.00 N/mm²
   facteur de réduction ........... ( Form. J.29 ) : kfc      =       1.00

   mode de ruine du T équivalent ( J.3.2.1 )

   résistance plastique du T équivalent ( Form. J.7 )
      plastification semelle ......................: Mpl1Rd =    28140.94 Nm
      ruine boulon et plastification semelle .......: Mpl2Rd =    28140.94 Nm

   mode 1: plastification semelle .................: F1Rd     =    2970.02 kN
   mode 2: ruine boulons et plastification semelle .: F2Rd    =    2381.72 kN
   mode 3: ruine boulons ..........................: F3Rd     =    3231.36 kN
   résistance .................................: FtRd(1,4)=       2381.72 kN

*  groupe entre rangées de boulons n° 2 et n° 3

   contrainte compression longitudinale semelle ....: Sigma   =       0.00 N/mm²
   facteur de réduction ........... ( Form. J.29 ) : kfc      =       1.00

   mode de ruine du T équivalent ( J.3.2.1 )

   résistance plastique du T équivalent ( Form. J.7 )
      plastification semelle ......................: Mpl1Rd =    21498.54 Nm
      ruine boulon et plastification semelle .......: Mpl2Rd =    21498.54 Nm

   mode 1: plastification semelle .................: F1Rd     =    2268.98 kN
   mode 2: ruine boulons et plastification semelle .: F2Rd    =    1381.57 kN
```

```
mode 3: ruine boulons ..........................: F3Rd      =     1615.68 kN
résistance ...................................: FtRd(2,3)=     1381.57 kN

* groupe entre rangées de boulons n° 2 et n° 4

contrainte compression longitudinale semelle ....: Sigma  =        0.00 N/mm²
facteur de réduction ........... ( Form. J.29 ) : kfc     =        1.00

mode de ruine du T équivalent ( J.3.2.1 )

résistance plastique du T équivalent ( Form. J.7 )
   plastification semelle ......................: Mpl1Rd =     24819.74 Nm
   ruine boulon et plastification semelle .......: Mpl2Rd =     24819.74 Nm

mode 1: plastification semelle .................: F1Rd      =     2619.50 kN
mode 2: ruine boulons et plastification semelle .: F2Rd      =     1881.65 kN
mode 3: ruine boulons ..........................: F3Rd      =     2423.52 kN
résistance ...................................: FtRd(2,4)=     1881.65 kN

* groupe entre rangées de boulons n° 3 et n° 4

contrainte compression longitudinale semelle ....: Sigma  =        0.00 N/mm²
facteur de réduction ........... ( Form. J.29 ) : kfc     =        1.00

mode de ruine du T équivalent ( J.3.2.1 )

résistance plastique du T équivalent ( Form. J.7 )
   plastification semelle ......................: Mpl1Rd =     14025.84 Nm
   ruine boulon et plastification semelle .......: Mpl2Rd =     14025.84 Nm

mode 1: plastification semelle .................: F1Rd      =     1480.30 kN
mode 2: ruine boulons et plastification semelle .: F2Rd      =     1189.72 kN
mode 3: ruine boulons ..........................: F3Rd      =     1615.68 kN
résistance ...................................: FtRd(3,4)=     1189.72 kN
```

2.1.2.3 raideur

```
* longueur effective du T équivalent
  rangées de boulons individuelles ou appartenant à un groupe

  rangée de boulons n° 1 ......................: beff(1)   =      168.92 mm
  rangée de boulons n° 2 ......................: beff(2)   =      168.92 mm
  rangée de boulons n° 3 ......................: beff(3)   =      168.92 mm
  rangée de boulons n° 4 ......................: beff(4)   =      168.92 mm

* coefficient de raideur ( Form. J.42 )

  rangée de boulons n° 1 ......................: k3(1)     =       18.09 mm
  rangée de boulons n° 2 ......................: k3(2)     =       18.09 mm
  rangée de boulons n° 3 ......................: k3(3)     =       18.09 mm
  rangée de boulons n° 4 ......................: k3(4)     =       18.09 mm
```

2.1.3 âme de la colonne en traction

2.1.3.1 résistance

rangée de boulons n°	coefficient d'interaction (Table J.5)	résistance (kN)
1	1.00	1304.72
2	1.00	1304.72
3	1.00	1304.72
4	1.00	1304.72

(59)

groupe entre rangées de boulons n°

1 - 2	1.00	1709.52
1 - 3	1.00	3025.12
1 - 4	1.00	3429.92
2 - 3	1.00	2620.32
2 - 4	1.00	3025.12
3 - 4	1.00	1709.52

2.1.3.2 raideur

```
rangée de boulons n° 1 .......................: k4(1)    =     6.25 mm
rangée de boulons n° 2 .......................: k4(2)    =     6.25 mm
rangée de boulons n° 3 .......................: k4(3)    =     6.25 mm
rangée de boulons n° 4 .......................: k4(4)    =     6.25 mm
```

2.1.4 plat d'about en flexion

```
paramètres géométriques ............ ( Fig. J.28 ) : e      =    85.00 mm
=======================                              m      =    56.06 mm

  rangée de boulons n° 1 (sous la semelle sup de la: m1     =    56.06 mm
                                                     m2     =    39.32 mm
     détermination du coefficient alpha ...........: Lambda1=     0.58
        ( Fig. J.27 )                                Lambda2=     0.41
                                                     ALPHA  =     5.48

  rangée de boulons n° 4 (jusqu'à la semelle inf de: m1     =    56.06 mm
                                                     m2     =    39.32 mm
     détermination du coefficient alpha ...........: Lambda1=     0.58
        ( Fig. J.27 )                                Lambda2=     0.41
                                                     ALPHA  =     5.48
```

2.1.4.1 longueur effective du T équivalent (Tables J.8) :

```
1) boulons pris individuellement

   rangée de boulons n° 1 (influence de la semelle supérieure de la poutre)
   * mécanismes circulaires :
        2 Pi m1 ..................................: leff   =    352.21 mm
   * autres mécanismes :
        Alpha m1 .................................: leff   =    307.28 mm

   rangée de boulons n° 2 et n° 3 (pas d'influence des semelles de la poutre)
   * mécanismes circulaires :
        2 Pi m1 ..................................: leff   =    352.21 mm
   * autres mécanismes :
        4 m1 + 1.25 e ............................: leff   =    274.22 mm

   rangée de boulons n° 4 (influence de la semelle inférieure de la poutre)
   * mécanismes circulaires :
        2 Pi m1 ..................................: leff   =    352.21 mm
   * autres mécanismes :
        Alpha m1 .................................: leff   =    307.28 mm

2) boulons appartenant d'un groupe

   groupe entre rangées de boulons n°
                              mécanismes circulaires        autres mécanismes
                                      (mm)                        (mm)
```

1 - 2	512.	387.2
1 - 3	1032.	647.2
1 - 4	1192.	760.3
2 - 3	872.	534.2
2 - 4	1032.	647.2
3 - 4	512.	387.2

2.1.4.2 résistance

```
1) boulons pris individuellement

*  rangée de boulons n° 1

   mode de ruine du T équivalent ( J.3.2.1 )

   résistance plastique du T équivalent ( Form. J.7 )
      plastification semelle .......................: Mpl1Rd =    6136.07 Nm
      ruine boulon et plastification semelle .......: Mpl2Rd =    6136.07 Nm

   mode 1: plastification semelle .................: F1Rd   =     437.85 kN
   mode 2: ruine boulons et plastification semelle .: F2Rd   =     464.16 kN
   mode 3: ruine boulons ..........................: F3Rd   =     807.84 kN
           ( Form. J.4 - J.5 - J.6 )

   résistance .................................: FtepRd(1)=     437.85 kN

*  rangée de boulons n° 2

   mode de ruine du T équivalent ( J.3.2.1 )

   résistance plastique du T équivalent ( Form. J.7 )
      plastification semelle .......................: Mpl1Rd =    5475.90 Nm
      ruine boulon et plastification semelle .......: Mpl2Rd =    5475.90 Nm

   mode 1: plastification semelle .................: F1Rd   =     390.75 kN
   mode 2: ruine boulons et plastification semelle .: F2Rd   =     450.42 kN
   mode 3: ruine boulons ..........................: F3Rd   =     807.84 kN

   résistance .................................: FtepRd(2)=     390.75 kN

*  rangée de boulons n° 3

   mode de ruine du T équivalent ( J.3.2.1 )

   résistance plastique du T équivalent ( Form. J.7 )
      plastification semelle .......................: Mpl1Rd =    5475.90 Nm
      ruine boulon et plastification semelle .......: Mpl2Rd =    5475.90 Nm

   mode 1: plastification semelle .................: F1Rd   =     390.75 kN
   mode 2: ruine boulons et plastification semelle .: F2Rd   =     450.42 kN
   mode 3: ruine boulons ..........................: F3Rd   =     807.84 kN

   résistance .................................: FtepRd(3)=     390.75 kN

*  rangée de boulons n° 4

   mode de ruine du T équivalent ( J.3.2.1 )

   résistance plastique du T équivalent ( Form. J.7 )
      plastification semelle .......................: Mpl1Rd =    6136.07 Nm
      ruine boulon et plastification semelle .......: Mpl2Rd =    6136.07 Nm

   mode 1: plastification semelle .................: F1Rd   =     437.85 kN
```

```
mode 2: ruine boulons et plastification semelle .: F2Rd   =      464.16 kN
mode 3: ruine boulons ...........................: F3Rd   =      807.84 kN

résistance ..................................: FtepRd(4)=      437.85 kN

2) boulons appartenant d'un groupe

*  groupe entre rangées de boulons n° 1 et n° 2

   mode de ruine du T équivalent  ( J.3.2.1 )

   résistance plastique du T équivalent  ( Form. J.7 )
      plastification semelle ......................: Mpl1Rd =     7733.57 Nm
      ruine boulon et plastification semelle .......: Mpl2Rd =     7733.57 Nm

   mode 1: plastification semelle .................: F1Rd   =      551.85 kN
   mode 2: ruine boulons et plastification semelle .: F2Rd   =      833.83 kN
   mode 3: ruine boulons ..........................: F3Rd   =     1615.68 kN

   résistance .................................: FtRd(1,2)=      551.85 kN

*  groupe entre rangées de boulons n° 1 et n° 3

   mode de ruine du T équivalent  ( J.3.2.1 )

   résistance plastique du T équivalent  ( Form. J.7 )
      plastification semelle ......................: Mpl1Rd =    12925.45 Nm
      ruine boulon et plastification semelle .......: Mpl2Rd =    12925.45 Nm

   mode 1: plastification semelle .................: F1Rd   =      922.33 kN
   mode 2: ruine boulons et plastification semelle .: F2Rd   =     1278.34 kN
   mode 3: ruine boulons ..........................: F3Rd   =     2423.52 kN

   résistance .................................: FtRd(1,3)=      922.33 kN

*  groupe entre rangées de boulons n° 1 et n° 4

   mode de ruine du T équivalent  ( J.3.2.1 )

   résistance plastique du T équivalent  ( Form. J.7 )
      plastification semelle ......................: Mpl1Rd =    15183.12 Nm
      ruine boulon et plastification semelle .......: Mpl2Rd =    15183.12 Nm

   mode 1: plastification semelle .................: F1Rd   =     1083.43 kN
   mode 2: ruine boulons et plastification semelle .: F2Rd   =     1661.75 kN
   mode 3: ruine boulons ..........................: F3Rd   =     3231.36 kN

   résistance .................................: FtRd(1,4)=     1083.43 kN

*  groupe entre rangées de boulons n° 2 et n° 3

   mode de ruine du T équivalent  ( J.3.2.1 )

   résistance plastique du T équivalent  ( Form. J.7 )
      plastification semelle ......................: Mpl1Rd =    10667.78 Nm
      ruine boulon et plastification semelle .......: Mpl2Rd =    10667.78 Nm

   mode 1: plastification semelle .................: F1Rd   =      761.22 kN
   mode 2: ruine boulons et plastification semelle .: F2Rd   =      894.92 kN
   mode 3: ruine boulons ..........................: F3Rd   =     1615.68 kN

   résistance .................................: FtRd(2,3)=      761.22 kN
```

* groupe entre rangées de boulons n° 2 et n° 4

mode de ruine du T équivalent (J.3.2.1)

résistance plastique du T équivalent (Form. J.7)

plastification semelle ....:	Mpl1Rd =	12925.45	Nm
ruine boulon et plastification semelle ....:	Mpl2Rd =	12925.45	Nm
mode 1: plastification semelle ....:	F1Rd =	922.33	kN
mode 2: ruine boulons et plastification semelle .:	F2Rd =	1278.34	kN
mode 3: ruine boulons ....:	F3Rd =	2423.52	kN
résistance ....:	FtRd(2,4)=	922.33	kN

* groupe entre rangées de boulons n° 3 et n° 4

mode de ruine du T équivalent (J.3.2.1)

résistance plastique du T équivalent (Form. J.7)

plastification semelle ....:	Mpl1Rd =	7733.57	Nm
ruine boulon et plastification semelle ....:	Mpl2Rd =	7733.57	Nm
mode 1: plastification semelle ....:	F1Rd =	551.85	kN
mode 2: ruine boulons et plastification semelle .:	F2Rd =	833.83	kN
mode 3: ruine boulons ....:	F3Rd =	1615.68	kN
résistance ....:	FtRd(3,4)=	551.85	kN

2.1.4.3 raideur

* longueur effective du T équivalent
  rangées de boulons individuelles ou appartenant à un groupe

rangée de boulons n° 1 ....:	leff(1) =	210.17	mm
rangée de boulons n° 2 ....:	leff(2) =	170.00	mm
rangée de boulons n° 3 ....:	leff(3) =	170.00	mm
rangée de boulons n° 4 ....:	leff(4) =	210.17	mm

* coefficient de raideur (Form. J.43)

rangée de boulons n° 1 ....:	k5(1) =	3.42	mm
rangée de boulons n° 2 ....:	k5(2) =	2.77	mm
rangée de boulons n° 3 ....:	k5(3) =	2.77	mm
rangée de boulons n° 4 ....:	k5(4) =	3.42	mm

2.1.4.4 boulons en traction

longueur du boulon .... (J.4.4.10) :	Lb =	65.50	mm
résistance .... (Table 6.5.3) :	BtRd =	403.92	kN
coefficient de raideur .... (Form. J.45) :	k7 =	13.70	mm

2.1.5 semelle de la poutre en compression

moment résistant de la poutre ....:	McRd =	989.39	kNm
résistance .... (Form. J.30) :	FcfbRd =	1856.96	kN

2.1.6 âme de la poutre en traction

largeur effective
  => égales à celles de la platine en flexion

2.1.6.1 résistance

rangée de boulons n°		résistance (kN) (Form. J.31) FtwbRd(i)
1	:	1210.85
2	:	1080.58
3	:	1080.58
4	:	1210.85

groupe entre rangées de b		FtwbRd(i,j)
1 - 2	:	1526.09
1 - 3	:	2550.62
1 - 4	:	2996.13
2 - 3	:	2105.11
2 - 4	:	2550.62
3 - 4	:	1526.09

2.2 ASSEMBLAGE DES DIFFéRENTES COMPOSANTES

2.2.1 résistance (Fig. J.34)

2.2.1.1 rangée de boulons n° 1

	résistance (kN)
âme de la colonne en compression ....:	1175.38
semelle de la colonne en flexion ....:	689.64
âme de la colonne en traction ....:	1304.72
plat d'about en flexion ....:	437.85
boulons en traction ....:	807.84
semelle de la poutre en compression ....:	1856.96
âme de la poutre en traction ....:	1210.85
	---------
résistance de la rangée de boulons n° 1 ....: Frd(1) =	437.85 kN

2.2.1.2 rangée de boulons n° 2

résistance (kN)

2.2.1.2.1 1) boulons pris individuellement

âme de la colonne en compression ....:	737.53
semelle de la colonne en flexion ....:	689.64
âme de la colonne en traction ....:	1304.72
plat d'about en flexion ....:	390.75
boulons en traction ....:	807.84
semelle de la poutre en compression ....:	1419.10
âme de la poutre en traction ....:	1080.58

2.2.1.2.2 2) boulons appartenant d'un groupe

groupe entre rangées de boulons n° 1 et n° 2

semelle de la colonne en flexion ....:	751.86
âme de la colonne en traction ....:	1271.67
plat d'about en flexion ....:	113.99
âme de la poutre en traction ....:	1088.24
	---------

résistance de la rangée de boulons n° 2 ....: Frd(2) = 113.99 kN

2.2.1.3 rangée de boulons n° 3

2.2.1.3.1 1) boulons pris individuellement

	résistance (kN)
âme de la colonne en compression ....:	623.54
semelle de la colonne en flexion ....:	689.64
âme de la colonne en traction ....:	1304.72
plat d'about en flexion ....:	390.75
boulons en traction ....:	807.84
semelle de la poutre en compression ....:	1305.11
âme de la poutre en traction ....:	1080.58

2.2.1.3.2 2) boulons appartenant d'un groupe

groupe entre rangées de boulons n° 1 et n° 3

semelle de la colonne en flexion ....:	1329.80
âme de la colonne en traction ....:	2473.27
plat d'about en flexion ....:	370.48
âme de la poutre en traction ....:	1998.77

groupe entre rangées de boulons n° 2 et n° 3

semelle de la colonne en flexion ....:	1267.58
âme de la colonne en traction ....:	2506.33
plat d'about en flexion ....:	647.23
âme de la poutre en traction ....:	1991.11

----

résistance de la rangée de boulons n° 3 ....: Frd(3) = 370.48 kN

2.2.1.4 rangée de boulons n° 4

2.2.1.4.1 1) boulons pris individuellement

	résistance (kN)
âme de la colonne en compression ....:	253.06
semelle de la colonne en flexion ....:	689.64
âme de la colonne en traction ....:	1304.72
plat d'about en flexion ....:	437.85
boulons en traction ....:	807.84
semelle de la poutre en compression ....:	934.63
âme de la poutre en traction ....:	1210.85

2.2.1.4.2 2) boulons appartenant d'un groupe

groupe entre rangées de boulons n° 1 et n° 4

semelle de la colonne en flexion ....:	1459.40
âme de la colonne en traction ....:	2507.60
plat d'about en flexion ....:	161.10
âme de la poutre en traction ....:	2073.81

groupe entre rangées de boulons n° 2 et n° 4

semelle de la colonne en flexion ....:	1397.17
âme de la colonne en traction ....:	2540.65
plat d'about en flexion ....:	437.85
âme de la poutre en traction ....:	2066.15

groupe entre rangées de boulons n° 3 et n° 4

semelle de la colonne en flexion ....:		819.24
âme de la colonne en traction ....:		1339.04
plat d'about en flexion ....:		181.37
âme de la poutre en traction ....:		1155.61
		---------
résistance de la rangée de boulons n° 4 ....:	Frd(4) =	161.10 kN

distribution plastique des efforts internes

2.2.1.5 résumé

résistance de la rangée de boulons n° 1 ....:	FRd(1) =	437.85 kN
résistance de la rangée de boulons n° 2 ....:	FRd(2) =	113.99 kN
résistance de la rangée de boulons n° 3 ....:	FRd(3) =	370.48 kN
résistance de la rangée de boulons n° 4 ....:	FRd(4) =	161.10 kN
résistance en flexion (ruine des soudures non consid:	MRdj =	313.40 kNm
résistance en flexion des soudures ....:	MRdw =	438.86 kNm
		---------
moment résistant .... (J.3.6) :		313.40 kNm
moment maximum élastique .... (J.2.1.2) :	Me =	208.93 kNm

2.2.2 raideur

2.2.2.1 détermination du coefficient de raideur équivalente

	raideur effective coefficient (mm) (Form. J.36)		bras de levier des forces internes	
rangée de boulons n°	1 : keff,1 =	1.72	h 1 =	476.40
rangée de boulons n°	2 : keff,2 =	1.54	h 2 =	396.40
rangée de boulons n°	3 : keff,3 =	1.54	h 3 =	136.40
rangée de boulons n°	4 : keff,4 =	1.72	h 4 =	56.40

bras de levier des forces internes . (Form. J.38) :	z =	383.76 mm
coefficient de raideur équivalente . (Form. J.36) :	keq =	4.53 mm

2.2.2.2 pourcentages de flexibilité

la flexibilité d'une rangée de boulons est la flexibilité relative de cette rangée en comparaison avec les autres (indépendamment des bras de levier)

pour la zone comprimée	29 %		
pour la zone tendue	71 %		
* rangée de boulons n° 1		24 %	
plat d'about en flexion			50 %
boulons en traction			13 %
* rangée de boulons n° 2		26 %	
plat d'about en flexion			56 %
boulons en traction			11 %
* rangée de boulons n° 3		26 %	
plat d'about en flexion			56 %
boulons en traction			11 %
* rangée de boulons n° 4		24 %	
plat d'about en flexion			50 %

```
boulons en traction                                  13 %
```

2.2.2.3 résumé

```
raideur initiale .................. ( Form. J.34 ) : Sji    =   98813.55 kNm/rad
raideur idéalisée ... ( J.2.1.2 - J.2.1.4 - T.J.3 ) : Sjn    =   49406.78 kNm/rad
raideur sécante ................... ( Form. J.34 ) : Sjs    =   33065.12 kNm/rad
```

2.2.3 résistance en cisaillement

```
résist cisaillement d'une rangée de ( Table 6.5.3 ) : FvRd   =     448.80 kN

semelle de la colonne en pression diamétrale ( Table 6.5.3 ):
                                         p1/(3d0)-0.25 =        0.56
                                         fub / fu      =        1.89
                                         =>      ALPHA =        0.56
   résist pression diamétrale d'une rangée de boulon: FbRd  =   674.38 kN

plat d'about en pression diamétrale :
                                         p1/(3d0)-0.25 =        0.56
                                         fub / fu      =        1.96
                                         =>      ALPHA =        0.56
   résist pression diamétrale d'une rangée de boulon: FbRd  =   347.13 kN

la résistance en cisaillement de la rangée de boulons soumise aux
   forces de traction et de cisaillement est réduite par un facteur 0,4/1,4 0.4/1.4
            ( J.3.1.2.(2b) )

résist cisaillement rangée de boulons n° 1 ........: Vrd(1) =     128.23 kN
résist cisaillement rangée de boulons n° 2 ........: Vrd(2) =     128.23 kN
résist cisaillement rangée de boulons n° 3 ........: Vrd(3) =     128.23 kN
résist cisaillement rangée de boulons n° 4 ........: Vrd(4) =     128.23 kN

résist cisaillement des soudures
   facteur de corrélation ......... ( 6.6.5.3.(5) ) : BETA  =       0.90
   longueur de la soudure .......................... : a     =     467.60 mm
   résist cisaillement des soudures ( 6.6.5.3.(4) ) : FwRd  =     734.32 kN

résistance au cisaillement de l'assemblage .........: VRd   =     512.91 kN
```

2.2.4 mode de ruine

```
rangée de boulons n° 1 : plat d'about en flexion
rangée de boulons n° 2 : plat d'about en flexion
rangée de boulons n° 3 : plat d'about en flexion
rangée de boulons n° 4 : plat d'about en flexion

capacité de rotation suffisante pour une analyse plastique
```

2.3 PROPRIéTéS DE CALCUL DU NOEUD POUR ANALYSE PLASTIQUE / VéRIFICATION PLASTIQUE DU NOEUD

```
moment résistant de calcul ........................: MRd    =     313.40 kNm

raideur initiale .................. ( Form. J.34 ) : Sji    =   98813.55 kNm/rad
raideur idéalisée ... ( J.2.1.2 - J.2.1.4 - T.J.3 ) : Sjn    =   49406.78 kNm/rad
```

3. RéFéRENCES

1 ENV 1993-1-1 : 1992,Eurocode 3: Design of steel structures.
Part 1.1: General rules and rules for buildings,
CEN, Brussels 1992.

2 ENV 1993-1-1 : 1992/A2, October 1998.
Revised Annex J of Eurocode 3, "Joints in Building Frames",
CEN, Brussels, October 1998.

68 23-10-2008

Annex 2: Single sided joint configuration with M30 10.9 bolts

CoP computation

Calcul d'assemblage de bâtiment suivant l'Eurocode 3 - Annexe J révisée

1. DONNéES

1.1 DONNéES DU PROJET

```
projet ......................: ROBUSTFIRE
structure ...................: Reference Structure
assemblage ..................: HEB300 S460 - IPE550 S355
identitif. de l'assemblage ..: Main joint - single-sided with M30
ingénieur ...................: JF Demonceau
date ........................: 23/10/2009

procédure de calcul .........: analyse plastique / vérification plastique du noeud

atmosphère ..................: non corrosive
système structural ..........: contreventé
```

1.2 principales données de l'assemblage

```
poutre :                   IPE 550,  S 355
colonne :                  HE 300 B,  S460 (MATéRIEL
plat d'about non débordan  590 X 210 X 15,  S 355
```

1.3 caractéristiques mécaniques

	limite élastique N/mm²	résistance ultime N/mm²
âme de la poutre .....:	355.00	510.00
semelle de la poutre .:	355.00	510.00
âme de la colonne ....:	460.00	530.00
semelle de la colonne :	460.00	530.00
plat d'about ....:	355.00	510.00
boulons en traction ..:	900.00	1000.00

1.4 caractéristiques géométriques

1.4.1 poutre : IPE 550, S 355

hauteur ....:	550.00	mm
largeur ....:	210.00	mm
épaisseur de semelle ....:	17.20	mm
épaisseur d'âme ....:	11.10	mm
rayon de gorge ....:	24.00	mm
inertie ....:	67116.52	cm4
aire ....:	134.42	cm²
longueur de la poutre connectée à la colonne ....:	10000.00	mm
inclinaison de la poutre ....:	0.00	°

1.4.2 colonne : HE 300 B, S460 (MATéRIEL

hauteur ....:	300.00	mm
largeur ....:	300.00	mm
épaisseur de semelle ....:	19.00	mm
épaisseur d'âme ....:	11.00	mm

rayon de gorge ....:	27.00	mm
inertie ....:	25165.68	cm4
aire ....:	149.08	cm²

1.4.3 plat d'about 590 X 210 X 15, S 355

distance verticale entre la semelle de la poutre et le bord du plat d'about ....:	20.00	mm
distance verticale entre les boulons et le bord du plat d'about ....:	85.00	mm
distance verticale entre les rangée de boulons 1 et 2 ....:	80.00	mm
distance verticale entre les rangée de boulons 2 et 3 ....:	260.00	mm
distance verticale entre les rangée de boulons 3 et 4 ....:	80.00	mm
distance horizontale entre les boulons ....:	130.00	mm
distance horizontale entre les boulons et le bord du plat d'about ....:	40.00	mm

1.4.4 boulons en traction 10.9

section résistante ....:	561.00	mm²
diamètre du fût ....:	30.00	mm
diamètre des trous ....:	33.00	mm
épaisseur de la tête de boulon ....:	19.00	mm
épaisseur de l'écrou ....:	24.00	mm
épaisseur totale des rondelles par boulon ....:	10.00	mm
diamètre des rondelles ....:	56.00	mm

1.5 facteurs de sécurité

gamma M0 ....:	1.00
gamma M1 ....:	1.00
gamma Mb ....:	1.25
gamma Mw ....:	1.25

1.6 Résultat de l'optimisation des soudures

épaisseurs minimales des soudures pour la procédure de calcul choisie de la structure et des noeuds
(soudures calculées pour développer la pleine capacité du noeud)

épaisseur de la soudure assemblant la semelle de la poutre ..:	7.3	mm
épaisseur de la soudure assemblant l'âme de la poutre ....:	3.0	mm

2. PROPRIéTéS DU NOEUD SOUS MOMENT POSITIF

2.1 CALCUL DES COMPOSANTES

2.1.1 panneau d'âme de la colonne en cisaillement

section cisaillée de la colonne ....:	Avc	=	47.43	cm²
coefficient beta .... (J.2.6.3) :	BETA	=	1.00	
résist plastique du panneau d'âme ....: (J.3.5.1)	VwpRd	=	1133.63	kN
résistance: vwprd/beta ....:	FwpRd	=	1133.63	kN
coefficient de raideur .... (Form. J.39) :	k1	=	4.70	mm

2.1.2 âme de la colonne en compression

```
largeur effective ................. ( Form. J.20 ) : l1     =     297.79 mm
                                                      l2     =     292.49 mm
                                                   => beff   =     292.49 mm

coefficient d'interaction .......... ( Table J.5 ) : RHO    =       0.79
contrainte de compression longitudinale dans l'âme adjacente
   au rayon de gorge .............................: Sigma  =       0.00 N/mm²
facteur de réduction .............. ( Form. J.22 ) : kwc    =       1.00

résistance : ( Form. J.17 )
   * voilement de l'âme :
     élancement ..................................: LAMBDA =       0.98
     résistance ..................................: Fc2    =    1170.69 kN

résistance .......................................: FcwcRd =     929.10 kN

coefficient de raideur ............ ( Form. J.40 ) : k2     =      10.83 mm
```

2.1.3 semelle de la colonne en flexion

```
paramètres géométriques ............ ( Fig. J.25 ) : e      =      85.00 mm
======================                               emin   =      40.00 mm
                                                     m      =      37.90 mm
                                                     n      =      40.00 mm
                                                     ew     =      14.00 mm
```

2.1.3.1 longueur effective du T équivalent (Tables J.6 - J.7)

```
1) boulons pris individuellement

   * mécanismes circulaires :
        2 Pi m ...................................: l      =     238.13 mm
   * autres mécanismes :
        4 m + 1.25 e .............................: l      =     257.85 mm

   pour toutes les rangées de boulons :
   * mécanismes circulaires ......................: leff   =     238.13 mm
   * autres mécanismes ...........................: leff   =     257.85 mm

2) boulons appartenant d'un groupe
```

groupe entre rangées de boulons n°	mécanismes circulaires (mm)	autres mécanismes (mm)
1 - 2	398.13	337.8
1 - 3	918.13	597.8
1 - 4	1078.13	677.8
2 - 3	758.13	517.8
2 - 4	918.13	597.8
3 - 4	398.13	337.8

2.1.3.2 résistance

```
( J.3.5.4.2 )
résistance d'un boulon ........... ( Table 6.5.3 ) : BtRd   =     403.92 kN

1) boulons pris individuellement
   ----------------------------
```

```
*  rangée de boulons n° 1

   contrainte compression longitudinale semelle ....: Sigma  =      0.00 N/mm²
   facteur de réduction ........... ( Form. J.29 ) : kfc    =      1.00

   mode de ruine du T équivalent ( J.3.2.1 )

   résistance plastique du T équivalent ( Form. J.7 )
      plastification semelle ......................: Mpl1Rd =   9886.08 Nm
      ruine boulon et plastification semelle .......: Mpl2Rd =  10704.64 Nm

   mode 1: plastification semelle .................: F1Rd   =   1043.39 kN
   mode 2: ruine boulons et plastification semelle .: F2Rd   =    689.64 kN
   mode 3: ruine boulons ..........................: F3Rd   =    807.84 kN
            ( Form. J.4 - J.5 - J.6 )

   résistance ..................................: FtRd(1)  =    689.64 kN

*  rangée de boulons n° 2

   contrainte compression longitudinale semelle ....: Sigma  =      0.00 N/mm²
   facteur de réduction ........... ( Form. J.29 ) : kfc    =      1.00

   mode de ruine du T équivalent ( J.3.2.1 )

   résistance plastique du T équivalent ( Form. J.7 )
      plastification semelle ......................: Mpl1Rd =   9886.08 Nm
      ruine boulon et plastification semelle .......: Mpl2Rd =  10704.64 Nm

   mode 1: plastification semelle .................: F1Rd   =   1043.39 kN
   mode 2: ruine boulons et plastification semelle .: F2Rd   =    689.64 kN
   mode 3: ruine boulons ..........................: F3Rd   =    807.84 kN
            ( Form. J.4 - J.5 - J.6 )

   résistance ..................................: FtRd(2)  =    689.64 kN

*  rangée de boulons n° 3

   contrainte compression longitudinale semelle ....: Sigma  =      0.00 N/mm²
   facteur de réduction ........... ( Form. J.29 ) : kfc    =      1.00

   mode de ruine du T équivalent ( J.3.2.1 )

   résistance plastique du T équivalent ( Form. J.7 )
      plastification semelle ......................: Mpl1Rd =   9886.08 Nm
      ruine boulon et plastification semelle .......: Mpl2Rd =  10704.64 Nm

   mode 1: plastification semelle .................: F1Rd   =   1043.39 kN
   mode 2: ruine boulons et plastification semelle .: F2Rd   =    689.64 kN
   mode 3: ruine boulons ..........................: F3Rd   =    807.84 kN
            ( Form. J.4 - J.5 - J.6 )

   résistance ..................................: FtRd(3)  =    689.64 kN

*  rangée de boulons n° 4

   contrainte compression longitudinale semelle ....: Sigma  =      0.00 N/mm²
   facteur de réduction ........... ( Form. J.29 ) : kfc    =      1.00

   mode de ruine du T équivalent ( J.3.2.1 )

   résistance plastique du T équivalent ( Form. J.7 )
```

```
   plastification semelle .......................: Mpl1Rd =     9886.08 Nm
   ruine boulon et plastification semelle .......: Mpl2Rd =    10704.64 Nm

mode 1: plastification semelle ..................: F1Rd   =     1043.39 kN
mode 2: ruine boulons et plastification semelle .: F2Rd   =      689.64 kN
mode 3: ruine boulons ...........................: F3Rd   =      807.84 kN
        ( Form. J.4 - J.5 - J.6 )

résistance ..................................: FtRd(4)   =      689.64 kN

2) boulons appartenant d'un groupe
   ------------------------------

*  groupe entre rangées de boulons n° 1 et n° 2

   contrainte compression longitudinale semelle ....: Sigma  =       0.00 N/mm²
   facteur de réduction ........... ( Form. J.29 ) : kfc    =       1.00

   mode de ruine du T équivalent ( J.3.2.1 )

   résistance plastique du T équivalent ( Form. J.7 )
      plastification semelle .......................: Mpl1Rd =    14025.84 Nm
      ruine boulon et plastification semelle .......: Mpl2Rd =    14025.84 Nm

   mode 1: plastification semelle ..................: F1Rd   =     1480.30 kN
   mode 2: ruine boulons et plastification semelle .: F2Rd   =     1189.72 kN
   mode 3: ruine boulons ...........................: F3Rd   =     1615.68 kN
   résistance ..................................: FtRd(1,2)=     1189.72 kN

*  groupe entre rangées de boulons n° 1 et n° 3

   contrainte compression longitudinale semelle ....: Sigma  =       0.00 N/mm²
   facteur de réduction ........... ( Form. J.29 ) : kfc    =       1.00

   mode de ruine du T équivalent ( J.3.2.1 )

   résistance plastique du T équivalent ( Form. J.7 )
      plastification semelle .......................: Mpl1Rd =    24819.74 Nm
      ruine boulon et plastification semelle .......: Mpl2Rd =    24819.74 Nm

   mode 1: plastification semelle ..................: F1Rd   =     2619.50 kN
   mode 2: ruine boulons et plastification semelle .: F2Rd   =     1881.65 kN
   mode 3: ruine boulons ...........................: F3Rd   =     2423.52 kN
   résistance ..................................: FtRd(1,3)=     1881.65 kN

*  groupe entre rangées de boulons n° 1 et n° 4

   contrainte compression longitudinale semelle ....: Sigma  =       0.00 N/mm²
   facteur de réduction ........... ( Form. J.29 ) : kfc    =       1.00

   mode de ruine du T équivalent ( J.3.2.1 )

   résistance plastique du T équivalent ( Form. J.7 )
      plastification semelle .......................: Mpl1Rd =    28140.94 Nm
      ruine boulon et plastification semelle .......: Mpl2Rd =    28140.94 Nm

   mode 1: plastification semelle ..................: F1Rd   =     2970.02 kN
   mode 2: ruine boulons et plastification semelle .: F2Rd   =     2381.72 kN
   mode 3: ruine boulons ...........................: F3Rd   =     3231.36 kN
   résistance ..................................: FtRd(1,4)=     2381.72 kN

*  groupe entre rangées de boulons n° 2 et n° 3
```

contrainte compression longitudinale semelle ....: Sigma = 0.00 N/mm²
facteur de réduction .... (Form. J.29) : kfc = 1.00

mode de ruine du T équivalent (J.3.2.1)

résistance plastique du T équivalent (Form. J.7)
plastification semelle ....: Mpl1Rd = 21498.54 Nm
ruine boulon et plastification semelle ....: Mpl2Rd = 21498.54 Nm

mode 1: plastification semelle ....: F1Rd = 2268.98 kN
mode 2: ruine boulons et plastification semelle .: F2Rd = 1381.57 kN
mode 3: ruine boulons ....: F3Rd = 1615.68 kN
résistance ....: FtRd(2,3)= 1381.57 kN

* groupe entre rangées de boulons n° 2 et n° 4

contrainte compression longitudinale semelle ....: Sigma = 0.00 N/mm²
facteur de réduction .... (Form. J.29) : kfc = 1.00

mode de ruine du T équivalent (J.3.2.1)

résistance plastique du T équivalent (Form. J.7)
plastification semelle ....: Mpl1Rd = 24819.74 Nm
ruine boulon et plastification semelle ....: Mpl2Rd = 24819.74 Nm

mode 1: plastification semelle ....: F1Rd = 2619.50 kN
mode 2: ruine boulons et plastification semelle .: F2Rd = 1881.65 kN
mode 3: ruine boulons ....: F3Rd = 2423.52 kN
résistance ....: FtRd(2,4)= 1881.65 kN

* groupe entre rangées de boulons n° 3 et n° 4

contrainte compression longitudinale semelle ....: Sigma = 0.00 N/mm²
facteur de réduction .... (Form. J.29) : kfc = 1.00

mode de ruine du T équivalent (J.3.2.1)

résistance plastique du T équivalent (Form. J.7)
plastification semelle ....: Mpl1Rd = 14025.84 Nm
ruine boulon et plastification semelle ....: Mpl2Rd = 14025.84 Nm

mode 1: plastification semelle ....: F1Rd = 1480.30 kN
mode 2: ruine boulons et plastification semelle .: F2Rd = 1189.72 kN
mode 3: ruine boulons ....: F3Rd = 1615.68 kN
résistance ....: FtRd(3,4)= 1189.72 kN

2.1.3.3 raideur

* longueur effective du T équivalent
rangées de boulons individuelles ou appartenant à un groupe

rangée de boulons n° 1 ....: beff(1) = 168.92 mm
rangée de boulons n° 2 ....: beff(2) = 168.92 mm
rangée de boulons n° 3 ....: beff(3) = 168.92 mm
rangée de boulons n° 4 ....: beff(4) = 168.92 mm

* coefficient de raideur (Form. J.42)

rangée de boulons n° 1 ....: k3(1) = 18.09 mm
rangée de boulons n° 2 ....: k3(2) = 18.09 mm
rangée de boulons n° 3 ....: k3(3) = 18.09 mm
rangée de boulons n° 4 ....: k3(4) = 18.09 mm

2.1.4 âme de la colonne en traction

2.1.4.1 résistance

rangée de boulons n°	coefficient d'interaction (Table J.5)	résistance (kN)
1	0.83	1077.97
2	0.83	1077.97
3	0.83	1077.97
4	0.83	1077.97
groupe entre rangées de boulons n°		
1 - 2	0.75	1274.84
1 - 3	0.53	1617.12
1 - 4	0.49	1671.02
2 - 3	0.59	1545.30
2 - 4	0.53	1617.12
3 - 4	0.75	1274.84

2.1.4.2 raideur

```
rangée de boulons n° 1 ......................: k4(1)    =     6.25 mm
rangée de boulons n° 2 ......................: k4(2)    =     6.25 mm
rangée de boulons n° 3 ......................: k4(3)    =     6.25 mm
rangée de boulons n° 4 ......................: k4(4)    =     6.25 mm
```

2.1.5 plat d'about en flexion

```
paramètres géométriques ............ ( Fig. J.28 ) : e        =    85.00 mm
======================                              m        =    56.06 mm

  rangée de boulons n° 1 (sous la semelle sup de la: m1       =    56.06 mm
                                                     m2       =    39.57 mm
     détermination du coefficient alpha ...........: Lambda1=      0.58
        ( Fig. J.27 )                                Lambda2=      0.41
                                                     ALPHA  =      5.48

  rangée de boulons n° 4 (jusqu'à la semelle inf de: m1       =    56.06 mm
                                                     m2       =    39.57 mm
     détermination du coefficient alpha ...........: Lambda1=      0.58
        ( Fig. J.27 )                                Lambda2=      0.41
                                                     ALPHA  =      5.48
```

2.1.5.1 longueur effective du T équivalent (Tables J.8) :

```
1) boulons pris individuellement

   rangée de boulons n° 1 (influence de la semelle supérieure de la poutre)
   * mécanismes circulaires :
        2 Pi m1 .................................: leff    =     352.21 mm
   * autres mécanismes :
        Alpha m1 ................................: leff    =     306.94 mm

   rangée de boulons n° 2 et n° 3 (pas d'influence des semelles de la poutre)
   * mécanismes circulaires :
        2 Pi m1 .................................: leff    =     352.21 mm
   * autres mécanismes :
        4 m1 + 1.25 e ...........................: leff    =     274.22 mm
```

```
   rangée de boulons n° 4 (influence de la semelle inférieure de la poutre)
   * mécanismes circulaires :
        2 Pi m1 ..................................: leff    =     352.21 mm
   * autres mécanismes :
        Alpha m1 .................................: leff    =     306.94 mm

2) boulons appartenant d'un groupe

   groupe entre rangées de boulons n°
                              mécanismes circulaires         autres mécanismes
                                       (mm)                        (mm)

               1 - 2                   512.                       386.9
               1 - 3                  1032.                       646.9
               1 - 4                  1192.                       759.6
               2 - 3                   872.                       534.2
               2 - 4                  1032.                       646.9
               3 - 4                   512.                       386.9
```

2.1.5.2 résistance

```
1) boulons pris individuellement

*  rangée de boulons n° 1

   mode de ruine du T équivalent ( J.3.2.1 )

   résistance plastique du T équivalent ( Form. J.7 )
      plastification semelle .......................: Mpl1Rd =     6129.29 Nm
      ruine boulon et plastification semelle .......: Mpl2Rd =     6129.29 Nm

   mode 1: plastification semelle ..................: F1Rd    =     437.37 kN
   mode 2: ruine boulons et plastification semelle .: F2Rd    =     464.02 kN
   mode 3: ruine boulons ...........................: F3Rd    =     807.84 kN
           ( Form. J.4 - J.5 - J.6 )

   résistance ..................................: FtepRd(1)=     437.37 kN

*  rangée de boulons n° 2

   mode de ruine du T équivalent ( J.3.2.1 )

   résistance plastique du T équivalent ( Form. J.7 )
      plastification semelle .......................: Mpl1Rd =     5475.90 Nm
      ruine boulon et plastification semelle .......: Mpl2Rd =     5475.90 Nm

   mode 1: plastification semelle ..................: F1Rd    =     390.75 kN
   mode 2: ruine boulons et plastification semelle .: F2Rd    =     450.42 kN
   mode 3: ruine boulons ...........................: F3Rd    =     807.84 kN

   résistance ..................................: FtepRd(2)=     390.75 kN

*  rangée de boulons n° 3

   mode de ruine du T équivalent ( J.3.2.1 )

   résistance plastique du T équivalent ( Form. J.7 )
      plastification semelle .......................: Mpl1Rd =     5475.90 Nm
      ruine boulon et plastification semelle .......: Mpl2Rd =     5475.90 Nm

   mode 1: plastification semelle ..................: F1Rd    =     390.75 kN
   mode 2: ruine boulons et plastification semelle .: F2Rd    =     450.42 kN
   mode 3: ruine boulons ...........................: F3Rd    =     807.84 kN
```

```
    résistance ..................................: FtepRd(3)=      390.75 kN

 *  rangée de boulons n° 4

    mode de ruine du T équivalent ( J.3.2.1 )

    résistance plastique du T équivalent ( Form. J.7 )
       plastification semelle ......................: Mpl1Rd =     6129.29 Nm
       ruine boulon et plastification semelle .......: Mpl2Rd =     6129.29 Nm

    mode 1: plastification semelle .................: F1Rd   =      437.37 kN
    mode 2: ruine boulons et plastification semelle .: F2Rd   =      464.02 kN
    mode 3: ruine boulons ..........................: F3Rd   =      807.84 kN

    résistance ..................................: FtepRd(4)=      437.37 kN

2)  boulons appartenant d'un groupe

 *  groupe entre rangées de boulons n° 1 et n° 2

    mode de ruine du T équivalent ( J.3.2.1 )

    résistance plastique du T équivalent ( Form. J.7 )
       plastification semelle ......................: Mpl1Rd =     7726.79 Nm
       ruine boulon et plastification semelle .......: Mpl2Rd =     7726.79 Nm

    mode 1: plastification semelle .................: F1Rd   =      551.36 kN
    mode 2: ruine boulons et plastification semelle .: F2Rd   =      833.69 kN
    mode 3: ruine boulons ..........................: F3Rd   =     1615.68 kN

    résistance ..................................: FtRd(1,2)=      551.36 kN

 *  groupe entre rangées de boulons n° 1 et n° 3

    mode de ruine du T équivalent ( J.3.2.1 )

    résistance plastique du T équivalent ( Form. J.7 )
       plastification semelle ......................: Mpl1Rd =    12918.67 Nm
       ruine boulon et plastification semelle .......: Mpl2Rd =    12918.67 Nm

    mode 1: plastification semelle .................: F1Rd   =      921.84 kN
    mode 2: ruine boulons et plastification semelle .: F2Rd   =     1278.19 kN
    mode 3: ruine boulons ..........................: F3Rd   =     2423.52 kN

    résistance ..................................: FtRd(1,3)=      921.84 kN

 *  groupe entre rangées de boulons n° 1 et n° 4

    mode de ruine du T équivalent ( J.3.2.1 )

    résistance plastique du T équivalent ( Form. J.7 )
       plastification semelle ......................: Mpl1Rd =    15169.56 Nm
       ruine boulon et plastification semelle .......: Mpl2Rd =    15169.56 Nm

    mode 1: plastification semelle .................: F1Rd   =     1082.46 kN
    mode 2: ruine boulons et plastification semelle .: F2Rd   =     1661.47 kN
    mode 3: ruine boulons ..........................: F3Rd   =     3231.36 kN

    résistance ..................................: FtRd(1,4)=     1082.46 kN

 *  groupe entre rangées de boulons n° 2 et n° 3
```

mode de ruine du T équivalent (J.3.2.1)

résistance plastique du T équivalent (Form. J.7)

plastification semelle ....:	Mpl1Rd =	10667.78 Nm
ruine boulon et plastification semelle ....:	Mpl2Rd =	10667.78 Nm

mode 1: plastification semelle ....:	F1Rd =	761.22 kN
mode 2: ruine boulons et plastification semelle .:	F2Rd =	894.92 kN
mode 3: ruine boulons ....:	F3Rd =	1615.68 kN

résistance ....: FtRd(2,3)= 761.22 kN

* groupe entre rangées de boulons n° 2 et n° 4

mode de ruine du T équivalent (J.3.2.1)

résistance plastique du T équivalent (Form. J.7)

plastification semelle ....:	Mpl1Rd =	12918.67 Nm
ruine boulon et plastification semelle ....:	Mpl2Rd =	12918.67 Nm

mode 1: plastification semelle ....:	F1Rd =	921.84 kN
mode 2: ruine boulons et plastification semelle .:	F2Rd =	1278.19 kN
mode 3: ruine boulons ....:	F3Rd =	2423.52 kN

résistance ....: FtRd(2,4)= 921.84 kN

* groupe entre rangées de boulons n° 3 et n° 4

mode de ruine du T équivalent (J.3.2.1)

résistance plastique du T équivalent (Form. J.7)

plastification semelle ....:	Mpl1Rd =	7726.79 Nm
ruine boulon et plastification semelle ....:	Mpl2Rd =	7726.79 Nm

mode 1: plastification semelle ....:	F1Rd =	551.36 kN
mode 2: ruine boulons et plastification semelle .:	F2Rd =	833.69 kN
mode 3: ruine boulons ....:	F3Rd =	1615.68 kN

résistance ....: FtRd(3,4)= 551.36 kN

2.1.5.3 raideur

* longueur effective du T équivalent
rangées de boulons individuelles ou appartenant à un groupe

rangée de boulons n° 1 ....:	leff(1) =	209.83 mm
rangée de boulons n° 2 ....:	leff(2) =	170.00 mm
rangée de boulons n° 3 ....:	leff(3) =	170.00 mm
rangée de boulons n° 4 ....:	leff(4) =	209.83 mm

* coefficient de raideur (Form. J.43)

rangée de boulons n° 1 ....:	k5(1) =	3.42 mm
rangée de boulons n° 2 ....:	k5(2) =	2.77 mm
rangée de boulons n° 3 ....:	k5(3) =	2.77 mm
rangée de boulons n° 4 ....:	k5(4) =	3.42 mm

2.1.5.4 boulons en traction

longueur du boulon	(J.4.4.10) :	Lb =	65.50 mm
résistance	(Table 6.5.3) :	BtRd =	403.92 kN
coefficient de raideur	(Form. J.45) :	k7 =	13.70 mm

2.1.6 semelle de la poutre en compression

moment résistant de la poutre	: McRd =	989.39	kNm
résistance .... (Form. J.30)	: FcfbRd =	1856.96	kN

2.1.7 âme de la poutre en traction

largeur effective
=> égales à celles de la platine en flexion

2.1.7.1 résistance

rangée de boulons n°		résistance (kN) (Form. J.31) FtwbRd(i)
1	:	1209.51
2	:	1080.58
3	:	1080.58
4	:	1209.51

groupe entre rangées de b		FtwbRd(i,j)
1 - 2	:	1524.75
1 - 3	:	2549.28
1 - 4	:	2993.46
2 - 3	:	2105.11
2 - 4	:	2549.28
3 - 4	:	1524.75

2.2 ASSEMBLAGE DES DIFFéRENTES COMPOSANTES

2.2.1 résistance (Fig. J.34)

2.2.1.1 rangée de boulons n° 1

	résistance (kN)
panneau d'âme de la colonne en cisaillement ....:	1133.63
âme de la colonne en compression ....:	929.10
semelle de la colonne en flexion ....:	689.64
âme de la colonne en traction ....:	1077.97
plat d'about en flexion ....:	437.37
boulons en traction ....:	807.84
semelle de la poutre en compression ....:	1856.96
âme de la poutre en traction ....:	1209.51
	---------
résistance de la rangée de boulons n° 1 ....: Frd(1) =	437.37 kN

2.2.1.2 rangée de boulons n° 2

résistance (kN)

2.2.1.2.1 1) boulons pris individuellement

panneau d'âme de la colonne en cisaillement ....:	696.26
âme de la colonne en compression ....:	491.73
semelle de la colonne en flexion ....:	689.64
âme de la colonne en traction ....:	1077.97
plat d'about en flexion ....:	390.75
boulons en traction ....:	807.84

semelle de la poutre en compression ....:	1419.59
âme de la poutre en traction ....:	1080.58

2.2.1.2.2 2) boulons appartenant d'un groupe

groupe entre rangées de boulons n° 1 et n° 2

semelle de la colonne en flexion ....:	752.35
âme de la colonne en traction ....:	837.47
plat d'about en flexion ....:	113.99
âme de la poutre en traction ....:	1087.38

résistance de la rangée de boulons n° 2 ....: Frd(2) = 113.99 kN

2.2.1.3 rangée de boulons n° 3

2.2.1.3.1 1) boulons pris individuellement

	résistance (kN)
panneau d'âme de la colonne en cisaillement ....:	582.27
âme de la colonne en compression ....:	377.74
semelle de la colonne en flexion ....:	689.64
âme de la colonne en traction ....:	1077.97
plat d'about en flexion ....:	390.75
boulons en traction ....:	807.84
semelle de la poutre en compression ....:	1305.59
âme de la poutre en traction ....:	1080.58

2.2.1.3.2 2) boulons appartenant d'un groupe

groupe entre rangées de boulons n° 1 et n° 3

semelle de la colonne en flexion ....:	1330.28
âme de la colonne en traction ....:	1065.75
plat d'about en flexion ....:	370.48
âme de la poutre en traction ....:	1997.92

groupe entre rangées de boulons n° 2 et n° 3

semelle de la colonne en flexion ....:	1267.58
âme de la colonne en traction ....:	1431.31
plat d'about en flexion ....:	647.23
âme de la poutre en traction ....:	1991.11

résistance de la rangée de boulons n° 3 ....: Frd(3) = 370.48 kN

2.2.1.4 rangée de boulons n° 4

2.2.1.4.1 1) boulons pris individuellement

	résistance (kN)
panneau d'âme de la colonne en cisaillement ....:	211.79
âme de la colonne en compression ....:	7.26
semelle de la colonne en flexion ....:	689.64
âme de la colonne en traction ....:	1077.97
plat d'about en flexion ....:	437.37
boulons en traction ....:	807.84
semelle de la poutre en compression ....:	935.12
âme de la poutre en traction ....:	1209.51

2.2.1.4.2 2) boulons appartenant d'un groupe

groupe entre rangées de boulons n° 1 et n° 4

semelle de la colonne en flexion ....:	1459.88
âme de la colonne en traction ....:	749.18
plat d'about en flexion ....:	160.62
âme de la poutre en traction ....:	2071.62

groupe entre rangées de boulons n° 2 et n° 4

semelle de la colonne en flexion ....:	1397.17
âme de la colonne en traction ....:	1132.65
plat d'about en flexion ....:	437.37
âme de la poutre en traction ....:	2064.81

groupe entre rangées de boulons n° 3 et n° 4

semelle de la colonne en flexion ....:	819.24
âme de la colonne en traction ....:	904.36
plat d'about en flexion ....:	180.88
âme de la poutre en traction ....:	1154.28

résistance de la rangée de boulons n° 4 ....: Frd(4) = 7.26 kN

distribution plastique des efforts internes

2.2.1.5 résumé

résistance de la rangée de boulons n° 1 ....: FRd(1) =	437.37	kN
résistance de la rangée de boulons n° 2 ....: FRd(2) =	113.99	kN
résistance de la rangée de boulons n° 3 ....: FRd(3) =	370.48	kN
résistance de la rangée de boulons n° 4 ....: FRd(4) =	7.26	kN
résistance en flexion (ruine des soudures non consid: MRdj =	304.49	kNm
résistance en flexion des soudures ....: MRdw =	426.30	kNm
moment résistant .... (J.3.6) :	304.49	kNm
moment maximum élastique .... (J.2.1.2) : Me =	203.00	kNm

2.2.2 raideur

2.2.2.1 détermination du coefficient de raideur équivalente

	raideur effective coefficient (mm) (Form. J.36)		bras de levier des forces internes
rangée de boulons n° 1 :	keff,1 =	1.72	h 1 = 476.40
rangée de boulons n° 2 :	keff,2 =	1.54	h 2 = 396.40
rangée de boulons n° 3 :	keff,3 =	1.54	h 3 = 136.40
rangée de boulons n° 4 :	keff,4 =	1.72	h 4 = 56.40

bras de levier des forces internes . (Form. J.38) : z = 383.73 mm
coefficient de raideur équivalente . (Form. J.36) : keq = 4.53 mm

2.2.2.2 pourcentages de flexibilité

la flexibilité d'une rangée de boulons est la flexibilité relative de cette rangée en comparaison avec les autres (indépendamment des bras de levier)

pour le panneau cisaille	40 %		
pour la zone comprimée	18 %		
pour la zone tendue	42 %		
* rangée de boulons n° 1		24 %	
plat d'about en flexion			50 %
boulons en traction			13 %
* rangée de boulons n° 2		26 %	
plat d'about en flexion			56 %
boulons en traction			11 %
* rangée de boulons n° 3		26 %	
plat d'about en flexion			56 %
boulons en traction			11 %
* rangée de boulons n° 4		24 %	
plat d'about en flexion			50 %
boulons en traction			13 %

2.2.2.3 résumé

raideur initiale .... (Form. J.34) : Sji = 58780.66 kNm/rad
raideur idéalisée ... (J.2.1.2 - J.2.1.4 - T.J.3) : Sjn = 29390.33 kNm/rad
raideur sécante .... (Form. J.34) : Sjs = 19669.26 kNm/rad

2.2.3 résistance en cisaillement

résist cisaillement d'une rangée de (Table 6.5.3) : FvRd = 448.80 kN

semelle de la colonne en pression diamétrale (Table 6.5.3):
p1/(3d0)-0.25 = 0.56
fub / fu = 1.89
=> ALPHA = 0.56
résist pression diamétrale d'une rangée de boulon: FbRd = 674.38 kN

plat d'about en pression diamétrale :
p1/(3d0)-0.25 = 0.56
fub / fu = 1.96
=> ALPHA = 0.56
résist pression diamétrale d'une rangée de boulon: FbRd = 347.13 kN

la résistance en cisaillement de la rangée de boulons soumise aux forces de traction et de cisaillement est réduite par un facteur 0,4/1,4 0.4/1.4 (J.3.1.2.(2b))

résist cisaillement rangée de boulons n° 1 ....: Vrd(1) = 128.23 kN
résist cisaillement rangée de boulons n° 2 ....: Vrd(2) = 128.23 kN
résist cisaillement rangée de boulons n° 3 ....: Vrd(3) = 128.23 kN
résist cisaillement rangée de boulons n° 4 ....: Vrd(4) = 128.23 kN

résist cisaillement des soudures
facteur de corrélation .... (6.6.5.3.(5)) : BETA = 0.90
longueur de la soudure ....: a = 467.60 mm
résist cisaillement des soudures (6.6.5.3.(4)) : FwRd = 734.32 kN

résistance au cisaillement de l'assemblage ....: VRd = 512.91 kN

2.2.4 mode de ruine

rangée de boulons n° 1 : plat d'about en flexion
rangée de boulons n° 2 : plat d'about en flexion

rangée de boulons n° 3 : plat d'about en flexion
rangée de boulons n° 4 : âme de la colonne en compression

aucune information sur la capacité de rotation donnée dans l'Eurocode 3

2.3 PROPRIéTéS DE CALCUL DU NOEUD POUR ANALYSE PLASTIQUE / VéRIFICATION PLASTIQUE DU NOEUD

moment résistant de calcul ....: MRd = 304.49 kNm

raideur initiale .... (Form. J.34) : Sji = 58780.66 kNm/rad
raideur idéalisée ... (J.2.1.2 - J.2.1.4 - T.J.3) : Sjn = 29390.33 kNm/rad

3. RéFéRENCES

1 ENV 1993-1-1 : 1992,Eurocode 3: Design of steel structures.
Part 1.1: General rules and rules for buildings,
CEN, Brussels 1992.

2 ENV 1993-1-1 : 1992/A2, October 1998.
Revised Annex J of Eurocode 3, "Joints in Building Frames",
CEN, Brussels, October 1998.

X.2. *Annex B: Matlab codes for the resolution of the simplified model*

X.2.1. Introduction

Within the present annex, a Matlab code to solve the system of equations given in Deliverable V, Annex C is reported. An explanation note can be found in §X.2.3.

X.2.2. Codes

<u>substructure.m</u>

```
%% Equations for the 3D-substructure, 1 storey
clear all
close all

%% Units: kN and m

%% Comments
% the "x" direction is following the primary frame
% the "y" direction is following the secondary frames

%%
% Input data's

global u0 L0x L0y KNx1 KNx2 KNy1 KNy2 M_Ax M_Bx M_Cx M_Dx N_Ax M_Ay M_By
M_Cy M_Dy N_Ay

L0x = 10;
L0y = 16;

% parameter for the deltaN-N law (assumed to be linear
KNx1 = 20000 ;
KNx2 = KNx1 ;
KNy1 = 15000 ;
KNy2 = KNy1 ;

% parameters for the M-N laws

% Following the x direction
M_Ax = 590;
M_Bx = 110.6;
M_Cx = 61;
M_Dx = -360;
N_Ax = 1577;
% interaction M-N law for the beam-to-colum joint in the principal frame

% Following the y direction
M_Ay =0;
M_By =0;
M_Cy =0;
M_Dy =0;
N_Ay = 1500;
% for the secondary frame, the joint is assumed to be a hinge so MA->Dy = 0
% the value given to N1y is useless, it just should be verified later that
% the Ny found can be sustained by this hinge

%% Initialisation of the given displacements

% As explained in the reports, to find the Q-delta (=P-u here) curve, the
% first step is to define a value of u, and then, find the corresponding
% value of P.
% Here, we define the values of u for which we want to find the
corresponding P
```

```
j = 2;
u_given(1)=0;
while u_given(j-1) < 1.5
    u_given(j)=u_given(j-1)+0.01;
    j = j+1;
end


%% Initialisation of the unknowns vector

x0 = ones(16,1); %16 is the number of unknowns

%% Resolution

% For each value of u that we have just defined, the system of equations,
% defined in the file "myfun.m" is solved.
% This system of equations is solved using the MATLAB function "fsolve"
% The results, for each value of u, are stored in a table called "results".
% In this table, each line corresponds to a value of u, and each column
% correspond to an unknown

val_stop = 0;
k = 1;

while (k<j && val_stop == 0)
    u0 = u_given(k);
    [x,fval,exitflag]=fsolve(@myfun,x0);
    results(k,:)= x; %the vector solution x is stored in a table
    verif(k,1)=exitflag; % the value of exitflag is stored in a vector
    x0 = results(k,:); %x0 is updated
    k = k+1;
end
```

<u>myfun.m</u>

```
function F = myfun(x)
%% Input data's
% The same as in the "substrucre.m" file

global u0 L0x L0y KNx1 KNx2 KNy1 KNy2 M_Ax M_Bx M_Cx M_Dx N_Ax M_Ay M_By
M_Cy M_Dy N_Ay

%% Definition of the unknowns
% The vector "x" is the unknowns-vector (16 unknowns)

P = x(1);
Nx = x(2);
Ny = x(3);
Mx1 = x(4);
Mx2 = x(5);
My1 = x(6);
My2 = x(7);
deltaN_x1 = x(8);
deltaN_x2 = x(9);
deltaN_y1 = x(10);
deltaN_y2 = x(11);
thetax = x(12);
thetay = x(13);
Lx = x(14);
Ly = x(15);
```

```
u = x(16);

%% Definition of the equations
% The vector F is the equations-vector (16 equations)
% Each element of the vector F is an equation, and the function fsolve
% tries to find the solution for F(x)=0, iterating from the starting point
x0.

F     = [u-u0
         tan(thetax) - (u/L0x)
         tan(thetay) - (u/L0y)
         Lx-(L0x/cos(thetax))
         Ly-(L0y/cos(thetay))
         P - (2*Nx*sin(thetax)+(2*((Mx2-Mx1)/Lx)*cos(thetax))) -
(2*Ny*sin(thetay)+(2*((My2-My1)/Ly)*cos(thetay)))
         L0x + deltaN_x1 + deltaN_x2 - Lx
         L0y + deltaN_y1 + deltaN_y2 - Ly
         KNx1*deltaN_x1-Nx
         KNx2*deltaN_x2-Nx
         KNy1*deltaN_y1-Ny
         KNy2*deltaN_y2-Ny
         Mx1 - M_SAG(Nx,N_Ax,M_Ax,M_Bx,M_Cx,M_Dx)
         Mx2 - M_HOG(Nx,N_Ax,M_Ax,M_Bx,M_Cx,M_Dx)
         My1 - M_SAG(Ny,N_Ay,M_Ay,M_By,M_Cy,M_Dy)
         My2 - M_HOG(Ny,N_Ay,M_Ay,M_By,M_Cy,M_Dy)];

% The M-N interaction laws are expressed in files M_HOG.m and M_SAG.m

end
```

M_HOG.m

```
function M = M_HOG(N,NA,MA,MB,MC,MD)

M = ((MB-MA)/NA)*N + MA;

end
```

M_SAG.m

```
function M = M_SAG(N,NA,MA,MB,MC,MD)

M = ((MC-MD)/NA)*N + MD;

end
```

X.2.3. Explicative notes on the codes

The 4 Matlab files are described in the present section.

substructure.m

This is the principal file. It is the one to be launched in the Matlab interface. The other files are called by this file or by a file that has itself already been called by “substructure.m” (Figure 30).

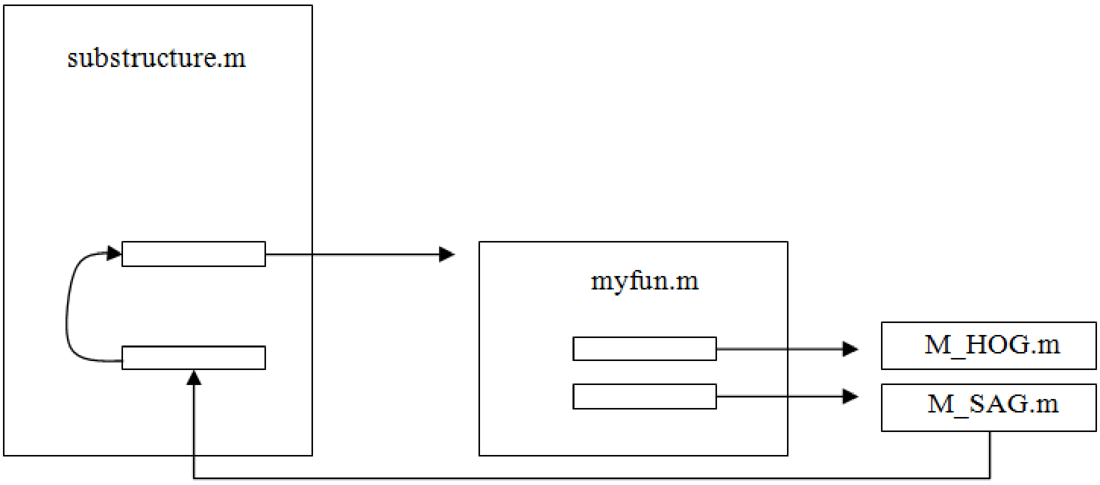

Figure 30. Links between the different Matlab-files

- Input data's
  - Initial lengths of the beams (L_{0x} is for the beams of the primary frame, $L_{0y}$for the beams of the secondary frame)
  - $N - \delta_N$ laws
    These laws are assumed to be linear: $K_N * \delta_N = N$.
    It is assumed that hinges in hogging and sagging have the same $N - \delta_N$ laws ($K_{N1} = K_{N2}$).
    For the primary frame,$K_{Nx} = 20000\ kN/m$, and for the secondary frame, $K_{Ny} = 15000\ kN/m$
  - $M - N$ laws
    The parameters $M_{A \to D, x\ or\ y}$ and $N_{A, x\ or\ y}$ are parameters that describe the $M - N$ interaction law, in hogging and sagging, and in the 2 main directions. Theses parameters will be defined in the paragraph describing M_HOG.m and M_SAG.m.

- Solving procedure

Initialisation of the u_given vector

As explained in this deliverable, the first step of the solving procedure is to define a value of u, and in a second step, solve the system of equations to determine the value of P corresponding to this value of u.

In this part of the matlab code, all the values of u for which the value of P will be calculated are defined (incremental step of 0.01 m, from u = 0 to u = 1.5 m).

Resolution of the equation system (description of the fsolve function)

For each value of u that has been defined, the system of equations defined in Deliverable V, Annex C is solved. This system of equations is defined in the file "myfun.m".

So, for each value of u, the system of equations is solved using the MATLAB function "`fsolve` ".

This function `fsolve` goes and find the equations in the file "myfun.m"."x" is the vector containing the unknowns and "F" is the vector containing the equations. The aim is to define x such as F(x)=0.

`[x,fval,exitflag]=fsolve(@myfun,x0)` means that the function `fsolve` will go in the file "`myfun`", find the vector F(x), and finally, after a certain number of iterations, find a vector solution "x" that verifies F(x)=0. To do these iterations, "`fsolve`" needs a starting point, which is "`x0`". `fval` is the value of the vector F(x) for the solution found (so, `fval` must be very close to 0). `exitflag` is a number, indicating if the iteration converged correctly (`fval` = 1 means that `fsolve` converged correctly).

So, for a certain value of u, `fsolve` finds the vector solution `x` and this solution is stored in a table called "results". In this table, each line corresponds to a value of u, and each column corresponds to an unknown (ex: the 3rd column corresponds to the 3rd unknown, which is N_y, the normal effort in the secondary beams). For each value of u, the value of the `exitflag` is also stored, to check in the end if, for every value of u, the `fsolve` converged correctly. The starting point "`x0`" is updated at each iteration: `fsolve` always starts iterating from the solution vector that it has just found.

<u>myfun.m</u>

In this file, all the unknowns are defined. It is in this file that the equations are written. In particular, the $M - N$ interaction laws refer to two other files, M_HOG and M_SAG, defined here below.

<u>M_HOG.m and M_SAG.m</u>

For the beam-to-column joints in the primary frame (x-direction), the $M - N$ law that is implemented is the following (Figure 31):

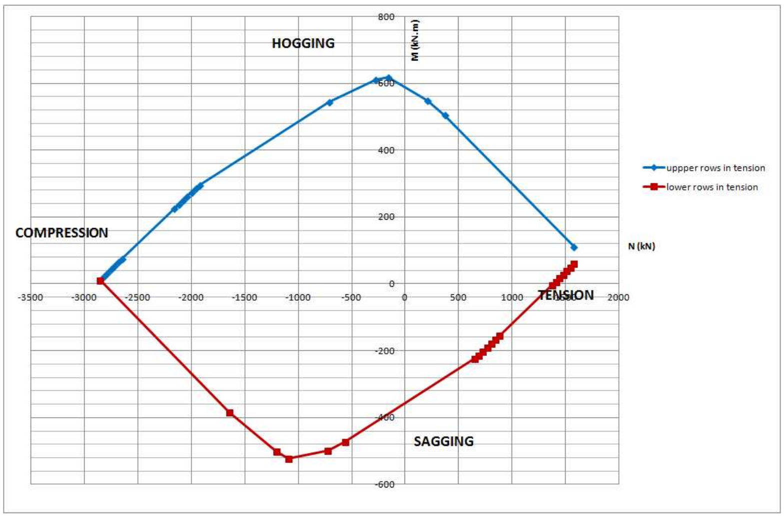

Figure 31. M-N interaction law for joints in the primary frame

It is simplified by considering only the tension part and by approximating the curves by lines (Figure 32):

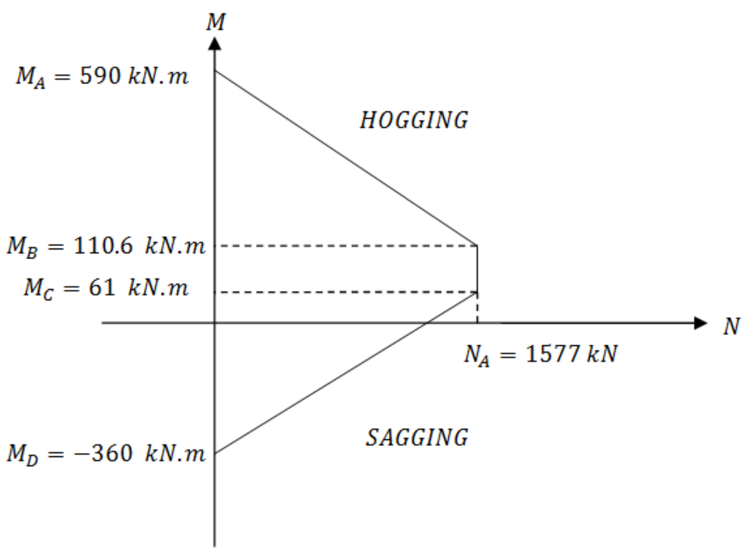

Figure 32. Simplification of the $M - N$ law

hogging	sagging
$M(N) = \frac{M_B - M_A}{N_A} * N + M_A$	$M(N) = \frac{M_C - M_D}{N_A} * N + M_D$

For the secondary frame (y-direction), the beam-to-column joint can be approximate by a hinge, so the values of the M-N law parameters are:

$$M_A = M_B = M_C = M_D = 0$$

The value of N_A is not relevant here.

XI. References

ADAPTIC user manual, Version 1.3b, Izzuddin, 2009, March.

Comeliau C., Demonceau J.-F., Huvelle C., Jaspart J.-P. (2012), "Simplified approach". Internal Report, University of Liège

Dai X.H., Wang Y.C., Bailey C.G. (2010). "Numerical modelling of structural fire behaviour of restrained steel beam-column assemblies using typical joint types", Engineering Structures, Vol. 32, 2337-2351.

De Martino A., Landolfo R., Mazzolani F.M. (1990). "The use of the Ramberg-Osgood law for materials of round-house type", Materials and Structures, 23, 59-67.

Demonceau J.-F. (2008), "Steel and composite building frames: sway response under conventional loading and development of membrane effects in beams further to an exceptional action", PhD Thesis realised at the ULg.

Demonceau J.F. (2008). "Steel and composite building frames: sway response under conventional loading and development of membrane effects in beams further to an exceptional action". Ph.D. Thesis, Faculty of applied sciences, University of Liege (BE), 2008.

EN 1991-1-2, "Eurocode 1 – Actions on structures – Part 1-2: General actions – Actions on

EN 1992-1-1:2004, "Eurocode 2: Design of concrete structures - Part 1-1: General rules and rules for buildings", European committee for standardization, December 2004.

EN 1992-1-2:2004, "Eurocode 2: Design of concrete structures – Part 1-2: General rules – Structural fire design", European committee for standardization, December 2004.

EN 1993-1-1:2005, "Eurocode 3: Design of steel structures – Part 1-1: General rules and rules for buildings", European committee for standardization, May 2005.

EN 1993-1-2:2005, "Eurocode 3: Design of steel structures – Part 1-2: General rules – Structural fire design", European committee for standardization, April 2005.

EN 1993-1-2:2005, "Eurocode 3: Design of steel structures – Part 1-2: General rules – Structural fire design", European committee for standardization, April 2005.

EN 1993-1-8:2005, "Eurocode 3: Design of steel structures – Part 1-8: Design of joints", European committee for standardization, May 2005.

EN ISO 377 (1997). "Steel and steel products – Location and preparation of samples and test pieces for mechanical testing", European Committee for Standardization, Brussels.

Fang C., Izzudin B., Elghazouli A., Nethercot D., Gernay T., Demonceau J.-F., Franssen J.-M., Robustfire report "Benchmark study for floor slabs", Imperial College and University of Liège

Izzuddin B.A. (1991). Nonlinear Dynamic Analysis of Framed Structures, PhD Thesis, Imperial College, University of London.

Izzuddin B.A., Vlassis A.G., Elghazouli A.Y. and Nethercot D.A. (2008). "Progressive Collapse of Multi-Storey Buildings due to Sudden Column Loss – Part I: Simplified Assessment Framework", Engineering Structures, 30:5, 1308-1318.

Jaspart et al. (2008). "Deliverable I: Definition of the problem and selection of the appropriate investigation ways", Robustness of car parks against localised fire, Grant Agreement Number RFSR-CT-2008-00036.

Kato B., Aoki H., Yamanouchi H. (1990). "Standardized mathematical expression for stress-strain relations of structural steel under monotonic and uniaxial tension loading", Materials and Structures, 23, 47-58.

Kodur V. K. R., Dwaikat M. M. S. (2010). "Effect of high temperature creep on the fire response of restrained steel beams", Materials and Structures, 43, 1327-1341.

Malvern, L. E. (1969). “Introduction to the Mechanics of a Continuous Medium”, Prentice-Hall, Englewood Cliffs, NJ.

NP EN 206-1:2007 (2007). “Concrete – Part 1: Specification, performance, production and conformity”, Norma Portuguesa, Instituto Português da Qualidade, Portugal.

Santiago A. (2008). “Behaviour of beam-to-column steel joints under natural fire”, Ph.D. Thesis, Department of Civil Engineering, University of Coimbra.

structures exposed to fire”, European committee for standardization, 2002.

Vila Real P., Couto C., Lopes N. (2011). “Modelling of multiple localised fires and steel structural members response using the software Elefir-EN”, Application of Structural Fire Engineering, Prague, Czech Republic.

Vlassis A.G., Izzuddin B.A., Elghazouli A.Y. and Nethercot D.A. (2008). “Progressive Collapse of Multi-Storey Buildings due to Sudden Column Loss – Part II: Application”, Engineering Structures, 30:5, 1424-1438.

Yang K. C., Lee H. H., Chan O. (2006). “Performance of steel H columns loaded under uniform temperature”, Journal of Constructional Steel Research, vol. 62, 262-270.